2010-04-23

Preliminary Design of Tall Buildings

Madison Radhames Paulino
Worcester Polytechnic Institute

PRELIMINARY DESIGN OF TALL BUILDINGS

by

Madison R Paulino

A thesis

Submitted to the Faculty

Of the

WORCESTER POLYTCHNIC INSTITUTE

in partial fulfillment of the requirements for the

Degree of Master of Science

in

Civil Engineering

May 2010

Approved by _____

Thesis Advisor: Prof. P. Jayachandran

_____

Prof. Leonard D. Albano

_____

Prof. T. El-Korchi, Head of the Department

ABSTRACT

Techniques for preliminary analysis of various tall building systems subjected to lateral loads have been studied herein. Three computer programs written in Matlab® graphical user interface language for use on any personal computer are presented. Two of these programs incorporate interactive graphics.

A program called Wall_Frame_2D is introduced for two-dimensional analysis of shear wall-frame interactive structures, using the shear-flexural cantilever analogy. The rigid outrigger approach was utilized to develop a program called Outrigger Program to analyze multi-outrigger braced tall buildings. In addition, a program called Frame Tube was developed which allows analysis of single and quad-bundled framed tube structures. The tube grids are replaced with an equivalent orthotropic plate, and the governing differential equations are solved in closed form.

Results for lateral deflections, rotations, and moment, shear, and torque distributions within the various resisting elements are compared against other preliminary and "exact" matrix analysis methods for several examples. SAP2000 was used to obtain "exact" results.

The approximate analyses are found to give reasonable results and a fairly good indication of the behavior of the actual structure.

These programs are proposed for inclusion in a knowledge-based approach to preliminary tall building design. The tall building design process is outlined and criteria are given for the incorporation of these "Resource Level Knowledge Modules" into an integrated tall building design system.

ACKNOWLEDGMENTS

The author wishes to express sincere thanks to Dr. P. Jayachandran for his timely advice and patience throughout this endeavor. Thanks are extended to all faculty members of the Civil & Environmental Engineering department at the Worcester Polytechnic Institute, especially to Dr. P. Albano, whom I had the opportunity to work with throughout this journey.

I sincerely appreciated my heroes, my parents, Carmelo and Milagros Paulino, for their unconditional love and endless sacrifice in bringing me up and offering me an opportunity to achieve my goals. Who I am at this point is directly the result of their courage, wisdom, and faith in their sons. I am thankful to my brothers, Enger, Edward, and Johan Paulino for their generous hospitality and support. To my uncle and cousins, Jose Paulino, Emmanuel Flores, and Chabelly Paulino for their special support too. And for all my family, I laid the path, and proved to all that anybody can reach any objectives desire with determination. I love you all and always will keep all of you close to me in my heart.

This work is also dedicated to God, who gave me encouragement, strength, and confident when I need it the most.

Table of Contents

List of Figures

List of Tables

I. INTRODUCTION

1 Introduction

An efficient and economical tall building cannot be designed without a thorough understanding of the significant factors affecting the selection of the structural system and knowledge of how the structural system will interrelate with architectural, mechanical and electrical aspects. Usually two to three different structural systems will be selected for comparison.

Long before the final “exact” analysis each system can be analyzed to provide a preliminary assessment of the structural response to lateral loading. At this stage it would be time consuming and wasteful to apply a large scale matrix computer analysis. In some instances, the hardware or software may not be readily available. The dominant behavior of each system can be addressed with preliminary design methods with consider the essential basic conditions for horizontal loads and stiffness requirement in terms of sway limitations.

In order for a preselected structural system to converge to an optimum design the initial member stiffness must be close to or, alternatively, the set of initial stiffness must be uniformly proportional in an approximate sense to the members of the optimum set ref (1). Rational approximate methods will provide good starting values for an “exact” analysis. We can observe the behavior of tall buildings subject to lateral loads in small-scale model tests ref (54), (3) and by using matrix analysis programs such as Etabs, SAP2000 or STRUDL. Heuristic knowledge may also be available in the form of industry experience and experts in tall building behavior ref (3). With this information we can make simplifying assumptions in order to provide the basis for an

approximate analysis formulation. Several approximate methods are available for various tall building lateral loads resisting systems ref (4), (5), (6), (7), (8), and (9). Specific examples include Coulland Bose's ref (10) approach to the analysis of framed tube structures and Heidebrecht and Stafford Smith's ref (11) method for analyzing shear wall-frame structures.

Using an approximate method we can analyze the structure based on the effects of its primary behavior. Conditions such as out-of-plane stiffness of the slabs can be neglected. Methods such Etabs, Sap2000, and STRUDL which are based on a large number of parameter make it difficult to observe macroscopic behavior and inhibit parameter design studies of the building system. Repeated analyses with these methods are economical prohibitive and usually will not provide for an optimized set of member proportions.

The approximate methods can be used to provide a basic for preliminary member sizing, provide a basic for relative evaluation of several design options, and to provide approximate values of shears, moments, lateral deflection, and rotations. Graphical displays are obviously useful to the student but also to the practicing engineer who can with a glance assess the analysis results.

With the advent of expert systems and knowledge based design approaches ref (12) to structural engineering ref (12), industry expertise, such as the preliminary approaches presented within, can be integrated with a non-algorithmic (symbolic) design advisor to allow for initial member sizing and subsequent optimization ref (3).

This work will first address lateral load resisting systems for tall buildings and outline the knowledge based approach to tall building design. Subsequent chapter present preliminary

analysis approaches and compare the results of several examples using computer programs developed in Matlab® graphical user interface with the results of more exact analyses.

In chapter II, shear wall and braced frame interactive structure in two dimensions are studied and a computer program, Wall_Frame_2D, develop from ref (11) and incorporating graphics is presented.

Multi-outrigger braced tall buildings are studied in Chapter III and a computer program called, Outrigger_Program capable of graphical display, is introduced and used to analyze two different structures with multiples outriggers. The program is based on the rigid outrigger approach ref (13).

Criteria for incorporating these programs into a knowledge based design approach are presented in chapter II. Conclusions and recommendations for future research conclude this thesis.

1.1 Development of Tall Building Systems- A Historical Perspective

The development of tall buildings and tall building structural systems closely follows that of material, analysis and non-structural system, (mechanical), developments. The earliest buildings were constructed of masonry. Chicago's sixteen stories Monadnock building (1981) is the tallest masonry structure ever built ref (14). At the base its walls were over six feet thick ref (15). Such seemingly ridiculous proportions were required by code. The taller the building, the greater the volume of masonry was required per unit area of floor space. These early structures provided inherent stability against overturning moments in their extreme dead loads.

An iron frame was first used in the United States for a lighthouse at Black Rock Harbor, Long Island Sound in 1843. Eventually cast iron use progressed from its use in building facades to that of a structural medium due to its fire-resistance and easy assembly. Subsequently wrought iron beams and columns were used simultaneously with masonry exterior walls. The six stories Harper Brothers Building of 1854 is an example of this technique ref (14). It was development of the Bessemer converter (1870) as well as the open hearth furnace with allowed widespread use of iron ore products in building material ref (16). The advent of hydraulic elevators (1870's) also made tall buildings more practical ref (27).

William Jenney's home Insurance Building of 1879 is considered the first extensive application of the internal skeleton and curtain wall to a high office building. Jenney's building also was one of the first to contain steel beams. Steel beams replaced cast and wrought iron as the industry standard in the early 1900's. The Chicago school of Architecture refined the use of beams and columns in steel and subsequently frame construction became widespread. Also at this time concrete slabs and columns were develop ref (17). Perret designed the Rue Franklin Apartment Buildings in 1903 which was the first use of a reinforced concrete skeleton structural system ref (14).

The first tall buildings of an all steel frame was constructed during the same year as the advent of riveting, 1889. Shortly thereafter the first use of an actual lateral bracing system to counter wind loads was developed for the Masonic temple in Chicago by E.C. Shankland.

The concentration of commerce in the constricted area of Manhattan and the subsequent increase in land values spurned taller and taller buildings and in 1931 the 102

stories Empire State Building was opened ref (14). This building had incorporated the states of the art in structural system, a braced steel frame in conjunction with a rigid concrete and masonry exterior. It was the rigid exterior which allowed the braced frame to be carried to such a height.

In the late 1940's, when adequate air conditioning and artificial lighting became available, a decrease in core size no longer required a corresponding decrease in over-all floor size ref (18). This resulted in the "slab" building and it was this time that concrete use increased in tall buildings. Shear walls in conjunction with flat slabs were first used on the Lake Meadows Housing Project in Chicago 1949. This type of construction became very popular for apartment buildings because the walls could be used to separate living apace. The advent of computer use in the 1950's now eliminated some of the tedium of structural calculations and subsequently economic structures could be more readily designed.

Encouragement from the architectural community now forced engineers to exercise ingenuity in design. Shear wall-frame interaction was an extension of the use of shear walls with simply supported exterior framing. The 38-stoty Brunswick Building is considerate the first use of such a system (1962) ref (19). In the years fallowing structural innovations such as the outrigger braced buildings in conjunction with perimeter belt trusses and many variations of the framed tube such as tube-in-tube, partial tube braced tube and bundled tube systems afforded economical tall building designs at any height to width ratio ref (19), (20), (22), (23), (24), and (25). The advent of high strength and lighter materials, better fastening and

construction methods, and more exact techniques of predicting behavior accompanied and certainly permitted practical application of these innovations.

1.2 Lateral Load Resisting Systems Far Tall Buildings

1.2.1 Introduction

As socio-economic trends demanded taller buildings, structural engineers were pressed to provide lateral load resisting systems that would minimize, (or at least optimize), cost of structural and reinforcing steel for buildings of greater height to width aspect ratios and varying vertical profiles. Initially, rigid frame construction was used extensively in tall buildings, but as aspect ratio increased, stiffness rather than strength criteria begins to control design and tall buildings pay a “premium for wind “, i.e. that amount of structural steel required beyond that required to sustain gravity loading ref (29). Figure 1 shows an acceptable wind premium for tall buildings. Figure 2 compare steel weight for various tall buildings. Those buildings to the upper left are most economical for a given number of stories.

In order to control building response to lateral loading structural engineers may utilize one or more of the fallowing ref (30):

1. Increase stiffness of the system
2. Increase building weight
3. Increase density of the structure with fill-ins
4. Use efficient shapes
5. Generate additional damping forces (tuned mass dampers)

This work will focus on systems that evolved from efforts to increase building stiffness.

Tall buildings structural system can be classified into four basic groups; rigid and semi-rigid frames, shear wall or braced frames structures, shear wall or truss-frame interactive structures, and tube structures. Tube structures can be further categorized into frames tube systems and high efficiency tube systems. High efficiency tube systems evolved from the basic frame tube. Figure 3, shows a comparison of tall building systems versus number of stories, and Figures 4 and 5shows a more detailed comparison of structural systems for steel and concrete structures respectively.

The sections following will discuss the general behavior and use of shear wall and truss-frame interactive structures. The reader is referred to ref (32) for a more detailed discussion of the non-structural parameters controlling the use of each particular system.

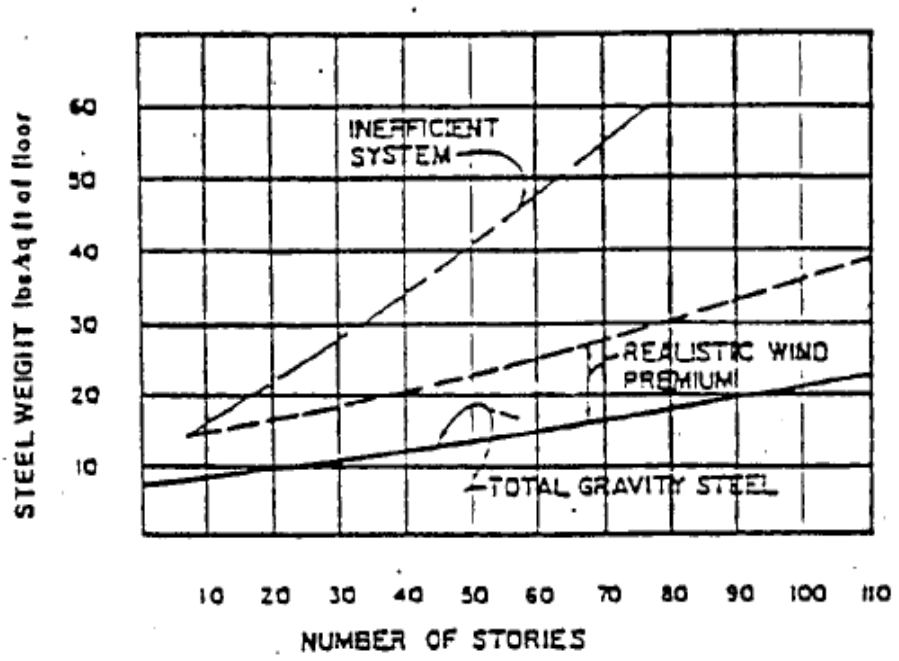

Figure 1Gravity Steel vs. Wind Premium ref (29)

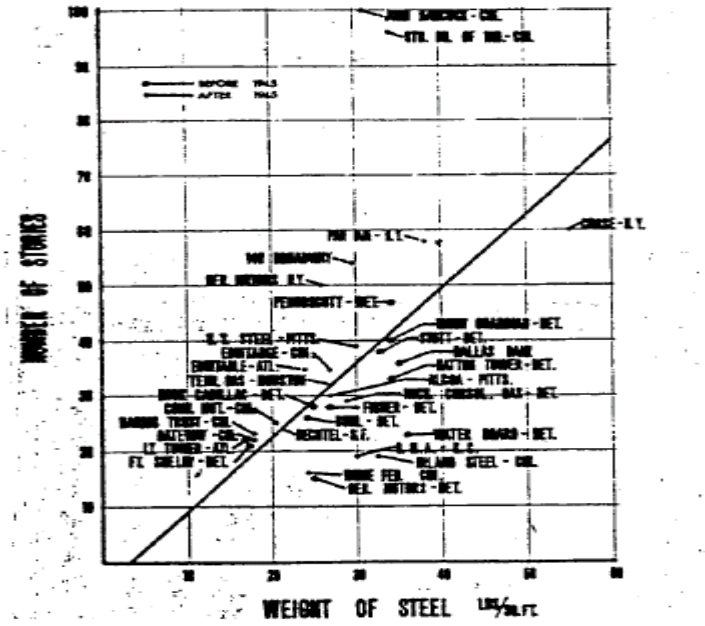

Figure 2 Comparison of Steel weight for various buildings ref (31)

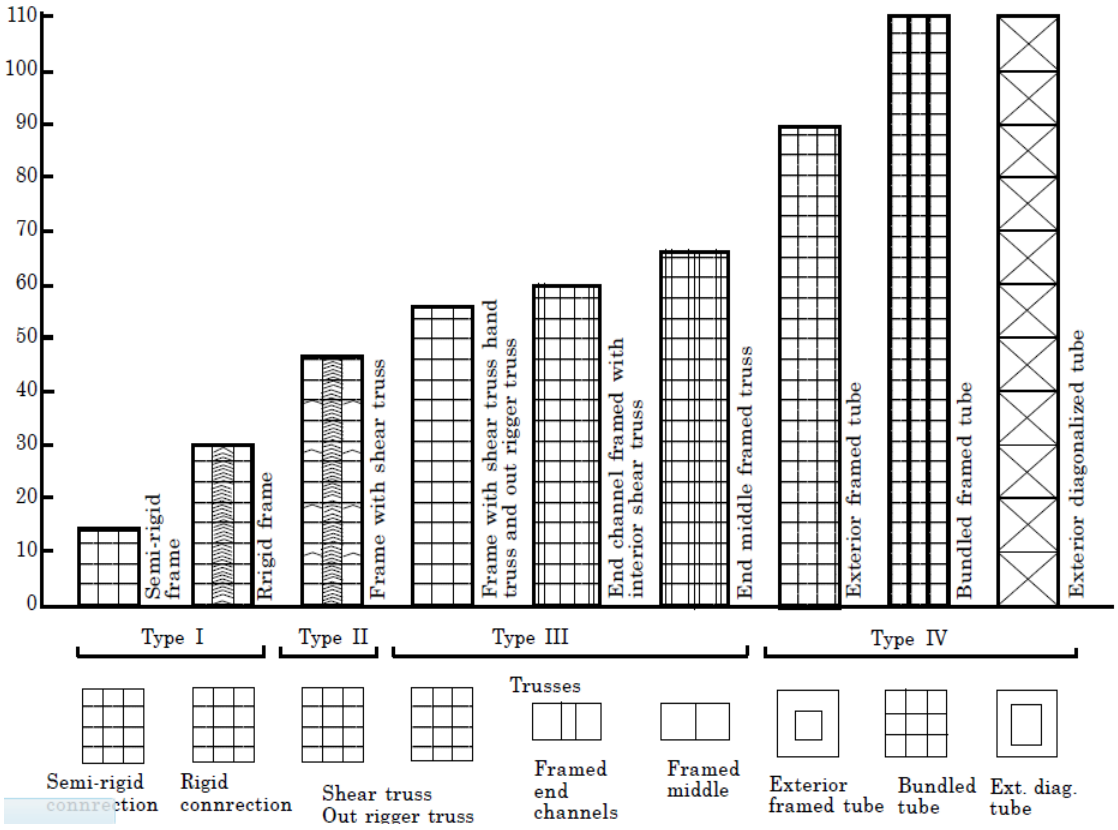

Figure 3 Comparisons of Structural Systems ref (29)

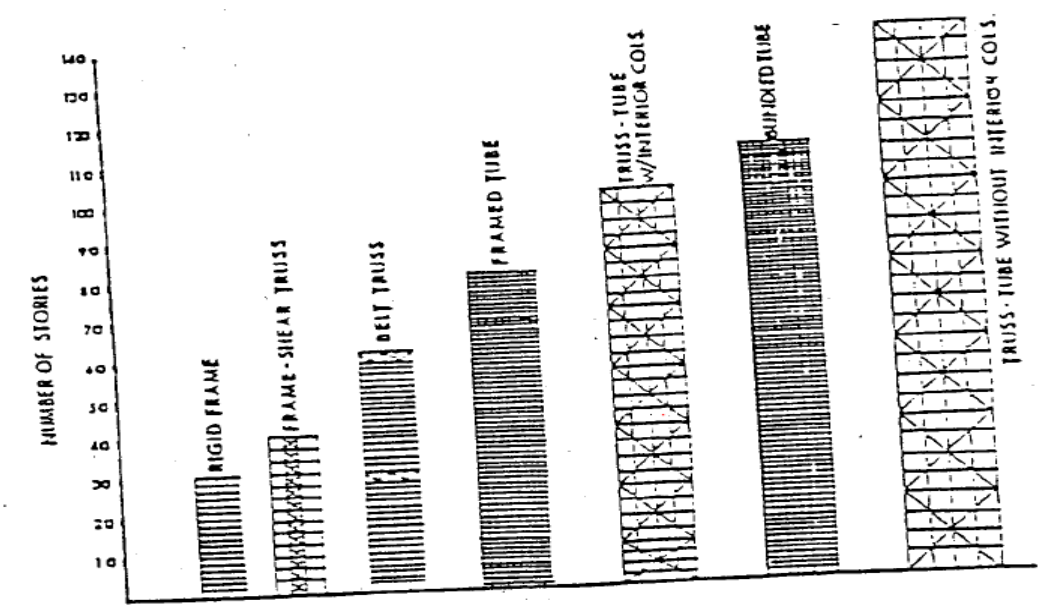

Figure 4 Types of steel structures ref (24)

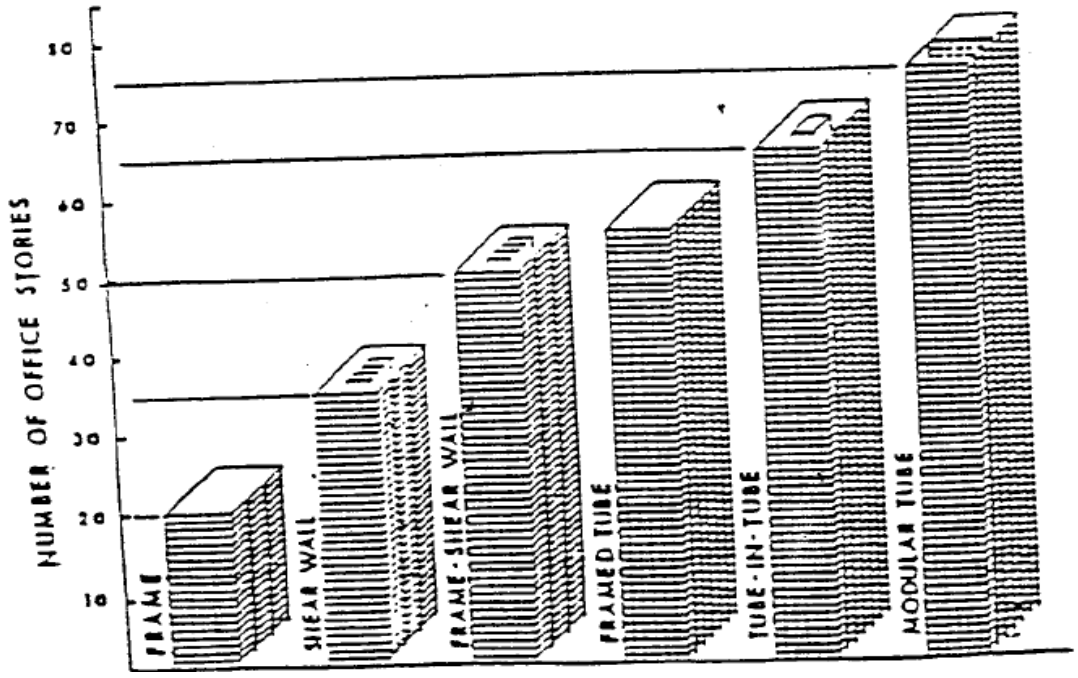

Figure 5 Concrete structure systems ref (24)

1.2.2 Shear Wall and Truss-Frame Interaction

Rigid and semi-rigid frames were found to be efficient only for buildings in the one to 20 story ranges. The flexibility of the beams and columns in these structures provides a shear mode response which is inefficient in resisting lateral drift. When vertical shear walls and or vertical trusses are introduced in the building plan they can provide the necessary lateral rigidity through a more efficient cantilever bending mode and interior frames can be designed for gravity loads only ref (41). May methods exist for analysis of building relying only on shear wall lateral stiffness ref (36), (37), (38), (39), and (40). Variations of some methods for analyzing coupled shear walls are discussed in section 2.1. Shear wall and truss building, staggered wall beams, and staggered trusses can provide rigidity up to forty stories and allow larger spans ref (34), and (35).

Shear wall can be placed to receive large gravity load tributary areas to increase resistances to overturning and uplift. No additional wind bracing should be required outside of the core area. Usually shear wall are located around the stair and elevators shafts and can serve a dual architectural/structural function. Figure 6 shows some typical shear wall arrangements. If they are unsymmetrical placed torsion effects must be considerate.

By using rigid connections in the exterior frame the frame and shear wall or trusses can be forced to interact. In concrete structures this interaction is inherent due to the monolithic construction. Here the combination of the characteristic deflections of the frame and wall or vertical truss trend to produce a “lazy S” deflection mode but usually the bending mode of the vertical elements governs. Figure 7 illustrates the basic response of each system and that of the interactive system. Here the shear wall could be replace by a vertical truss. Hereafter the terms

shear wall and vertical truss are used interchangeably. It is this shear-flexural cantilever behavior which forms the basis for development of the computer programs in chapter II.

Normally the rigid wall will sustain the majority of shears and moments at the base. Near the building top, the frame will tend to pull back on the wall and hence a point of contra flexure develops in the shear wall. Unlike buildings of a system where lateral loads can be distributed based on relative stiffness, the presence of varied behavioral modes coupled with rigid floor slabs results in non-uniform interaction forces which complicate the analysis. See Figure 7c. Shear wall-frame interaction has been successfully used in apartment buildings up to 70 stories high ref (44). Notable examples include the 38 stories concrete Brunswick building and the Chase Manhattan building in New York ref (19).

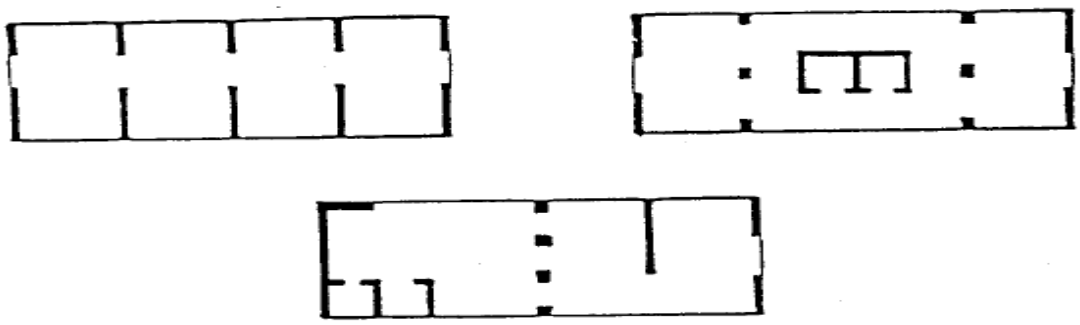

Figure 6 Typical shear wall arrangements ref (42)

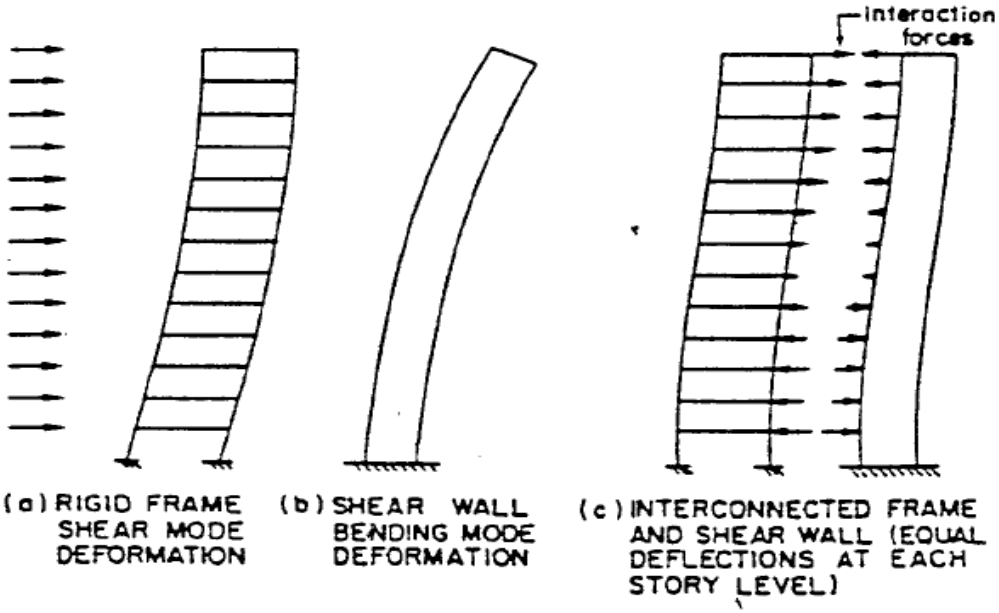

Figure 7 Interaction between shear wall & frame ref (43)

1.2.3 Braced Frames with Outrigger Trusses

To accomplish shear truss-frame interaction in steel buildings a large number of expressive rigid moment connections will be required. In order to increase the interaction between the core and exterior columns thereby improving cantilever action and reducing shear deflection horizontal outrigger trusses can be introduced to “link” the core and exterior columns. Frequently belt trusses are used to engage a greater number of exterior columns to reduce vertical deflection and improve action due to thermal effects ref (48). These trusses most often are located at mechanical levels in the building. Figure 8 show a schematic of the outrigger-belt truss system.

Outrigger trusses were first introduced by Jack Barbacki in 1961 ref (45). Figures 9 a, b illustrate their use on the 43 stories Yasuda Building in Tokyo designed by the structural department of the Tasei Corporation. The belt truss located at the top floor is sometimes called a “hat-truss’. Belt trusses can improve system stiffness by as much as twenty five percent ref (29).

The outrigger trusses should be fixed to the core and pinned to the exterior columns to improve bending efficiency. When the core bends outrigger trusses act as lever arms that transfer vertical shears and put direct axial stresses into the perimeter columns. The columns act as struts to resist bending and the core moment is reduced due to the transfer of overturning moment to axial loads.

Observe Figure 10a.When the frame is hinged to the core it behaves as a cantilever beam and it is free to rotate at any height. The resulting moment diagram due to a distributed lateral force is shown. In Figure 10b an outrigger truss has been introduced in the top story. The

building now resists rotation at the top level and a point of inflation and subsequent reduction in core moment results. The building now deflects in the “lazy S” mode of a wall-frame system. Figure 10c illustrates the behavior of a double outrigger system. Additional outriggers reduce lateral drift less dramatically and four outriggers can be considered a practical limit. By considering the outriggers infinitely rigid and writing equations for rotation compatibility at the outrigger locations, these buildings can be solved in a preliminary sense ref (46).

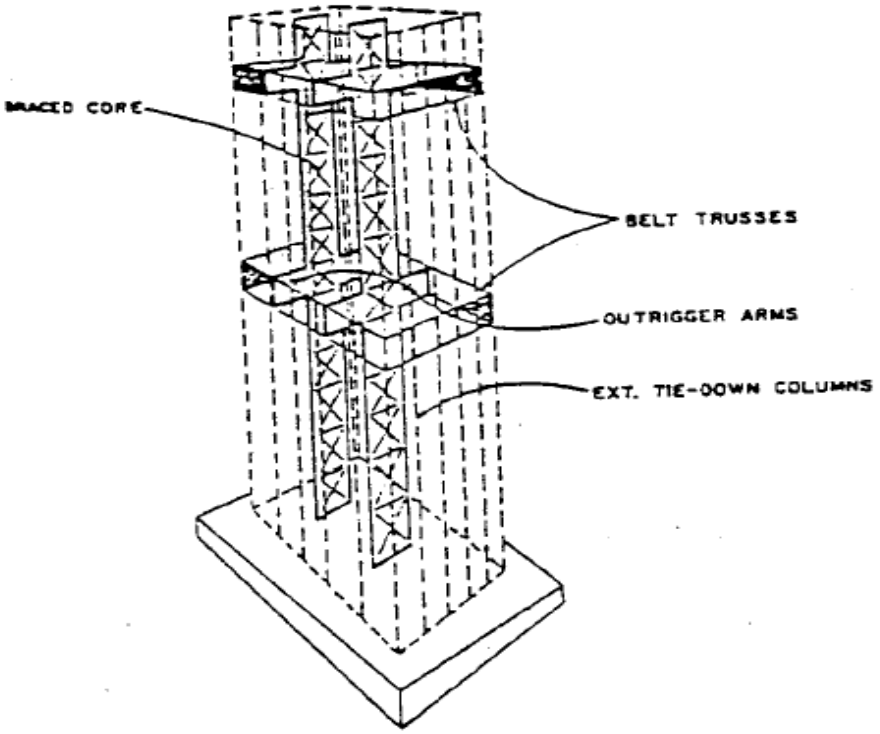

Figure 8 Outrigger-Belt truss system ref (46)

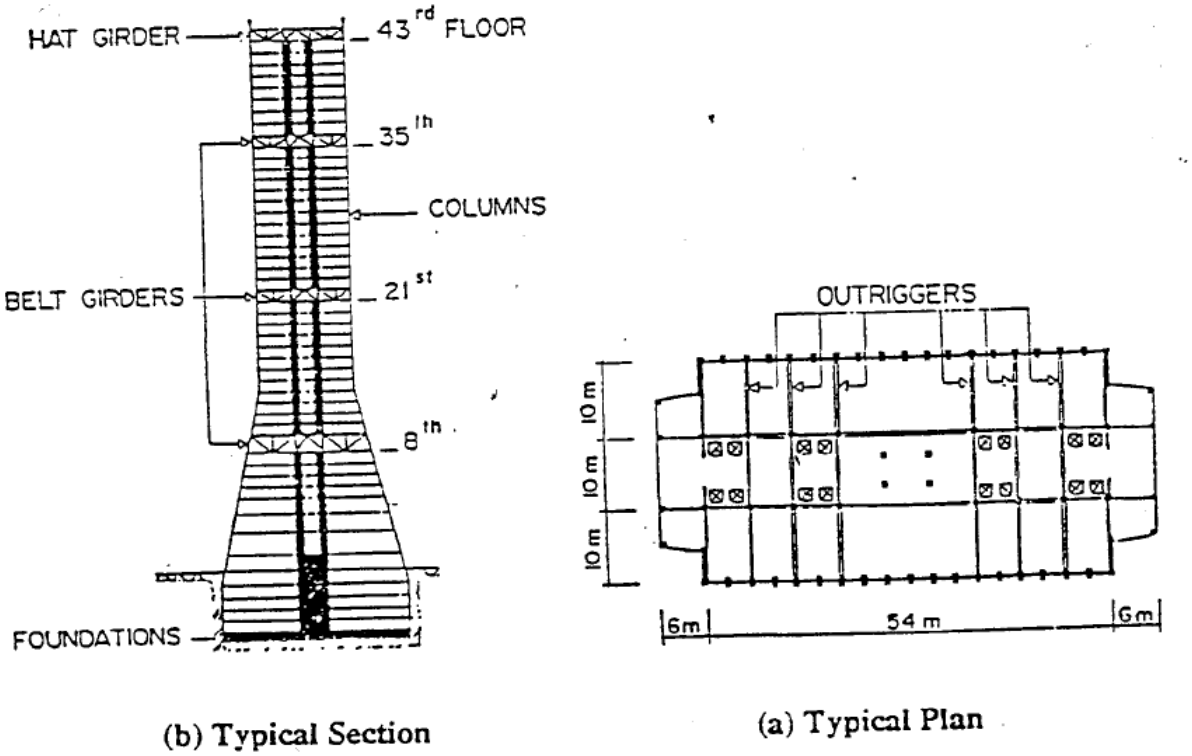

Figure 9 Yasuda building ref (47)

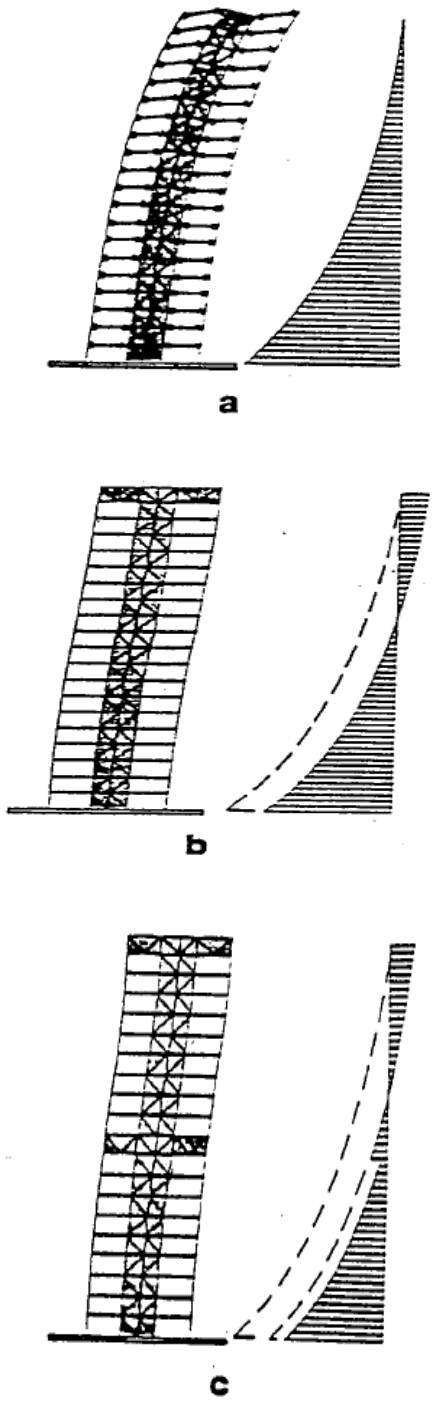

Figure 10 Behavior of Outrigger truss system ref (49)

1.2.4 Framed Tube Systems

1.2.4.1 Introduction

In both simple frames and wall-truss type structures the axial stiffness of members away from the buildings neutral axis will play a major role in reducing deflections. In framed tube systems, this idea are extended whereby the entire lateral loads resisting system is located at the building perimeter forming a perforated tube ref (25). The framed tube efficiency in resisting lateral loads also results from the use of deeper spandrel beams and shorter spans.

The framed tube itself was the original application of the tubular concept. The bundled tube developed as a means of creating "modular" space.

1.2.4.2 Framed Tube

The framed tube system consists of closely spaced exterior columns, (usually between3& 10 feet) tied at each floor level with deep spandrel beams (usually 2-5 feet) ref (29). See Figure 11. An important criterion for efficient use of the framed tube is optimization of the opening sizes and relative column and girder stiffnesses ref (29). The framed tube allows the core framing to be constructed independently therefore the exterior can be constructed while the interior layout is being finalized. Mullions and additional framing for cladding and window arrangements are eliminated if the window system is incorporated in the perforated tube. Also, prefabricated steel "structural trees" can be utilized to speed erection.

The tube system resists lateral forces three dimensional through the axial stiffness of the exterior columns on the "flange" sides and the bending of beams and columns on the “web" sides. Due to the flexibility of the web sides of the frame a shear lag effect is produced which

increases corner column stresses and reduces the cantilever efficiency. Al so differential column shortening due to the proximity of the columns to the exterior must be considered in the final design. Figure 12 illustrates the shear lag effect in a framed tube. Approximate analysis methods such as the equivalent orthotropic tube of Coull ref (52), utilized in Chapter V recognize this behavior and further applications of the framed tube were developed to limit the shearing effect. This system was first used for the Dewitt-Chesmut apartment Building in Chicago in 1963. It has been used successfully in buildings up wards of 70-80 stories including the 82 story Standard Oil of Indiana Building ref (31).

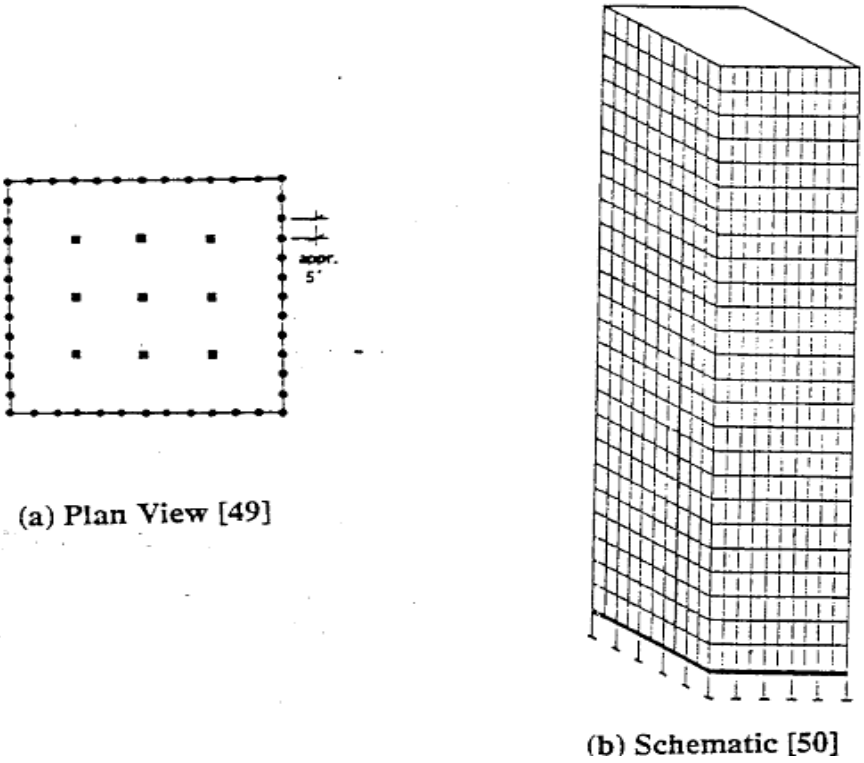

Figure 11 Framed tube structure ref (49), and (50)

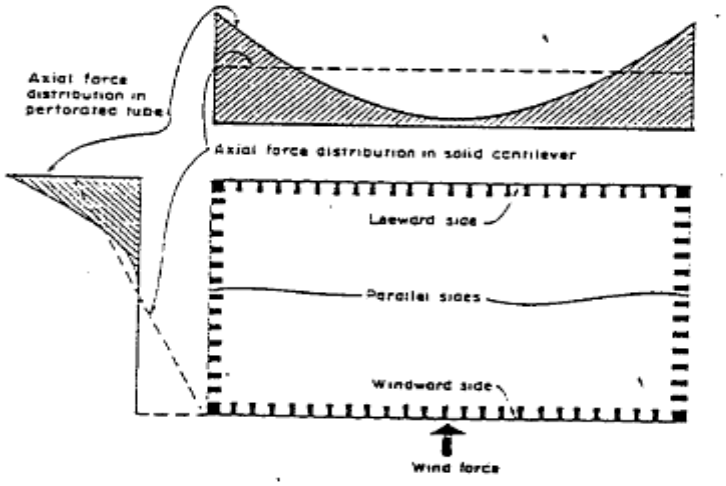

Figure 12 Shear lag effect in framed tube ref (1)

1.3 Tall Building Design Approach

The design procedure can be considered composed of two pans - functional design which assures adequate working areas, provides for HVAC, transportation facilities, mechanical systems and aesthetics and structural framework design which is the selection of member proportions in an adequate arrangement to carry service loads ref (16). This work is primarily concerned with the structural framework design and specifically the preliminary analysis of candidate structural systems.

The tall building design process (although this also applies in less detail to most types of structures) can be summarized in five major phases:

1. **Planning**. Owner, architect and principals of the design team establish functions for which the structure must serve. Building use areas and major building parameters are determined.

2. **Preliminary Structural System Selection.** This involves establishing, (in conjunction with local code) vertical, wind, and earthquake loads and subsequently an approximate indication of moments, shears, and dynamic properties of the structure ref (58).
Wind tunnel tests may be required. Fundamental criteria for strength, stability, serviceability, human comfort, (in extremely tall buildings), and acceptable damage levels are required. Using the information above preliminary member sizes can be established for each particular structural system considered for further study.

3. **Preliminary Analysis and Evaluation.** This stage involves iterative application of tools such as Wall_Frame_2D and Outrigger_Program, (See Chapters II and III) to assess drift levels and distribution of lateral loads until satisfactory member sizes and proportions are realized.

For steel structures the structural engineer is concerned with least weight of structural steel per square foot of usable building space. Each system(s) can now be evaluated as a plausible candidate for optimization. Figure 13 presents preliminary design in more detail.

4. **Optimization.** This involves extensive design optimization studies of substructures, usually four to five floor sub-systems for gravity and lateral loads ref (3).Parametric examination of girder, column and/or bracing proportions are undertaken to minimize drift vs. steel weight. In symmetrical buildings planar bents can be studied. Economic constraints often dictate the degree of optimization undertaken by the structural engineer. Steps 3 &4 may be repeated several times. Concrete systems will require more iteration due to self-weight constraints.

5. **Final** Analysis. Here extensive two and three dimensional computer analyses using programs such as SAP2000 and STRUDL are utilized for final assessment of drift and stress levels. Inelastic dynamic analysis, for lateral time dependent loads may be required for odd shaped plans. Fabrication and erection considerations are addressed during final design. The steps above outline a very complex procedure. The design team is interested in designing a building that will provide a suitable environment for its intended use and often it is non-structural parameters that control the final outcome.

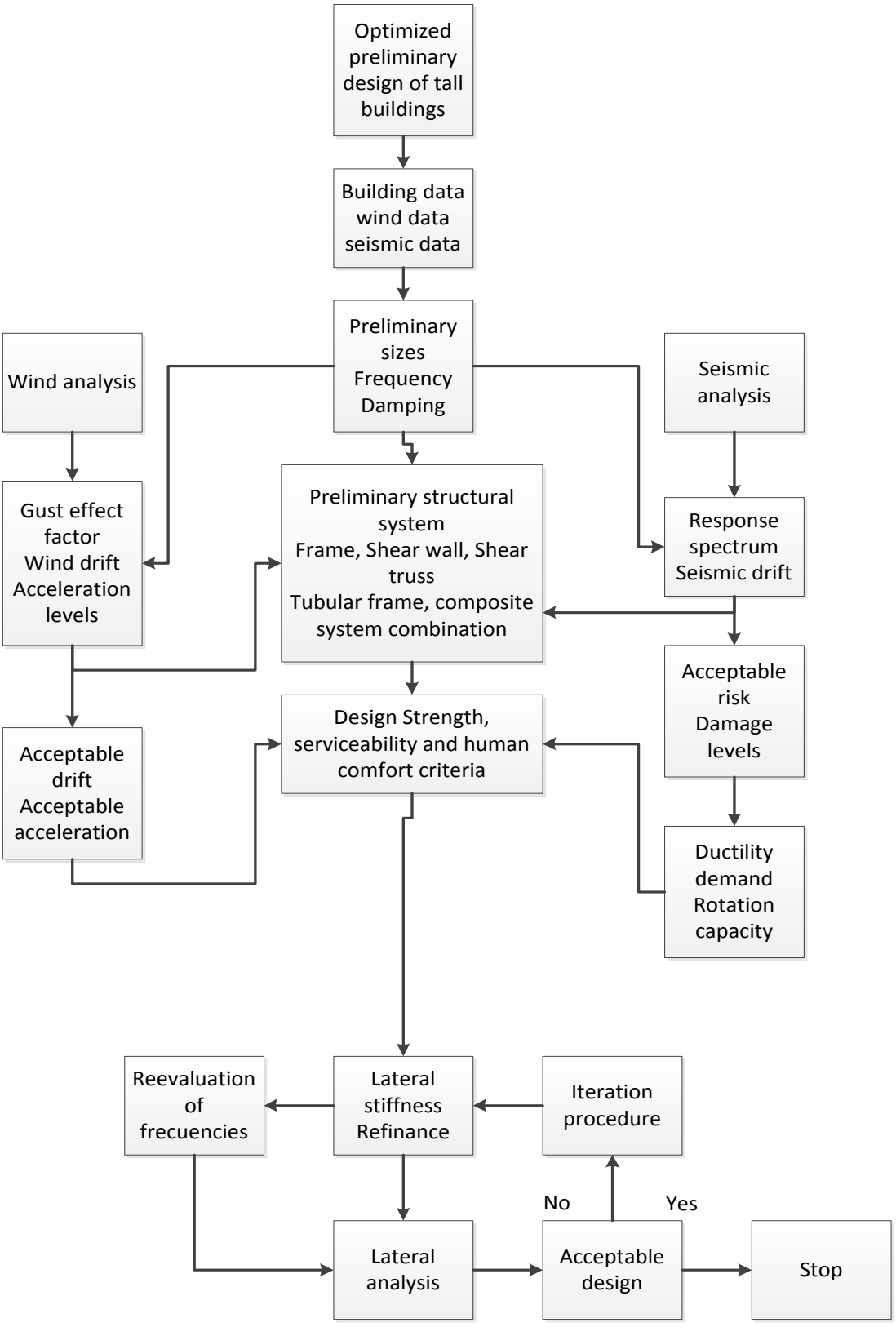

Figure 13 Methodology of preliminary design ref (58)

1.4 Knowledge Based Expert Systems

1.4.1 Introduction

Expert Systems, also called Knowledge Based Systems, (KBS), instruct computers to perform tasks with the knowledge and intuition of human experts. In this way problems without any rigid solution process can be solved. By organizing knowledge into a sophisticated "Knowledge Base" of patterns and rules, expert systems allow computers to act as intelligent assistants whereby the user need not possess a complete knowledge of the subject matter to perform design tasks ref (60). Unlike conventional computer programs which rely on algorithmic schemes using strict languages such as C++, a KBS incorporates the ability to utilize heuristic knowledge bases.

The knowledge based approach has been applied to design of concrete columns ref (61), and many non-structural problems ref (62). HI-RISE is an example of an expert system developed for design of rectangular commercial or residential buildings ref (12). The detailed discussion of expert system techniques is out of the scope of this project. Following is a discussion of the application of a KBS for tall building design and how the algorithmic programs introduced within will fit into the knowledge based design scheme.

1.4.2 A Knowledge Based System for Tall Buildings

The knowledge of tall building engineering is both heuristic, (i.e. the knowledge of recognized experts), and algorithmic, that based on structural mechanics principles. The latter is considered "deep" knowledge and is most prevalent in the industry. Heuristic knowledge is best represented symbolically whereas algorithmic procedures are primarily numerical.

A KBS for tall building design would incorporate this knowledge (heuristic and algorithmic), into Knowledge Modules (KMs) manipulated by a controlling mechanism which would identify which knowledge base to execute at a particular time in the solution process. Figure 12 defines the Knowledge Modules proposed by Connor, Jayachandrali, and Sriram for a KBS approach to tall building currently in development at WPI and MIT ref (3).

The implementation of this approach categorizes the KMs into three levels briefly described below ref (3):

1. **Strategy** Level KMs such as the controller in Figure 12

2. **Specialist** Level KMs which perform individual tasks that contributes to the solution. Examples include the Conceptualized and the Preliminary Sizer and Analyzers.

3. **Resource** Level KMs which provide for algorithmic analyses and contain primarily deep knowledge. Computer programs UNSWFS, NUSWFS and FRMTUB previously developed at WPI are examples of Resource Level KMs. The Resource Level KMs developed herein function as individual "preliminary Analyzers" for various lateral load resisting structural systems but can also be used for preliminary sizing of individual structural elements. Most importantly the Resource Level KMs provide the building response data, (deflections, shears, moments, etc.), required by the Preliminary Global Evaluator to rank the candidate systems based on structural feasibility.

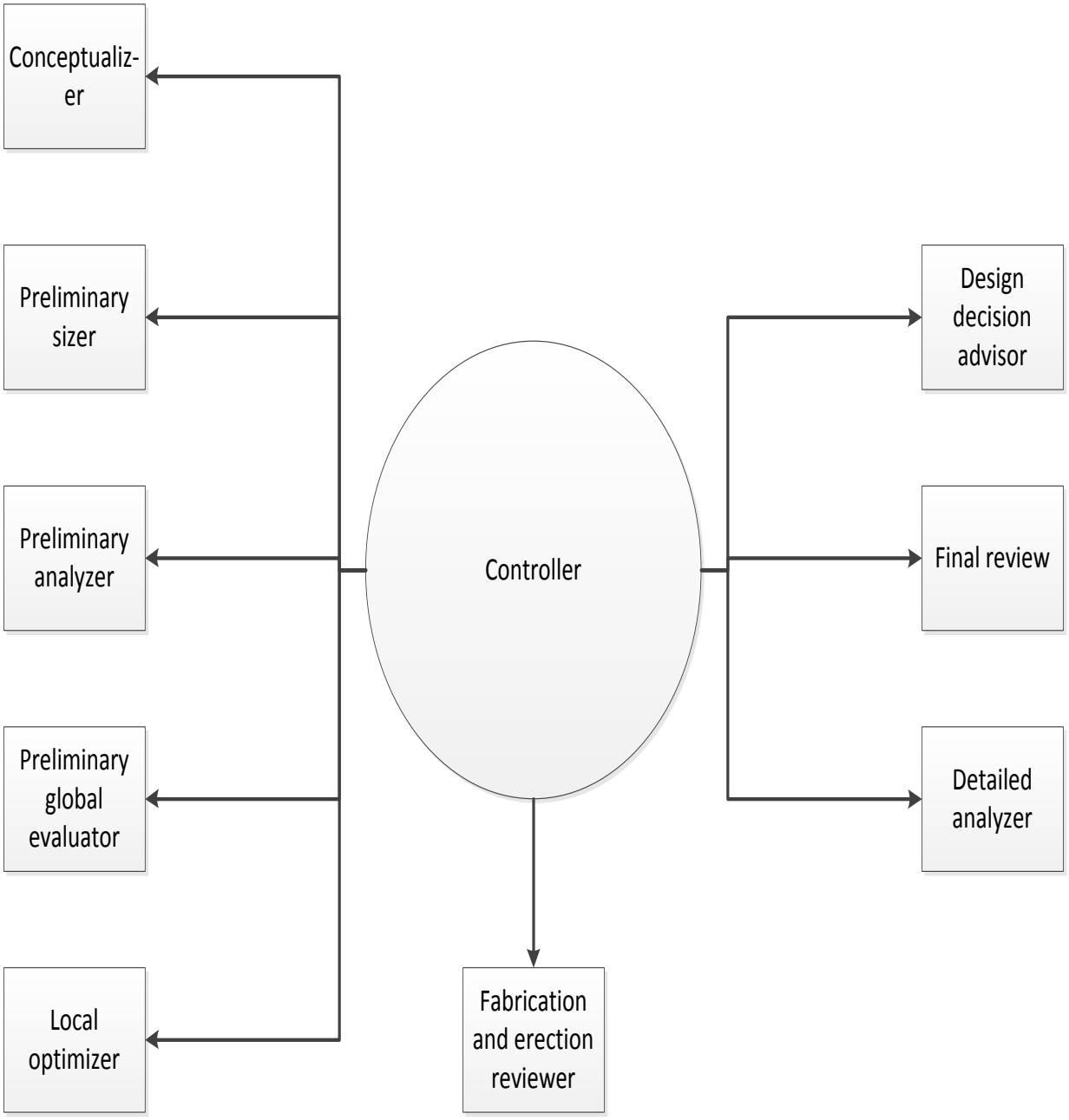

Figure 14 Knowledge modules ref (3)

1.5 Statement of Problem

Tall building knowledge is currently limited to a select group of consulting firms. Development of a KBS for tall building design that incorporates all types of buildings would allow for diffusing this knowledge throughout the industry.

Computer programs which analyze tall buildings based on continuum techniques and closed form solutions would allow designers to observe macroscopic behavior and subsequently allow parametric studies. Graphical displays would provide immediate indication of response patterns. Output from these programs could be used in an integrated tall building analysis and design program.

Herein four such computer programs are presented for preliminary design of shear wall-frame interactive buildings in two and three dimensions, outrigger braced tall buildings and framed and bundled tube structures.

The implementation of these knowledge modules and their potential uses in developing preliminary designs for candidate structural systems for typical building projects are examined. Future research would examine ways of incorporating this Resource Level Knowledge Modules in the Knowledge Based Expert System (KBES) being implemented at WPI and MIT under the direction of Professors Jayachandran and Jerome Connor. An industrial advisory group consisting of Dr. Joseph Colaco, Hal Iyengar, Robert Macnamaraand others will give expert advice on the actual use and verification of this KBES for the preliminary design and analysis of tall buildings.

1.6 Objectives of Study

The objectives of this study are as follows:

1. To gain Knowledge about the behavior of various tall building lateral load resisting systems.

2. To learn about the preliminary design methods used to analyze these various systems.

3. To study these approaches in order to subsequently provide computer programs for use by practicing engineers and the student of tall buildings in the preliminary analysis and design of tall buildings, and study of tall building behavior respectively.

4. To provide the student of tall buildings a synopsis of tall building systems, the tall building design approach, and computational approaches to tall building design.

5. To provide an insight on applying the output of these resource level KMs to show how knowledge based approach can be used for analysis and design of tall buildings.

6. To develop Resource Level Knowledge Modules for the approximate analysis and preliminary design of the following types of tall buildings:

I. Planar (2-D) shear wall-frame buildings

II. Multi-outrigger braced tall buildings with or without belt trusses

III. Framed tube structures

7. To develop computer graphics for the post-processing of data from the Resource level Knowledge Modules.

II. SHEAR WALL AND TRUSS-FRAME INTERACTION 2-DIMENSIONAL ANALYSIS

2 Introduction

When vertical elements are arranged symmetrically in the building plan individual bents in the structure can be analyzed, (for symmetrical loading cases), to represent the entire buildings response to lateral loadings. Shear walls and vertical trusses respond similarly to lateral loads, (see Figure 7), and although methods exist which analyze frames combined with shear *trusses* exclusively ref (64), and (65), the literature review herein will discuss methods of analyzing shear *wall-frame* structures in two dimensions only. A method for adapting vertical shear trusses to these methods will be discussed in Section 2.2.

Existing approximate analysis techniques consist of iterative (66), and (5), simplified matrix methods, ref (67), (68), (69), (70), and (72), and differential equation approaches, ref (73), (74), (75), and (77), All are of various degrees of complexity and usefulness. The reader is referred to extensive literature reviews for a complete bibliography ref (78), (79), and (44).

Section 2.1 will provide a cursory review of several of these methods and discuss in more detail those of Rosman ref (80) a plane frame approach ref (44), and Coull's approach to coupled shear walls. The shear-flexural cantilever analogy as interpreted by Heidebrecht and Stafford Smith ref (11) will be presented in Section 2.2. This method was used as the basis for computer program Wall_Frame_2D. The program analyzes uniform shear wall-frame structures and applies a subroutine to determine equivalent uniform properties for analysis of non-uniform structures. The program is capable of graphical displays of lateral drift and distribution of shears and moments between the wall and frame components. Results

fromWall_Frame_2Dwill be compared to those of NUSWFS ref (63) for a 30 story concrete building and SAP2000 for a 60 story steel building.

2.1 Literature Review

When the frame portion of a structure consisting of shear walls and a frame is capable of making a significant contribution to lateral stiffness or the system is constructed deliberately for interaction it will be necessary to assess the distribution of forces between the wall and frame components. Assuming the wall sustains all the load is not conservative because shear walls with openings may behave in a shear mode (see Figure 18b) and conversely frames with rigid in fills may behave in a flexural mode ref (81). Methexls to determine accurate load distribution are discussed below.

The method of Khan and Sbarounis is an iterative technique. It provides for axial deformation of columns, variation of properties with height, and points of contra flexure not at column mid-height. Provisions also exist to account for non-rigid foundations ref (66). The analysis is performed in two stages. First the deflected shape and the amount of lateral load distributed to the walls and frames respectively is determined. The authors then divide the structure into separate wall and frame systems and apply a repeated force fitting analysis until the deflections and rotations of the wall system converge. After convergence of the iteration solution the final deflected shape of the structure is used to distribute moments and shears to every member in each bent of the structure ref (66). The influence charts presented for an equivalent ten story structure can be used to expedite design.

Design charts are also provided by Parme ref (68). This procedure relates the total load at each floor level to the displacements of that floor and those floors immediately above and

below it For every level an equation is written in terms of the relative stiffnesses of the columns, girders, and shear wall and the applied loading ref (68); a series of simultaneous equations results. Axial deformation is neglected and floors are considered rigid in plane such that all columns and shear walls translate equally at each level. Although shear walls do not have to start at the base level, an -average shear wall stiffness is required for non-uniform structures.

Clough, King, and Wilson ref (67) developed a simplified matrix method for analyzing frames with or without shear walls included in the plan. Each story stiffness matrix is combined to obtain a stiffness matrix for each frame. Each frame stiffness is superimposed to obtain the total building stiffness in tri-diagonal form ref (67). Recursive relationships are used to eliminate the vertical and rotational terms. This results in a lateral stiffness matrix with only one degree of freedom per story for each frame. The lateral displacements are solved for simultaneously using Gaussian elimination.

The plane frame approach can be applied to a shear wall-frame structure provided floors can be modeled as rigid in their own plane and torsion can be neglected i.e., symmetric structures and loading ref (44). Figure 13 illustrates the idealization of the structure for plane frame analysis. Understanding of the principles of this approach is essential for structural designers of tall buildings. Here the vertical elements are connected by link elements which represent the rigid floor slabs.

Axial deformation of beams may be neglected but neglecting axial deformation of columns can be critical for tall, slender structures. Equations 1 and 2 can be used to assess column deformation contribution (44).

$$\Delta_a = \frac{WH^3 F_n}{E_c A_c B^2}$$ Equation 1

Where: Δ_a = deflection at top of frame due to axial deformation of exterior columns

F_n= function of n, dependent on type of loading

n= area of exterior column at top of frame divided by the area of exterior column at bottom of frame

A_c= area of exterior columns at first story level

B= total width of frame

E_c= Young's modulus of elasticity of columns

$$\Delta_b = \frac{Wh^2 H}{12\sum(E_c \mathrm{I}_c)}\left(F_s(1-\beta_d)^3 + 2\lambda F_g(1-\beta_c)^3\right)$$ Equation 2

Where: Δ_b= deflection at top of frame due to bending of members

W = total lateral load, h= story height, H= total building height

I_c= column moment of inertia at first story level

I_b = moment of inertia of beam at bottom of the structure

F_s,F_g= functions of s and g respectively

s= I_c at top of frame / I_c at bottom of frame

g= I_b at top of frame / I_b at bottom of frame

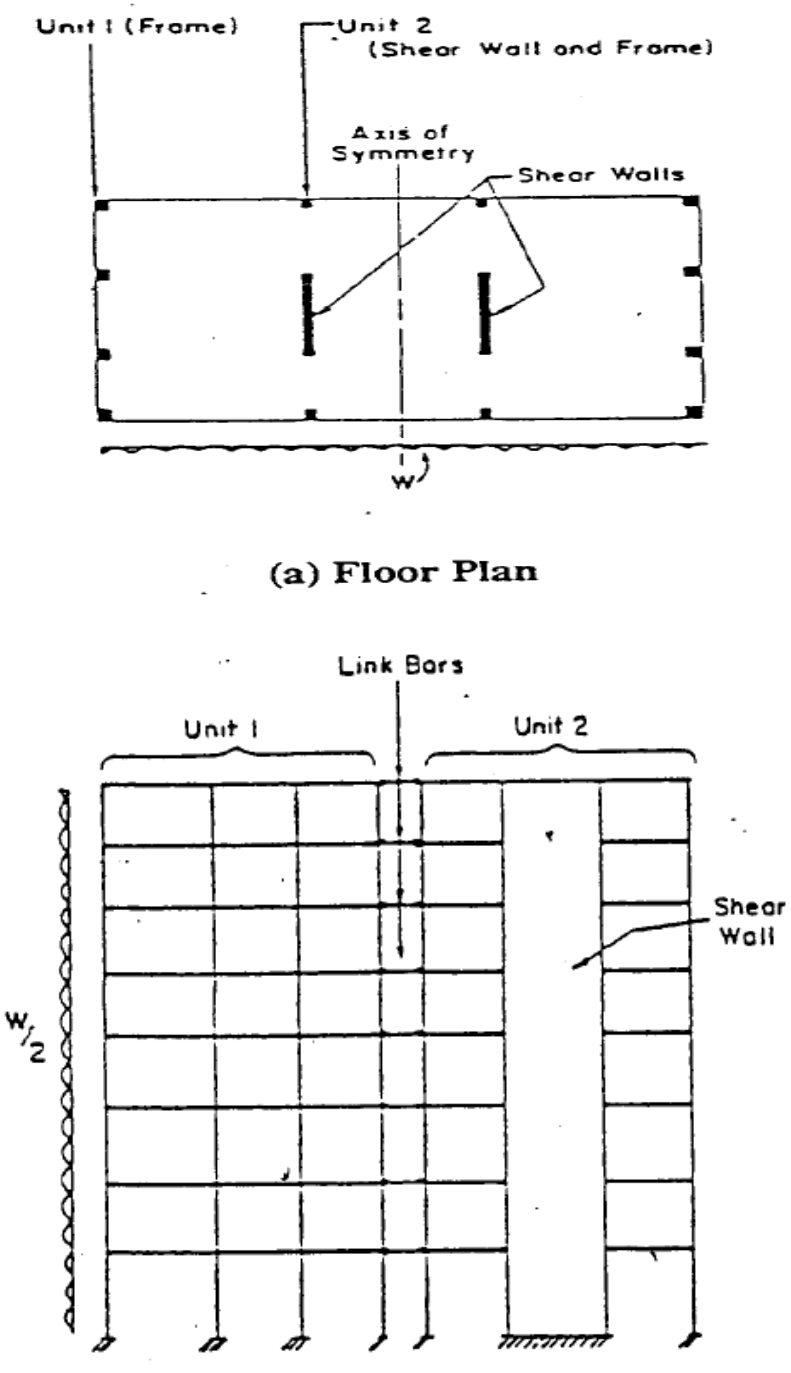

Figure 15 Idealization for plane frame analysis ref (44)

B_d= D/h, where D is beam depth

B_c= c/l, where c is column width and I is the distance between column center lines

$$\lambda = \frac{\sum\left(\frac{E_c \mathrm{I}_c}{h}\right)}{2\sum\frac{E_b \mathrm{I}_b}{l}}$$ i.e., summation over width of structure at first story level

Many bays can be lumped together to save computer memory, but only if axial deformation is neglected ref (44). In order to account for finite widths of shear walls and depths of beams eq. 2 can be used. The resulting model (Figure 13 b) can then be analyzed using standard plane-frame analysis programs.

In contrast to the methods above Cardan ref (82) applies a differential equation formulation to the problem. He assumes that lateral loads and reactions from parallel frames connected to a shear wall can be continuously distributed along the full length of the wall. Properties of the walls and frames are assumed constant. Conditions of equilibrium of external and internal forces lead to a single second order differential equation. Solutions for standard load cases are presented.

Gould ref (83) suggested a method of distributing lateral loads between shear walls and frames based on deformation compatibility. Each story of the frame is represented as an elastic spring connected to the shear wall at each floor by a rigid bar and a rotational spring, and connected to each of the adjacent floors through a rigid joint Spring constants for each floor depend on the location of the shear walls in the plan. A finite difference equation is used to solve for the displacements.

An early application of the shear-flexure cantilever analogy to be discussed in Section 2.2were utilized by Rosman ref (80).He applies the subgrade modulus of the soil to allow for flexibility at the foundation level. Floors are assumed rigid in plane and all building properties are assumed constant throughout the building height. The wall is assumed to act as a cantilever beam and its flexural stiffness is denoted by:

$$K_w = E\mathrm{I}$$ Equation 3

Frame stiffness (shear stiffness of the shear cantilever) is denoted by:

$$K_s = \frac{12E_R \sum \mathrm{I}}{h^2\left(1+\left(\frac{2\mathrm{I}l}{\bar{\mathrm{I}}h}\right)\right)}$$ Equation 4

Where: ∑I= sum of all moments of inertia of columns in the frames

E_R= modulus of elasticity of frame material, h= story height

l, I, $\bar{\mathrm{I}}$ = span and moments of inertia of the columns and of the beams with stiffness coefficients equal to one

The foundation stiffness is given by:

$$K_B = 2c\mathrm{I}_B$$ Equation 5

Where: I_B= moment of inertia of the base of the footing of the wall

c= soil sub grade modulus for axial compression

The Rosman substitute system is shown in Figure 14.A free body diagram of the substitute system is shown in Figure 15. Equilibrium of horizontal forces on the upper part of the system requires that:

$$M' + T = \eta \quad \text{Equation 6}$$

Where: η = total shear at an arbitrary cross section of the system

T= shear in the shear cantilever, M'= shear force in the flexural cantilever

Using eq. 6 the complementary energy of the system is determined to be [80]:

$$\cup = \int_0^H \left(\frac{M^2}{2K_W} + \frac{(\eta - M')^2}{2K_S} \right) dx + \frac{(M_H)^{23}}{2K_B} \quad \text{Equation 7}$$

The Subscript H denotes the base of the building. By applying the calculus of variations to eq. 7 the governing differential equation of the substitute system is determined to be:

$$M'' - \frac{K_S}{K_W} M = w \quad \text{Equation 8}$$

Where: M, M"= moment in the flexural cantilever as a function of x and the second derivative of M with respect to x respectively.

w= magnitude of distributed lateral load per unit height

The corresponding boundary conditions are:

$$M'_H + \frac{K_S}{K_W} M_H = \eta_H \text{ at x=H and } M_O=0 \text{ at x=0} \quad \text{Equation 9}$$

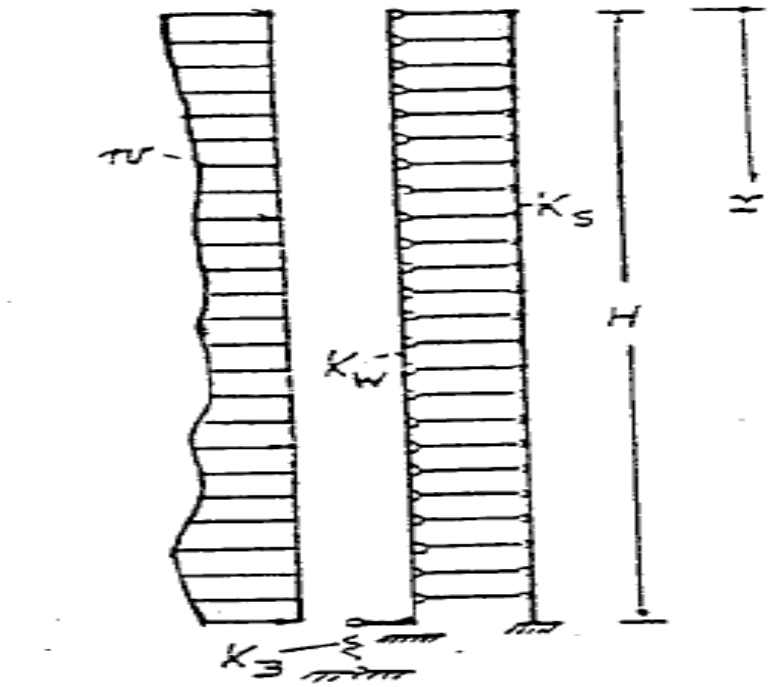

Figure 16 The Rosman substitute system ref (80)

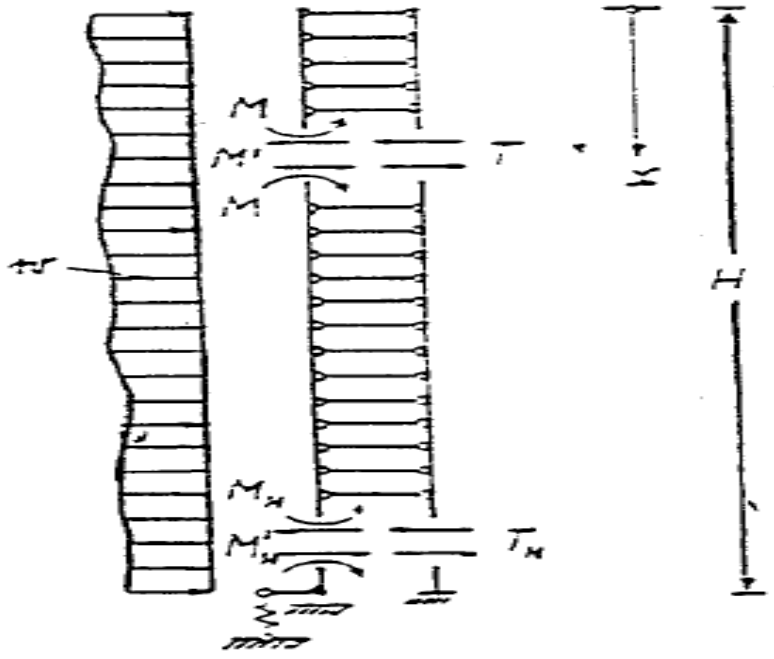

Figure 17 Free body diagram of Rosman system ref (80)

The problem is solved by determining the equation of the bending moment which satisfies equations 8 and 9 ref (80).

As previously stated regular openings in shear walls can result in frame deformation of the shear walls depending on the stiffness of the connecting beams. A shear-flexure analogy would be subsequently invalid unless the wall was considered a section of frame. A brief review of approximate coupled wall theory is provided to give the user of Wall_Frame_2Da method to accommodate them into the analysis. Figure 16 a shows a typical coupled shear wall and Figure 16 b shows its deflected shape.

To analyze the coupled shear wall structure the individual connecting beams of flexural Stiffness EI_p are replaced by an equivalent continuous medium (lamina) of stiffness EI_p/h per unit height [84]. Since it is assumed that the connecting beams do not deform axially the walls deflect equally with a point of contra flexure at mid-span of the connecting beams. When the laminas are cut at their midpoints a shear force of q per unit length acts along the cut sections. By considering compatibility conditions the following second order differential equation results ref (84):

$$\frac{d^2\mathrm{T}}{dx^2} - \alpha^2\mathrm{T} = -\beta x^2 \quad \text{Equation 10}$$

Where $\mathrm{T} = \int_0^x q dx$ is the integral of the shear force in the continuous connection from the top of the wall to point x and

$$\alpha^2 = \frac{12\mathrm{I}_p}{hb^3}\left(\frac{l^2}{\mathrm{I}} + \frac{\mathrm{A}}{\mathrm{A}_1\mathrm{A}_2}\right)$$

$$\beta = 0.5wl\left(\frac{12\mathrm{I}_p}{hb^3}\right)\frac{l}{\mathrm{I}}$$

With $I = I_1 + I_2$ and $A = A_1 + A_2$

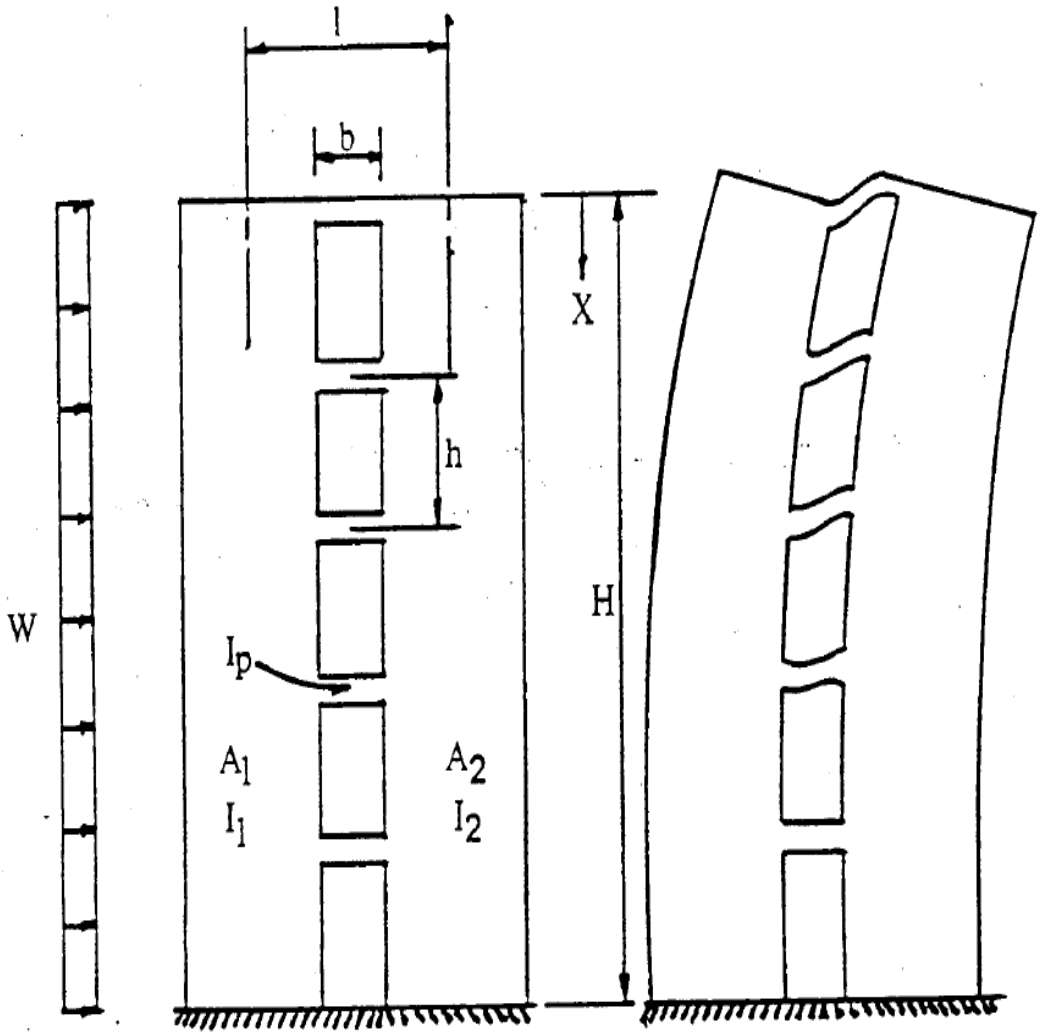

Figure 18 Coupled shear wall system ref (80)

A study by Marshall Ref (85) indicated that when α H>13 the walls may be considered a single homogeneous cantilever. When α H<O.8 the two walls can be considered separately and when 0.8< α H<13 the stiffness of the connecting beams should be considered ref (79). In this case a frame analogy can be applied ref (89). Additional loading conditions ref (86), coupled shear walls of variable thickness ref (87), and cross section ref (88) can also be addressed. For shear walls with two vertical rows of openings the tables of Schwaighofer and Tai ref (102) can be used for preliminary design.

2.2 The Shear-Flexural Cantilever Beam Analogy

The shear-flexural beam analogy can be utilized for analyzing structures that rely on Shear wall or braced frame interaction with a moment resisting frame for lateral stiffness (shear wall and braced frame are considered interchangeable for this discussion). Based on the dominant behavioral modes of the shear wall and frame shown in Figures 7b and 7a respectively, the shear wall is assumed to act as a flexural cantilever with infinite shear stiffness and the frame as a shear cantilever with infinite flexural stiffness. By forcing compatible deflections at each floor level the deflected shape of Figure 7c results. Rosman's approach discussed in Section 2.1 is an early application of this method but he assumes that interaction only occurs when base rotation is present.

Heidebrecht and Stafford Smith developed the shear-flexural analogy for symmetrical structures and solved the governing differential equation in closed form ref (11). From beam theory the governing differential equation for the flexural cantilever is:

$$\mathrm{EI}\frac{d^4 y_B}{dx^4} = w_B(x) \quad \text{Equation 11}$$

Where: EI= flexural stiffness at height x above the base

$\frac{d^4 y_B}{dx^4}$ = Fourth derivative of deflection of beam at height x

$W_B(x)$ =distributed load resisted by the flexural beam

And for the shear cantilever the governing equation is:

$$-GA\frac{d^2 y_S}{dx^2} = w_S(x)$$ Equation 12

Where: GA= equivalent shear stiffness at height x

$\frac{d^2 y_S}{dx^2}$ = Second derivative of deflection of shear beam at height x

$W_S(x)$=distributed load resisted by shear beam

The flexural stiffness EI is equal to the modulus of elasticity, E, times the moment of inertia, I, of the shear wall. For a bent with several shear walls the EI parameter is simply the summation of all the EI terms. The designer should be cautioned however that this is only valid when the shear walls interact through the direct horizontal action of rigid "linkbeams" which negate any possibility of bending interactions through the connecting beams.

Section 2.1 gives some rules of thumb for approaching coupled walls. Finite element methods can also be used to determine I (inertia) although these may defeat the purpose of approximate analysis ref (92), and (93). For un perforated walls I is calculated from $I= (1/12)bH^3$ where b is the wall thickness and H equals the width parallel to the load.

The moment of inertia of a braced frame can be approximated using simple statics and the truss efficiency factors developed by Iyengar ref (29). For a frame with n columns:

$$I = \sum_{i=1}^{n} I_i + E_f \sum_{i=1}^{n} A_i d_i^{\,2}$$ Equation 13

Where: $\sum I_i$= sum of the individual. Moments of inertia of the columns about an axis normal to the applied load

$A_i d_i$ = area of column i times the distance d from the centroid of the truss to the

Centroid of column i

E_f=truss efficiency factor (0.9 for X-bracing, el.8 for K-bracing, 0.7 for partial

K-bracing)

The equivalent shear stiffness, GA, of the frame portion is defined as the inter story shear force required to give a unit horizontal shearing deformation over the one story height. Rigid joint sizes and shearing deformations of individual elements are neglected. See ref.(136) to allow for shearing deformations of the frame components. Figure 17a shows a one story frame segment of story height h. If a unit shearing force P is applied resulting in as hearing deformation Δ, and points of contra flexure are assumed at mid-span of the beams a single column line segment can be represented by Figure 17 b. I_{b1}, b1 and I_{b2} , b2represent the moments of inertia and spans of the beams on either side of a column of moment of inertia I_c From the force-deflection relationship of the column the shearing stiffness is given by:

$$GA = \frac{12EI_c}{h^2} \frac{1}{\left(1 + \frac{2I_c}{h\left(\frac{I_{b1}}{b1} + \frac{I_{b2}}{b2}\right)}\right)}$$ Equation 14

The total GA parameter for the frame is the sum of the GA terms for all the columns in a single column line. For exterior columns an adjacent beam I is set equal to zero. Section2.3.2 discusses an application of eq. 14 to frames of varied column and girder sizes.

The floors are assumed rigid in plane and no twisting of the floor plan is allowed. If the shear and flexural beams are considered linked along their heights a uniform interactive force of q(x) and a concentrated force Q at the top of the structure are required for equilibrium. The floor diaphragms are modeled as rigid links as in the plane frame analogy of Section 2.1. The governing differential equations of the shear-flexural beam are ref (11):

$$\mathrm{EI}\frac{d^4y}{dx^4} = w_B(x) + q(x) \quad \text{Equation 15}$$

$$-GA\frac{d^2y}{dx^2} = w_S(x) - q(x) \quad \text{Equation 16}$$

Adding eq. 15 and 16 and dividing by EI gives:

$$\frac{d^4y}{dx^4} - \alpha^2\frac{d^2y}{dx^2} = \frac{w(x)}{\mathrm{EI}} \quad \text{Equation 17}$$

Where $w(x) = w_B(x) + w_S(x)$ and $= \alpha^2 = GA/EI$.

The solution of eq. 17 for a uniformly distributed load of magnitude W_0 is:

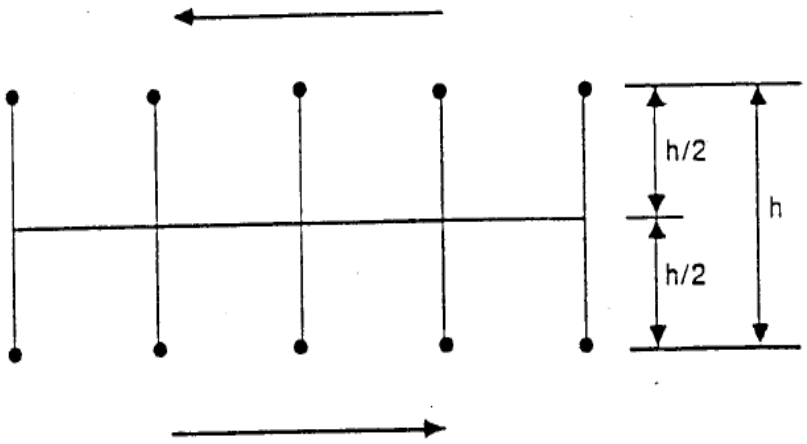

(a) One-story Frame Segment

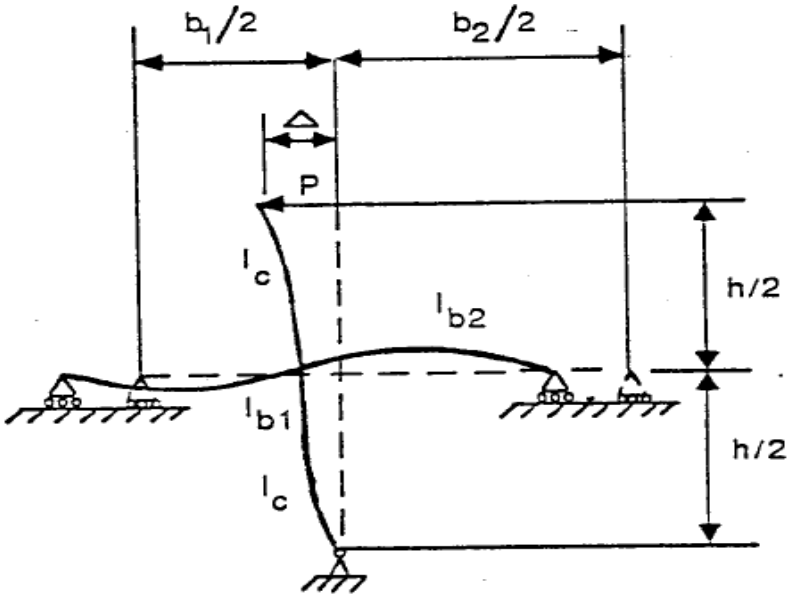

(b) Horizontal Deformation In One Column In Frame

Figure 19 Shear behavior in frame ref (11)

$$y(x) = C_1 + C_2 x + C_3 \cosh \alpha x + C_4 \sinh \alpha x - \frac{W0x^2}{2\mathrm{EI}\alpha^2}$$ Equation 18

The constants C1-C4 are determined from the following boundary conditions [11]:

(a) At the fixed base displacement and slope equal zero i.e. at x=0, y(0)=0 and y'(0)=0

(b) At the free end total moment and total shear equal zero i.e. at x=H,

$M(H)= M_B(H) + M_S(H)= 0$, $S(H)= S_S(H) + S_B(H)= 0$

$M_B(H)$ and $M_S(H)$ equal zero independently from statics. Substituting the expressions

For M_B, $Ss_{,\text{ and}}$ S_B from beam theory gives :

$$\mathrm{M}_B(\mathrm{H}) = \mathrm{EI}\frac{d^2y}{dx^2}(\mathrm{H}) = 0$$ Equation 19

And

$$S(\mathrm{H}) = GA\frac{dy}{dx}(\mathrm{H}) - \mathrm{EI}\frac{d^3y}{dx^3}(\mathrm{H}) = 0$$ Equation 20

Upon evaluating the constants of integration eq. 18 becomes:

$$y(x) = \frac{W0\mathrm{H}^4}{\mathrm{EI}(\alpha\mathrm{H})^4}\left[\left(\frac{\alpha\mathrm{H}\sinh(\alpha\mathrm{H})+1}{\cosh(\alpha\mathrm{H})}\right)(\cosh(\alpha x)-1) - \alpha\mathrm{H}\sinh(\alpha x) + (\alpha\mathrm{H})^2\left(\frac{x}{\mathrm{H}} - \frac{1}{2}\left(\frac{x}{\mathrm{H}}\right)^2\right)\right]$$ Equation 21

Subsequently for the case of uniformly distributed load the equations for shears, moments, and the interactive force q as a function of the distance from the base, x, are as follows:

$$\mathrm{M}_B(x) = \frac{2\mathrm{M}_O}{(\alpha\mathrm{H})^2}\left(\left(\frac{\alpha\mathrm{H}\sinh(\alpha\mathrm{H})+1}{\cosh(\alpha\mathrm{H})}\right)(\cosh(\alpha x)) - (\alpha\mathrm{H}\sinh(\alpha x) - 1)\right)$$ Equation 22

$$\mathrm{M}_S(x) = \mathrm{M}_O\left(1 - \frac{x}{\mathrm{H}}\right)^2 - \mathrm{M}_B(x)$$ Equation 23

$$S_B(x) = \frac{S_O}{\alpha\mathrm{H}}\left(\alpha\mathrm{H}\cosh(\alpha x) - \left(\frac{\alpha\mathrm{H}\sinh(\alpha\mathrm{H})+1}{\cosh(\alpha\mathrm{H})}\right)\sinh(\alpha x)\right)$$ Equation 24

$$S_S(x) = S_O\left(1-\frac{x}{\mathrm{H}}\right) - S_B(x)$$ Equation 25

$$q(x) = w_S + \frac{(\alpha\mathrm{H})^2\,\mathrm{M}_B(x)W0}{2\mathrm{M}_O}$$ Equation 26

M_O and S_O represent the total moment and shear at x=0.

The equations for shear and moment of the shear cantilever are written in terms of the total shear and moment at x and the shear and moment in the flexural cantilever. Note that $M_S(x)$ cannot be obtained directly.

To provide for a more accurate application of static wind and seismic loads, equations for a linearly distributed lateral load with a maximum magnitude W_1 at the top of the building and zero at the base (triangular loading) have been developed as well as equations for the application of a concentrated load P at the top of the structure. To do so the last term of eq. 18 is replaced by $-W_1x^3/2H\alpha^2EI$ for the triangular load case and $-PH^2/2\alpha^2EI$ for the case of a concentrated load when solving for the y(x) function. Design equations for the triangular load case become ref (11):

$$w(x) = \frac{W_1 x}{\mathrm{H}}$$ Equation 27

$$y(x) = \frac{W_1\mathrm{H}^4}{\mathrm{EI}(\alpha\mathrm{H})^2}\left[\left(\left(\frac{\sinh(\alpha\mathrm{H})}{2\alpha\mathrm{H}}\right) - \left(\frac{\sinh(\alpha\mathrm{H})}{(\alpha\mathrm{H})^3}\right) + \left(\frac{1}{(\alpha\mathrm{H})^2}\right)\right)\left(\frac{\cosh(\alpha x)-1}{\cosh(\alpha\mathrm{H})}\right) + \left(\frac{x}{\mathrm{H}} - \frac{\sinh(\alpha x)}{\alpha\mathrm{H}}\right)\left(\frac{1}{2} - \frac{1}{(\alpha\mathrm{H})^2}\right) - \left(\frac{1}{6}\left(\frac{x}{\mathrm{H}}\right)^3\right)\right]$$ Equation 28

$$\mathrm{M}_B(x) = \frac{3\mathrm{M}_O}{(\alpha\mathrm{H})^3}\left[\left(\frac{(\alpha\mathrm{H})^2\sinh(\alpha\mathrm{H})}{2} - \sinh(\alpha\mathrm{H}) + \alpha\mathrm{H}\right)\left(\frac{\cosh(\alpha x)}{\cosh(\alpha\mathrm{H})}\right) - \left(\frac{(\alpha\mathrm{H})^2}{2} - 1\right)\sinh(\alpha x) - \alpha\mathrm{H}\left(\frac{x}{\mathrm{H}}\right)\right]$$ Equation 29

$$\mathrm{M}_S(x) = \mathrm{M}_O\left(1 - \frac{3}{2}\left(\frac{x}{\mathrm{H}}\right) + \frac{1}{2}\left(\frac{x}{\mathrm{H}}\right)^3\right) - \mathrm{M}_B(x)$$ Equation 30

$$S_B(x) = -\frac{2S_O}{(\alpha H)^2}\left[\left(\frac{(\alpha H)^2 \sinh(\alpha H)}{2} - \sinh(\alpha H) + \alpha H\right)\left(\frac{\sinh(\alpha x)}{\cosh(\alpha H)}\right) - \left(\frac{(\alpha H)^2}{2} - 1\right)\cosh(\alpha x) - 1\right]$$ Equation 31

$$S_S(x) = S_O - S_O\left(\frac{x}{H}\right)^2 - S_B(x)$$ Equation 32

$$q(x) = w(x) + \frac{W_1}{3}(\alpha H)^2\left(\frac{M_B(x)}{M_O}\right)$$ Equation 33

And for a concentrated load P the design equations are given by ref (11):

$$y(x) = \frac{PH^3}{EI}\left[\left(\frac{\sinh(\alpha H)}{(\alpha H)^3 \cosh(\alpha H)}\right)(\cosh(\alpha x) - 1) - \left(\frac{\sinh(\alpha x)}{(\alpha H)^3}\right) + \left(\frac{1}{(\alpha H)^2}\right)\left(\frac{x}{H}\right)\right]$$ Equation 34

$$M_B(x) = \left(\frac{M_O}{\alpha H}\right)(\tanh(\alpha H)\cosh(\alpha x) - \sinh(\alpha x))$$ Equation 35

$$M_S(x) = M_O\left(1 - \frac{x}{H}\right) - M_B(x)$$ Equation 36

$$S_B(x) = P(\cosh(\alpha x) - \tanh(\alpha H)\sinh(\alpha x))$$ Equation 37

$$S_S(x) = P - S_B(x)$$ Equation 38

$$q(x) = PH\alpha^2\left(\frac{M_B(x)}{M_O}\right)$$ Equation 39

Since we are considering elastic material behavior only, various combinations of these three standard loading cases could be combined to represent various static wind and seismic loading requirements.

This approach is most convenient for macroscopic study of the individual component contributions. Heidebrecht and Stafford Smith ref (11) present design curves in terms of the α (alpha) parameter for the distributed loading case. Comparisons can be made for various combinations of shear wall and braced frame stiffness and by using a computer program

preliminary member sizes can be determined rapidly. The method does not include second order effects or axial deflections but these effects can be superimposed. This approach has been previously programmed on the W.P.I. main frame computer (DEC-20) by Lefrancois Ref (63).Lefrancois also applied the transfer matrix method to this approach to analyze structures of non-uniform stiffness. This program is called NUSWFS. The author presents a computer program for use on IBM compatible personal computer utilizing the shear-flexural cantilever analogy for analyzing shear wall-frame interactive structures in two dimensions in Section 2.3

2.3 Computer Program SWLFRM·2D

2.3.1 Program Description and Use

Computer program SWLFRM-2D was written to solve equations 21-25, 27-32, and 34-38 for the shear wall-frame interactive structures. The interactive force q(x) was not considered. The program was written in Matlab® graphical user interface and compiled withversion2009a.

The analysis assumes no twisting of the building is allowed. Floors must be assumed rigid in plane. The material is assumed to behave within its elastic range therefore gravity load effects can be superimposed. All building components (shear walls, trusses, or frames) must be of equal height and extend the full length of the structure. Bents with setbacks must be addressed separately [90]. The foundations must be considered rigid at the base to satisfy the boundary conditions.

The program structure consists of a main program called Wall_Frame_2D.EXE and Subroutines AlPHA.EXE to calculate the alpha parameter for uniform or non-uniform buildings.

Descriptions of the subroutines are included in Appendix A. A condensed variable list for the program is found in Section 2.3.1.1.

To start the program the user simply double clicks Wall_Frame_2D.EXE at the appropriate PC prompt, then select from the drop up menu bottom the loading case to be study, as is illustrate it in Figure 20, can be selected three different loading cases, distribute, triangular, and concentrated.

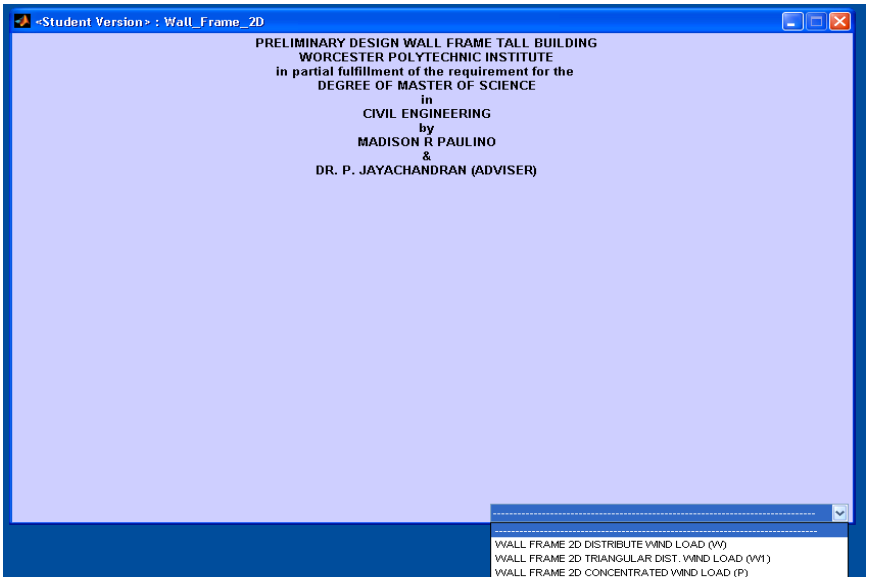

Figure 20 Wall_Frame_2D Program Loading Selection

In this program the input values can be change at any time in the screen. The required input variables are: Moment of elasticity shear wall or truss (E) in K/ft^2, Total moment of inertia of shear wall or truss (I) in ft^4, Building height (H) in ft., Number of segments for output (N), Load in k/ft., and the applicable load type distribute (W), concentrated (P), or triangular (W_1) .Only one type of load is allowed per analysis. The user has the choice of pre-calculating alpha, (in which case ALPHA is required input), or providing the input required for ALPHA program to calculate alpha.

The additional input required for the ALPHA program consists of the frame inertia of the columns, frame inertia of the girder, height of the story, number of columns in the story, number of similar story, frame material modulus of elasticity, wall/truss moment of inertia, and wall/truss material modulus of elasticity. Units must be kept consistent for reliable results.

The user has two output options, the output consists of a full input echo and the lateral deflections and shears and moments in the shear and flexural cantilevers at evenly spaced intervals along H. The user controls the fineness of the mesh with the N (number of story to study) variable. Note however that since this is a closed form solution the number of output points has no effect on the accuracy of the analysis.

2.3.1.1 Condensed Variable List· Wall_Frame_2D

Listed below is a condensed variable list for program Wall_Frame_2D.

- The Load type: uniform Distribute (W_o), Triangular (W_1), Concentrated (P)
- Uniform (W_o): Value of distributed lateral load
- Concentrated (P): Value of distributed lateral load
- Triangular (W_1): Maximum value of a linearly distributed load which has a magnitude of W_1 at the top of the building and zero at the base of the building
- Building Height (H)
- Modulus of elasticity of shear wall/truss (E)
- Flexural cantilever moment of inertia about an axis normal to the applied load
- Alpha $\sqrt{\frac{EI}{GA}}$
- Number of Segment for output (N)

2.3.2 Analyzing Buildings of Non-Uniform Stiffness

In program NUSWFS, Lefrancois (63) applied the transfer matrix method to the shear-flexure analogy to directly account for step changes in the building properties.

Although it is very useful, and provides good results, the program would require considerable input preparation for a building with many step changes. Reasonable results can also be obtained by averaging the building properties over the building height. This is easily done for monolithic shear walls and slightly more tedious for vertical trusses.

Calculating an average GA value for step changes in the frame properties by hand calculation would be most involved. Therefore the program ALPHA, has this capabilities, to allow interactive input of column and girder properties for subsequent calculation of alpha. By using this approach the user may easily analyze bents with horizontal as well as vertical step changes in stiffness. Also the user can quickly observe changes in behavior for various ratios of girder and column stiffness. The input utilized by ALPHA program is listed in Section 2.3.1.The number of levels of different stiffness and numbers of bays in the frame portion of the bent are currently unlimited.

The following rules apply to the frame input:

1. Story height is equal throughout the building.

2. Column moments of inertia are equal within each level of different stiffness.

3. The girder moments of inertia within each bay of a particular level of constant column stiffness are equal.

4. The bay widths may differ but each bay width must be constant throughout the height of the building.

5. The number of stories is equal for all bays.

The girder moment of inertia used in eq. 14 at a boundary between "levels" is that of the lower level and the column moment of inertia used there is an average between adjacent levels. For situations where exterior columns differ from interior columns an average column moment of inertia can be used with sufficient accuracy.

2.3.3 Description of Graphics

Graphical displays have obvious advantages over hard copy of data. The component contributions of the shear-flexural beam can be instantly assessed for reasonable distribution of shear and moment. Wall_frame_2D will plot the lateral deflection, moment, and shear vs. building height. For the latter two cases the individual contributions of the shear and flexural cantilevers are displayed. The program graphs only that data which has been immediately calculated.

2.4 Example Analyses

In this section three examples will be presented using program Wall_Frame_2Ddeveloped as part of this research. The first example is a bent from a 36 story reinforced concrete structure. It will be analyzed using Wall_Frame_2Dand program NUSWFS which was previously discussed.

The second and third example is a bent from a 60 story composite structure consisting of a reinforced concrete core and steel exterior. The results of the Wall_Frame_2D analysis will be compared to those of a SAP2000analysis. SAP2000 is a full scale commercial matrix analysis program. The SAP2000 results are considered "exact" for comparison purposes.

2.4.1 Example 2-1: 36 Story Reinforced Concrete Building

2.4.1.1 Statement of the Problem

Figure 20 shows a model of a bent of the 36 story reinforced concrete building to be analyzed in this section. The author wishes to show a comparison of results for four separate models of this bent with various equivalent loading conditions. The bent will be analyzed as a single uniform segment using Wall_Frame_2Dand as a two, four, and six segment structure

with program NUSWFS. The six segment model is shown in Figure20the properties of the six, four, two, and one segment models are shown in Table1 for all analyses the segments are numbered starting at the base. Units for this example are kips (k) and feet (ft.).

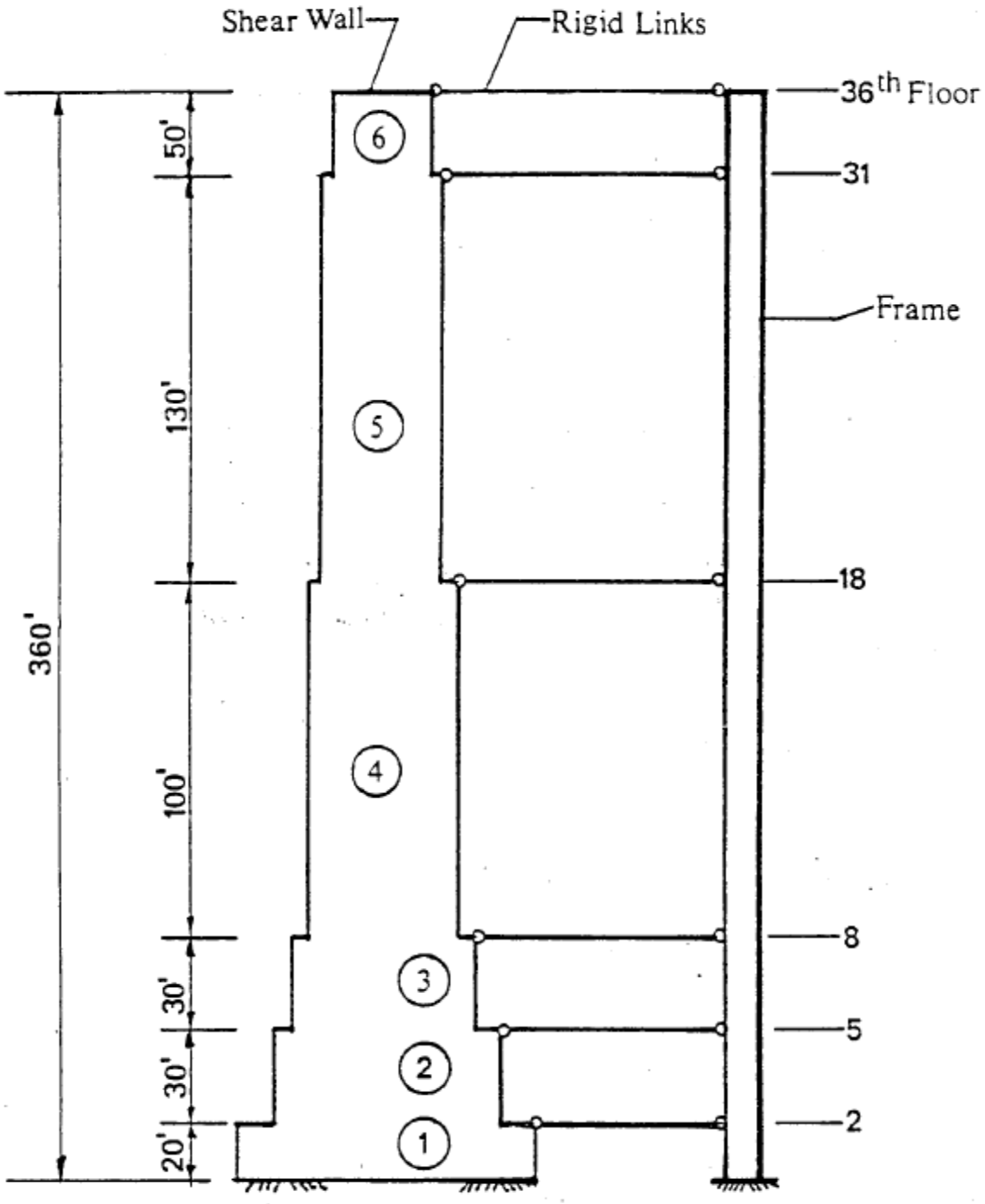

Figure 21Wall_Frame_2D model example 2-1

Table 1Example 2-1: Input Data 36 Story Reinforced Concrete Building

Number of segments	Segment No.	I (ft^4)	GA (Kips)	ALPHA (1/ft) (*10e-4)	Segment Length (ft)
6	1	49872	9500	5.874	20
	2	46042	8731	5.861	30
	3	42125	8674	6.107	30
	4	36662	7530	6.099	100
	5	32121	6750	6.169	130
	6	30091	6400	6.207	50
4	1	47574	9039	5.866	50
	2	37923	7794	6.101	130
	3	32121	6750	6.169	130
	4	30091	6400	6.207	50
2	1	45531	8902	5.951	80
	2	33080	6966	6.148	280
1	1	36080	7396	6.093	360

Notes: 1. E= 5.521 * 10^5 k/ft2

2. Analysis for 6, 4, and 2 segments with NUSWFS and WO= 4.75 k/ft.

3. Analysis for 1 segment with Wall_Frame_2D and W_o= 4.75 k/ft., W_1= 7.125 k/ft., P= 855 k

2.4.1.2 Methods of Analysis

The bent will be analyzed a total of six times. Program Wall_Frame_2Dwill be used to analyze the non-uniform structure with equivalent uniform properties for three lateral load conditions: uniform distributed loading *(W_O),* linearly distributed loading *(W_1),* and a concentrated load at the top of the structure (P). Each loading results in the same base overturning moment. The two, four, and six segment model will be analyzed using NUSWFS for a uniform loading of 4.75 k/ft. only. NUSWFS is incapable of other loading conditions. Input data for all six analyses is shown in Table 1the complete input data for the Wall_Frame_2Danalyses is shown in Tables 2, 3, and 4 as it is output from the program. Results of the analyses are presented in Section 2.4.1.3.

2.4.1.3 Results

The output files for the SWLFRM-2D analyses are shown in Tables 2, 3, and4 for the uniform, triangular, and concentrated load cases respectively. NUSWFS output is not given here.

Figure 22 compares the lateral deflection vs. building height for the Wall_Frame_2D and NUSWFS analyses. Figure 23 shows a plot of the normalized shear wall moments vs. height above the base for each analysis. The shear wall moments were divided by the total overturning moment of 307800 k/ft. to yield the normalized values. Figure 23 compares plots of the normalized shear in the frame component vs. height above the base. Each load type results in a different base shear, V, (V_P=855 k, V_{WO}= 1710k, and V_{W1} =1282.5 k). Therefore Figure 23 shows the frame shears normalized with respect to the applicable load type.

Table 2 Example 2-1: 36 Story Reinforce Concrete Building Wall_Frame_2D Output, Uniform Load

```
      PRELIMINARY ANALYSIS OF WALL OR TRUSS-FRAMED BLDGS.
             METHOD DEV. BY HEIDEBRECHT & SMITH
      THIS METHOD TO BE USED FOR 2-DIMENSIONAL ANALYSIS.
      REF: J. OF STRL. DIV, ASCE, VOL 99, NO. ST2. FEB. 1973
             MADISON R. PAULINO M.S.C.E. W.P.I. 2010


 Input Data:
 Wind Load (Wo) (K/ft): 4.75000
 Building Height (ft): 360.00
 Truss or Wall Mon. of elasticity (K/ft^2): 5.52100e+005
 Total moment of Inertia Truss or Wall (ft^4): 3.60800e+004
 Alpha: 6.09300e-004
 Number of output (N):   10.0
```

Height(ft)	Lateral Deflection	Shear Wall		Frame	
H	y	Moment	Shear	Moment	Shear
0.00	0.00000	3.04166e+005	1.71000e+003	3.63438e+003	0.00000e+000
36.00	0.00924	2.45752e+005	1.53533e+003	3.56602e+003	3.66779e+000
72.00	0.03451	1.93613e+005	1.36140e+003	3.37917e+003	6.59684e+000
108.00	0.07241	1.47723e+005	1.18813e+003	3.09891e+003	8.87085e+000
144.00	0.11995	1.08061e+005	1.01543e+003	2.74733e+003	1.05732e+001
180.00	0.17456	7.46065e+004	8.43213e+002	2.34350e+003	1.17869e+001
216.00	0.23405	4.73445e+004	6.71405e+002	1.90353e+003	1.25950e+001
252.00	0.29666	2.62615e+004	4.99920e+002	1.44054e+003	1.30800e+001
288.00	0.36101	1.13473e+004	3.28676e+002	9.64663e+002	1.33244e+001
324.00	0.42613	2.59492e+003	1.57589e+002	4.83079e+002	1.34107e+001
360.00	0.49146	0.00000e+000	-1.34212e+001	0.00000e+000	1.34212e+001

Table 3Example 2-1: 36 Story Reinforce ConcreteBuildingWall_Frame_2D Output, Triangular Load

```
      PRELIMINARY ANALYSIS OF WALL OR TRUSS-FRAMED BLDGS.
            METHOD DEV. BY HEIDEBRECHT & SMITH
      THIS METHOD TO BE USED FOR 2-DIMENSIONAL ANALYSIS.
      REF: J. OF STRL. DIV, ASCE, VOL 99, NO. ST2. FEB. 1973
            MADISON R. PAULINO M.S.C.E. W.P.I. 2010


 Input Data:
 Wind Load (W1) (K/ft): 7.12500
 Building Height (ft): 360.00
 Truss or Wall Mon. of elasticity (K/ft^2): 5.52100e+005
 Total moment of Inertia Truss or Wall (ft^4): 3.60800e+004
 Alpha: 6.09300e-004
 Number of output (N):   10.0
```

Height(ft)	Lateral Deflection	Shear Wall		Frame	
H	y	Moment	Shear	Moment	Shear
0.00	0.00000	3.03803e+005	1.28250e+003	3.99727e+003	-2.27374e-013
36.00	0.00938	2.57856e+005	1.26592e+003	3.92788e+003	3.75258e+000
72.00	0.03555	2.12957e+005	1.22430e+003	3.73438e+003	6.89709e+000
108.00	0.07558	1.70007e+005	1.15762e+003	3.43835e+003	9.45355e+000
144.00	0.12669	1.29909e+005	1.06585e+003	3.06040e+003	1.14540e+001
180.00	0.18627	9.35677e+004	9.48932e+002	2.61980e+003	1.29427e+001
216.00	0.25196	6.18884e+004	8.06824e+002	2.13400e+003	1.39759e+001
252.00	0.32171	3.57795e+004	6.39453e+002	1.61819e+003	1.46218e+001
288.00	0.39382	1.61519e+004	4.46739e+002	1.08491e+003	1.49611e+001
324.00	0.46702	3.91953e+003	2.28589e+002	5.43567e+002	1.50865e+001
360.00	0.54053	0.00000e+000	-1.51029e+001	0.00000e+000	1.51029e+001

Table 4Example 2-1: 36 Story Reinforce ConcreteBuildingWall_Frame_2D Output, Concentrated Load

```
PRELIMINARY ANALYSIS OF WALL OR TRUSS-FRAMED BLDGS.
       METHOD DEV. BY HEIDEBRECHT & SMITH
THIS METHOD TO BE USED FOR 2-DIMENSIONAL ANALYSIS.
REF: J. OF STRL. DIV, ASCE, VOL 99, NO. ST2. FEB. 1973
       MADISON R. PAULINO M.S.C.E. W.P.I. 2010


Input Data:
Wind Load (P) (K/ft): 855.00000
Building Height (ft): 360.00
Truss or Wall Mon. of elasticity (K/ft^2): 5.52100e+005
Total moment of Inertia Truss or Wall (ft^4): 3.60800e+004
Alpha: 6.09300e-004
Number of output (N):   10.0
```

Height(ft)	Lateral Deflection	Shear Wall		Frame	
H	y	Moment	Shear	Moment	Shear
0.00	0.00000	3.02957e+005	8.55000e+002	4.84326e+003	0.00000e+000
36.00	0.00952	2.72247e+005	8.51156e+002	4.77284e+003	3.84361e+000
72.00	0.03676	2.41669e+005	8.47722e+002	4.57143e+003	7.27768e+000
108.00	0.07972	2.11206e+005	8.44696e+002	4.25375e+003	1.03039e+001
144.00	0.13642	1.80846e+005	8.42076e+002	3.83443e+003	1.29236e+001
180.00	0.20488	1.50572e+005	8.39862e+002	3.32811e+003	1.51382e+001
216.00	0.28315	1.20371e+005	8.38051e+002	2.74933e+003	1.69487e+001
252.00	0.36925	9.02274e+004	8.36644e+002	2.11264e+003	1.83559e+001
288.00	0.46121	6.01275e+004	8.35639e+002	1.43253e+003	1.93606e+001
324.00	0.55709	3.00565e+004	8.35037e+002	7.23498e+002	1.99633e+001
360.00	0.65492	-3.89480e-011	8.34836e+002	3.89480e-011	2.01641e+001

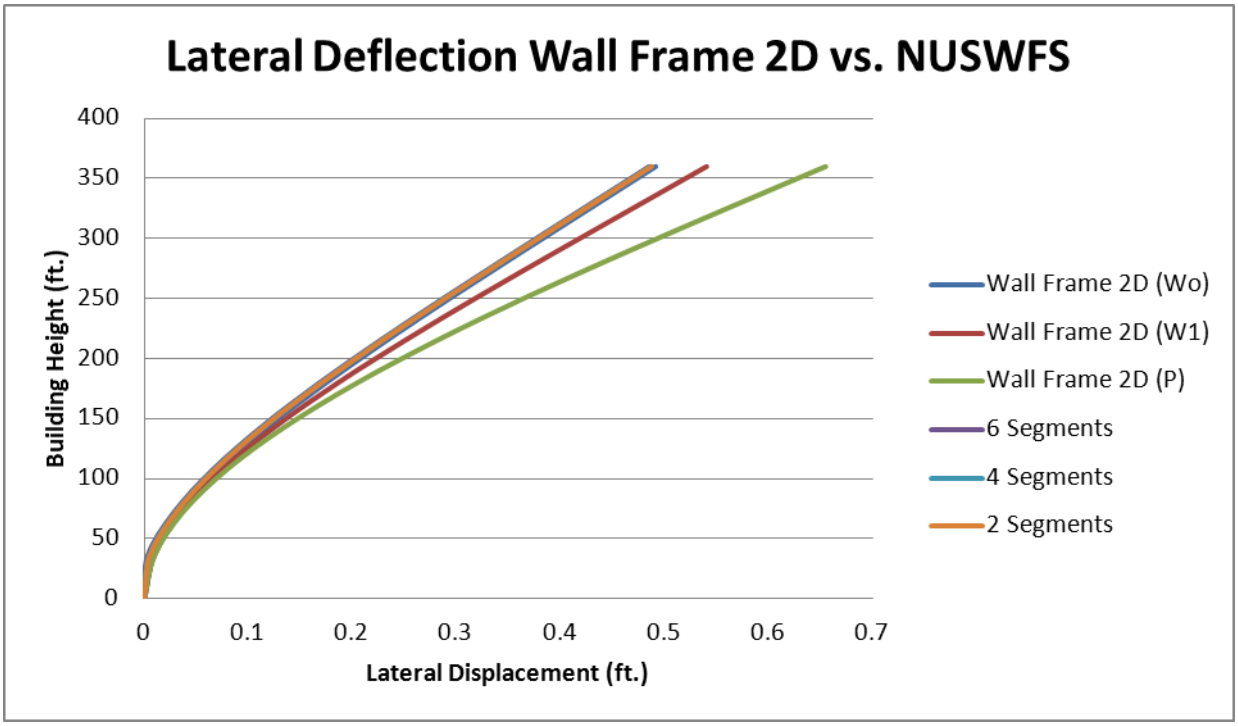

Figure 22: Example 2-1 36 Story Reinforce Concrete Building. Lateral Deflection Wall Frame 2D vs. NUSWFS

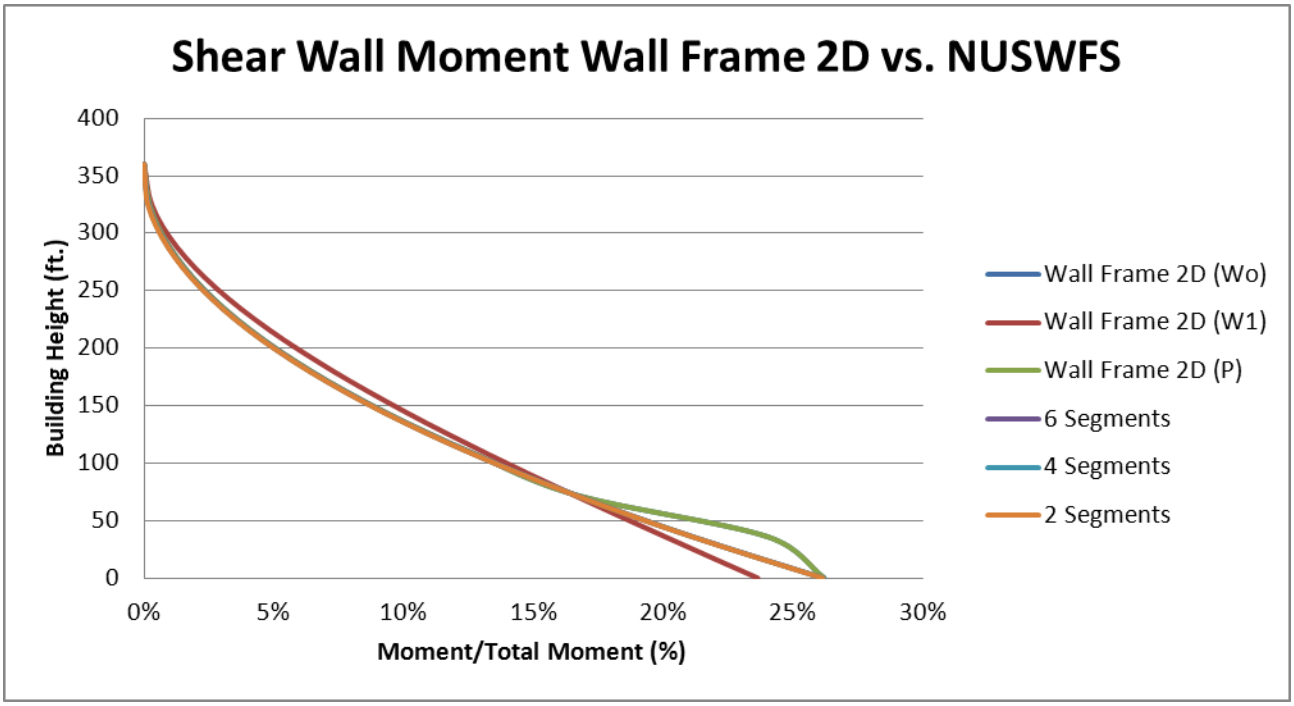

Figure 23: Example 2-1 36 Story Reinforce Concrete Building. Shear Wall Moment Wall Frame 2D vs. NUSWFS

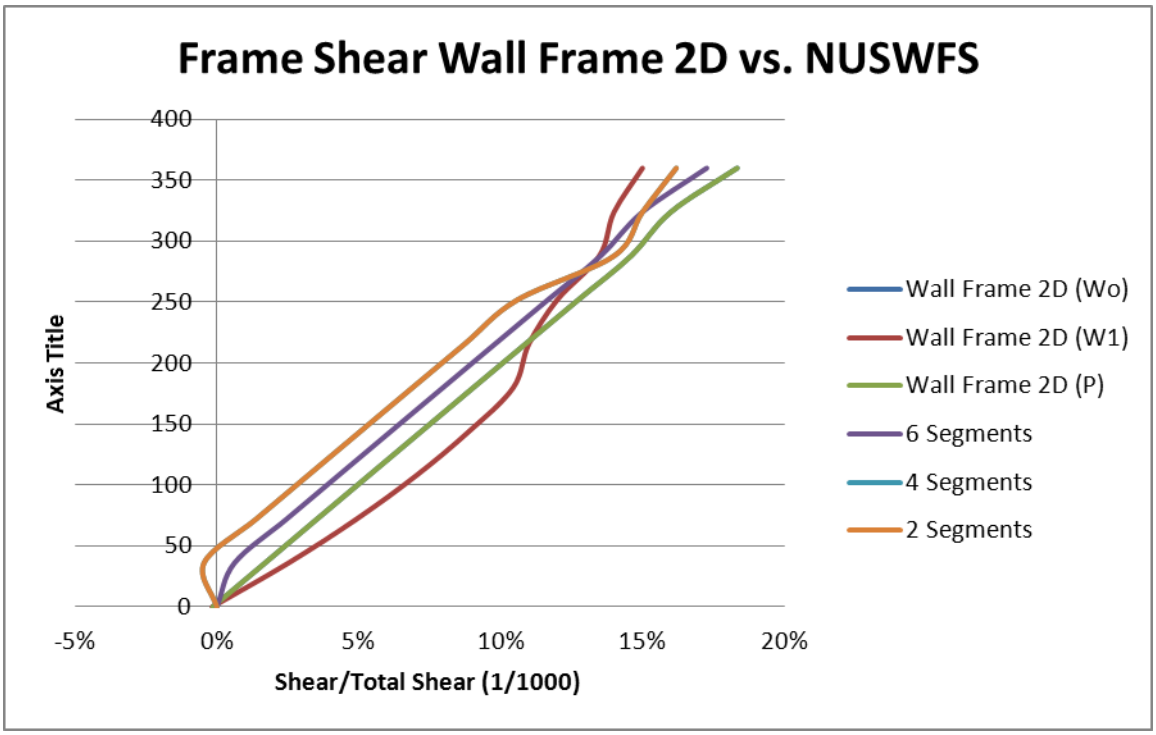

Figure 24: Example 2-1 36 Story Reinforce Concrete Building. Frame Shear Wall Frame 2D vs. NUSWFS

2.4.2 Example 2-2 and 2-3: 60 Story Composite Building

2.4.2.1 Statement of the Problem

A typical bent from a 60 story composite structure will be analyzed using Wall_Frame_2Dand SAP2000 to allow comparison with a more "exact" method. The SAP2000 model is shown in Figure 26-27 and the equivalent uniform building for the Wall_Frame_2Danalysis is shown in Figure 25. The member proportions for the SAP2000 analysis are shown in Table 6.

For the analyses a uniform lateral load was used to compare output. Table 5 lists the input data for the Wall Framed 2D analyses.

2.4.2.2 Methods of Analysis

The composite bent will be analyzed with two different approaches. A Wall_Frame_2Danalysis using Figure 25 and Tables 5 will be carried out for a concentrated and uniformly distributed load case. The ALPHA program will be used to calculate the alpha parameter by averaging the GA terms for the twelve different levels of stiffness. Since the frame consists of two "exterior" bays only, the GA parameter for a typical story was calculated by summing the GA terms for two exterior columns per story. This is equivalent to a frame with one bay.

The EI parameter for the flexural cantilever, in this case a vertical wall, was calculated using program ALPHA listed in Appendix. The SAP2000 model of Figure 26-27 was subjected to a uniformly distributed load of 0.600 k/ft. and to a concentrated load of 100.0 Kips.

The version of SAP2000 is a V12 version. For the SAP2000 analysis all columns are considered continuous through the joints. Girder connections to the columns are assumed to provide full moment resistance. Results of the analyses are given in Section 2.4.2.3.

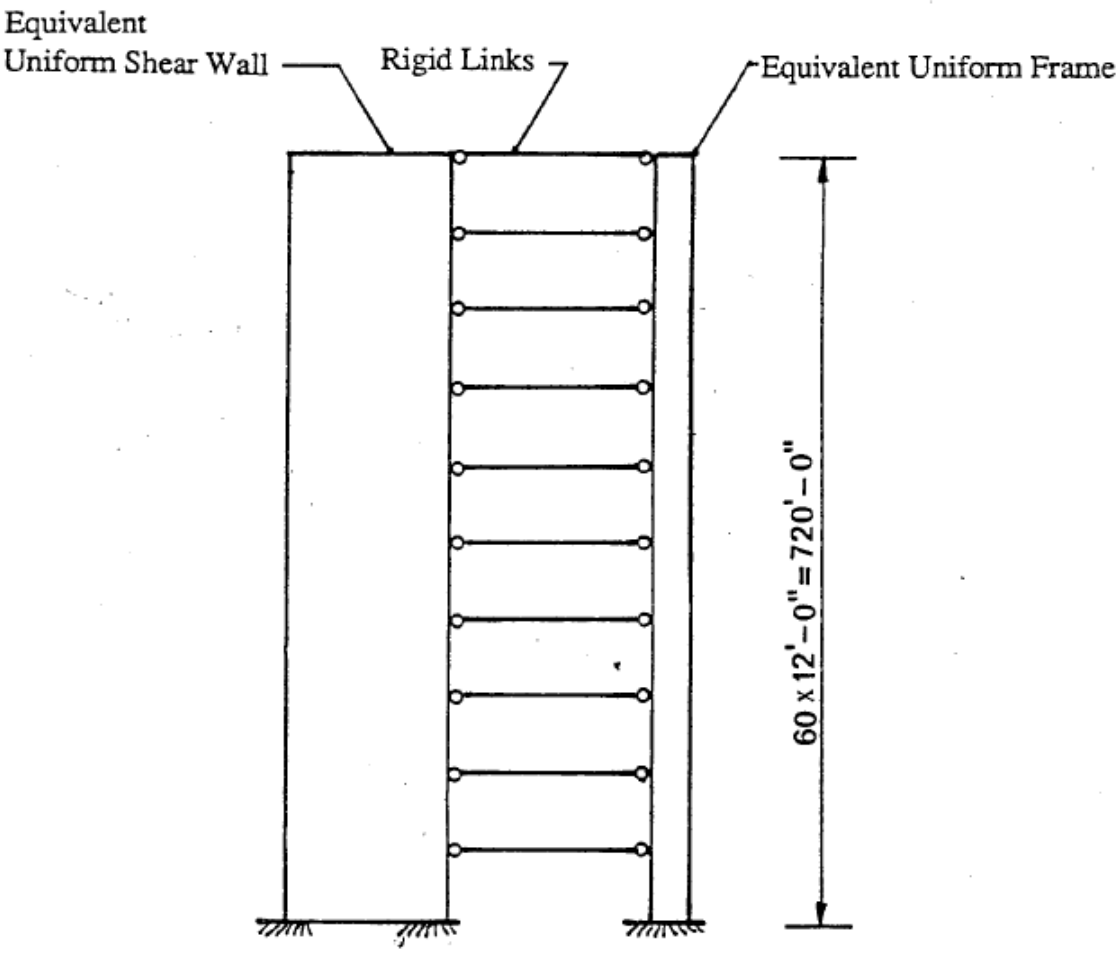

Figure 25 Wall_Frame_2D Model Example 2-2 and 2-3

Table 5 Example 2-2: Input Data for Wall_Frame_2D. 60 story Composite Building

Distribute Wind Load (w) (k/ft)	0.6	Concentrated Wind Load (p) (kips)	100
Building Height (H) (ft)	720	Building Height (H) (ft)	720
Moment of elasticity Shear Wall or Truss (E) (k/ft^2)	519119.5	Moment of elasticity Shear Wall or Truss (E) (k/ft^2)	519119.5
Moment of Inertia of Shear Wall or Truss (I) (ft^4)	8444.44	Moment of Inertia of Shear Wall or Truss (I) (ft^4)	8444.44
Alpha	0.0037	Alpha	0.0037
Number of segments for output (N)	20	Number of segments for output (N)	20

Notes: Alpha calculated by ALPHA program using inertia of the columns, inertia of the girder, height of the story, number of columns in the story, number of similar story, frame material modulus of elasticity, wall moment of inertia, and wall material modulus of elasticity. The input data shown the Appendix.

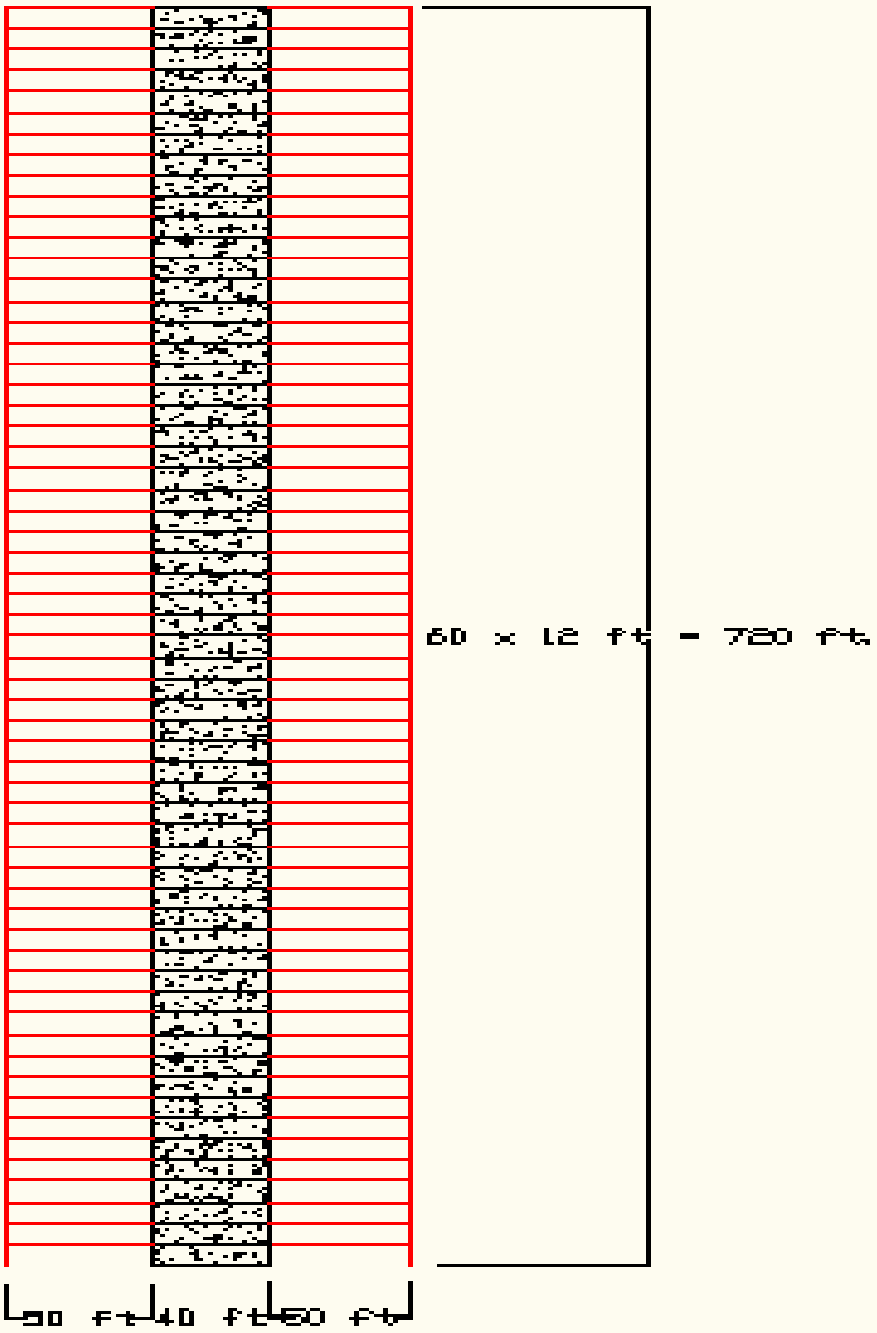

Figure 26: SAP2000 Model Example 2-2 and 2-3

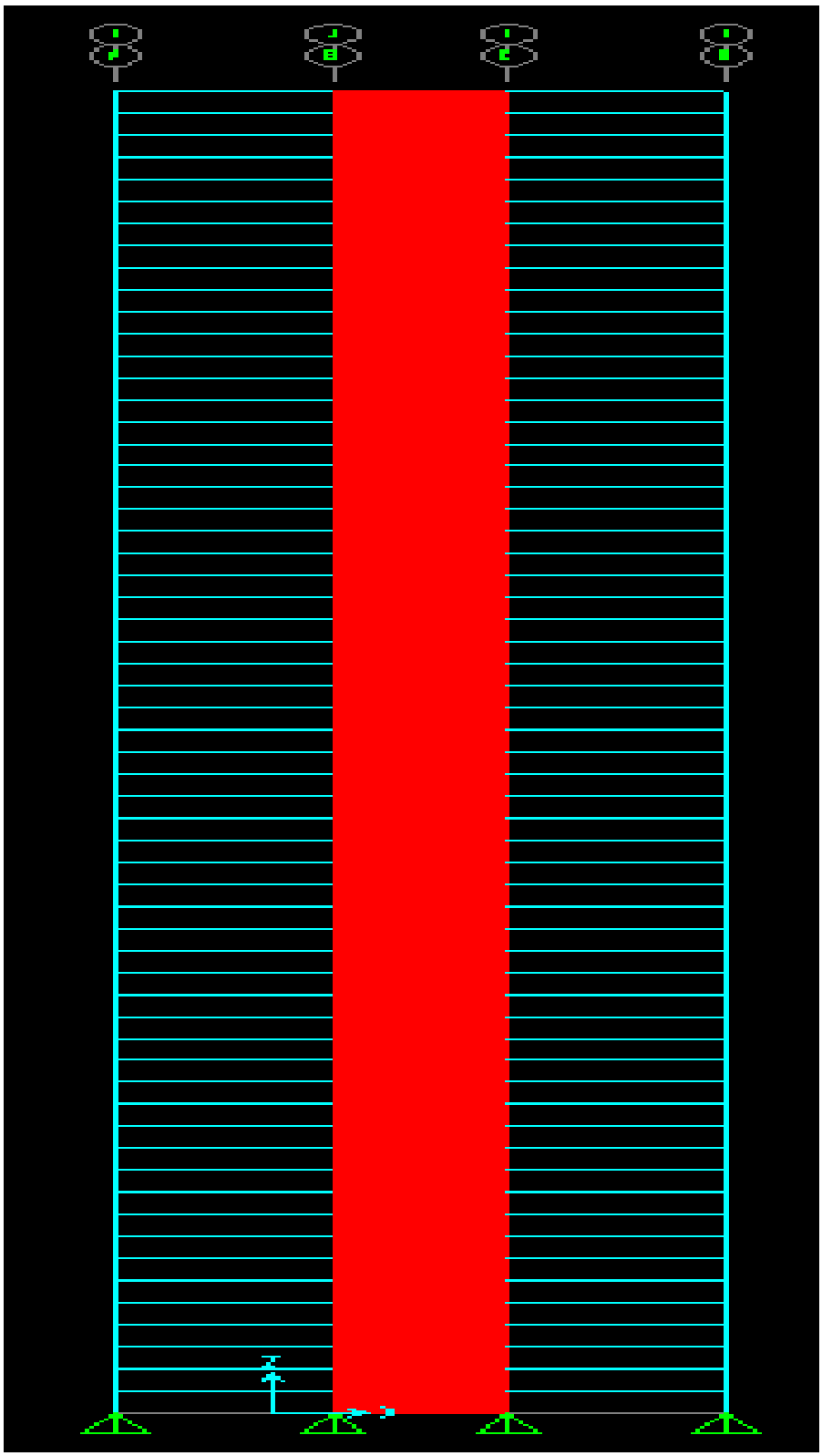

Figure 27: SAP2000 Model Example 2-2 and 2-3

Table 6: Member Proportion 60 Story Composite Building

	Columns		Girders				
Building Floors	Section	Section Ix (in^4)	Section	Section Ix (in^4)	Frame material modulus of elasticity (ksi)	Shear wall thickness (in)	Wall material modulus of elasticity (k/in)
60-55	W14X283	3840	W36X256	16800	29000	8	3605
55-50	W14X311	4330	W36X262	17900	29000	10	3605
50-45	W14X342	4900	W36X282	19500	29000	12	3605
45-40	W14X370	5440	W36X302	21100	29000	14	3605
40-35	W14X398	6000	W36X330	23300	29000	16	3605
35-30	W14X426	6600	W36X361	25700	29000	18	3605
30-25	W14X455	7190	W36X395	28500	29000	20	3605
25-30	W14X500	8210	W36X411	32100	29000	22	3605
20-15	W14X550	9430	W36X487	36000	29000	24	3605
15-10	W14X605	10800	W36X529	39600	29000	26	3605
10`-5	W14X665	12400	W14X652	50600	29000	28	3605
5`-0	W14X730	14300	W36X800	64700	29000	30	3605

2.4.2.3 Results

The outputs file for the Wall_Frame_2D analysis is shown in Table 7 and 8.The output file created from the frame input session is found in Appendix. SAP2000 output is to voluminous to include here.

Figures 28-31 illustrate the graphics from the Wall_Frame_2D analysis for the uniform distribute load. Figure 28 is a plot of the lateral deflection vs. height above the base. Figures 29-30 and 30-32 show the normalized moment and shear distributions in the shear-flexure cantilevers respectively, example 2-3 graphs are not illustrate.

Figures 33 and 34 compare the output data for the two analyses. Figure 33 and 34 is a plot of the lateral deflections vs. height above the base.

Table 7 Example 2-2: 60 story composite Building Wall_Frame_2D Output, Uniform Load

```
      PRELIMINARY ANALYSIS OF WALL OR TRUSS-FRAMED BLDGS.
            METHOD DEV. BY HEIDEBRECHT & SMITH
      THIS METHOD TO BE USED FOR 2-DIMENSIONAL ANALYSIS.
      REF: J. OF STRL. DIV, ASCE, VOL 99, NO. ST2. FEB. 1973
            MADISON R. PAULINO M.S.C.E. W.P.I. 2010


 Input Data:
 Wind Load (Wo) (K/ft): 0.60000
 Building Height (ft): 720.00
 Truss or Wall Mon. of elasticity (K/ft^2): 5.19120e+005
 Total moment of Inertia Truss or Wall (ft^4): 8.44444e+003
 Alpha: 3.70000e-003
 Number of output (N):   20.0
```

Height(ft)	Lateral Deflection	Shear Wall		Frame	
H	y	Moment	Shear	Moment	Shear
0.00	0.00000	7.78786e+004	4.32000e+002	7.76414e+004	0.00000e+000
36.00	0.01077	6.33618e+004	3.75679e+002	7.69950e+004	3.47212e+001
72.00	0.04032	5.07496e+004	3.26033e+002	7.52216e+004	6.27672e+001
108.00	0.08492	3.98179e+004	2.82180e+002	7.25453e+004	8.50200e+001
144.00	0.14132	3.03725e+004	2.43341e+002	6.91603e+004	1.02259e+002
180.00	0.20674	2.22455e+004	2.08826e+002	6.52345e+004	1.15174e+002
216.00	0.27876	1.52926e+004	1.78021e+002	6.09122e+004	1.24379e+002
252.00	0.35533	9.39007e+003	1.50380e+002	5.63171e+004	1.30420e+002
288.00	0.43470	4.43316e+003	1.25410e+002	5.15540e+004	1.33790e+002
324.00	0.51540	3.33786e+002	1.02669e+002	4.67110e+004	1.34931e+002
360.00	0.59622	-2.98091e+003	8.17527e+001	4.18609e+004	1.34247e+002
396.00	0.67617	-5.56983e+003	6.22885e+001	3.70626e+004	1.32112e+002
432.00	0.75450	-7.47896e+003	4.39311e+001	3.23622e+004	1.28869e+002
468.00	0.83063	-8.74223e+003	2.63543e+001	2.77934e+004	1.24846e+002
504.00	0.90419	-9.38208e+003	9.24579e+000	2.33789e+004	1.20354e+002
540.00	0.97499	-9.40990e+003	-7.69844e+000	1.91299e+004	1.15698e+002
576.00	1.04302	-8.82616e+003	-2.47795e+001	1.50470e+004	1.11179e+002
612.00	1.10847	-7.62049e+003	-4.23008e+001	1.11197e+004	1.07101e+002
648.00	1.17167	-5.77148e+003	-6.05737e+001	7.32668e+003	1.03774e+002
684.00	1.23318	-3.24628e+003	-7.99230e+001	3.63508e+003	1.01523e+002
720.00	1.29375	0.00000e+000	-1.00692e+002	0.00000e+000	1.00692e+002

Table 8 Example 2-3: 60 story composite Building Wall_Frame_2D Output, Concentrated Load

```
      PRELIMINARY ANALYSIS OF WALL OR TRUSS-FRAMED BLDGS.
             METHOD DEV. BY HEIDEBRECHT & SMITH
      THIS METHOD TO BE USED FOR 2-DIMENSIONAL ANALYSIS.
      REF: J. OF STRL. DIV, ASCE, VOL 99, NO. ST2. FEB. 1973
             MADISON R. PAULINO M.S.C.E. W.P.I. 2010


 Input Data:
 Wind Load (P) (K/ft): 100.00000
 Building Height (ft): 720.00
 Truss or Wall Mon. of elasticity (K/ft^2): 5.19120e+005
 Total moment of Inertia Truss or Wall (ft^4): 8.44444e+003
 Alpha: 3.70000e-003
 Number of output (N):   20.0
```

Height(ft)	Lateral Deflection	Shear Wall		Frame	
H	y	Moment	Shear	Moment	Shear
0.00	0.00000	2.67659e+004	1.00000e+002	4.52341e+004	0.00000e+000
36.00	0.00378	2.33931e+004	8.76581e+001	4.50069e+004	1.23419e+001
72.00	0.01450	2.04359e+004	7.68737e+001	4.43641e+004	2.31263e+001
108.00	0.03126	1.78418e+004	6.74552e+001	4.33582e+004	3.25448e+001
144.00	0.05330	1.55647e+004	5.92353e+001	4.20353e+004	4.07647e+001
180.00	0.07995	1.35642e+004	5.20680e+001	4.04358e+004	4.79320e+001
216.00	0.11062	1.18047e+004	4.58258e+001	3.85953e+004	5.41742e+001
252.00	0.14479	1.02550e+004	4.03979e+001	3.65450e+004	5.96021e+001
288.00	0.18199	8.88747e+003	3.56877e+001	3.43125e+004	6.43123e+001
324.00	0.22182	7.67787e+003	3.16117e+001	3.19221e+004	6.83883e+001
360.00	0.26392	6.60469e+003	2.80974e+001	2.93953e+004	7.19026e+001
396.00	0.30798	5.64887e+003	2.50823e+001	2.67511e+004	7.49177e+001
432.00	0.35372	4.79342e+003	2.25130e+001	2.40066e+004	7.74870e+001
468.00	0.40087	4.02314e+003	2.03436e+001	2.11769e+004	7.96564e+001
504.00	0.44921	3.32435e+003	1.85357e+001	1.82757e+004	8.14643e+001
540.00	0.49854	2.68462e+003	1.70571e+001	1.53154e+004	8.29429e+001
576.00	0.54866	2.09260e+003	1.58817e+001	1.23074e+004	8.41183e+001
612.00	0.59941	1.53776e+003	1.49884e+001	9.26224e+003	8.50116e+001
648.00	0.65060	1.01024e+003	1.43615e+001	6.18976e+003	8.56385e+001
684.00	0.70210	5.00671e+002	1.39897e+001	3.09933e+003	8.60103e+001
720.00	0.75374	0.00000e+000	1.38665e+001	0.00000e+000	8.61335e+001

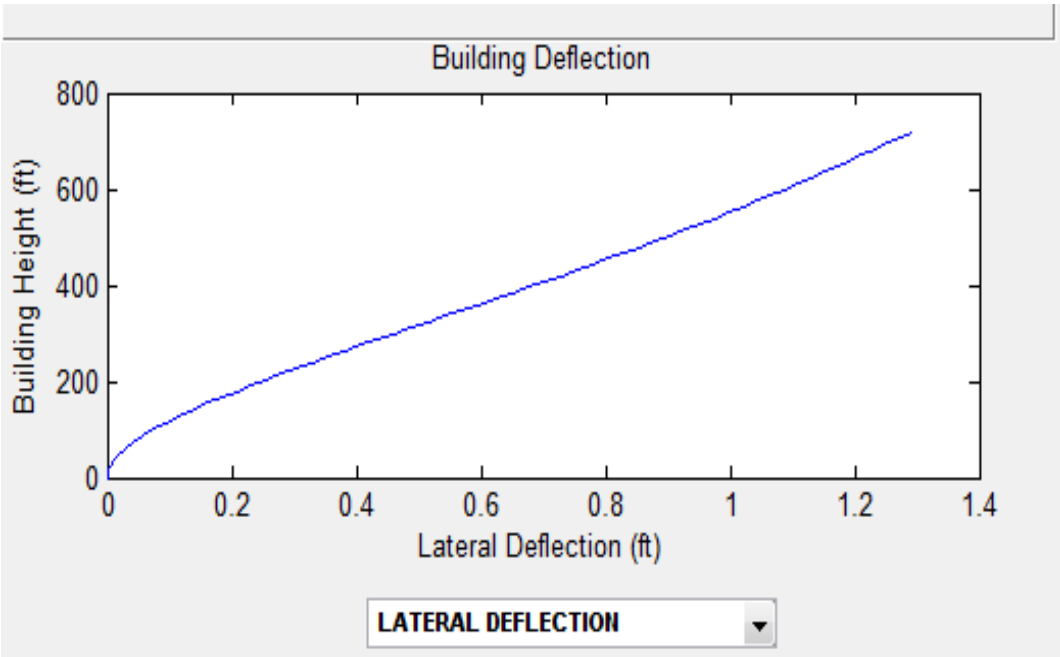

Figure 28: Example 2-2 Lateral Deflection vs. Height Wall_Frame_2D Graphics

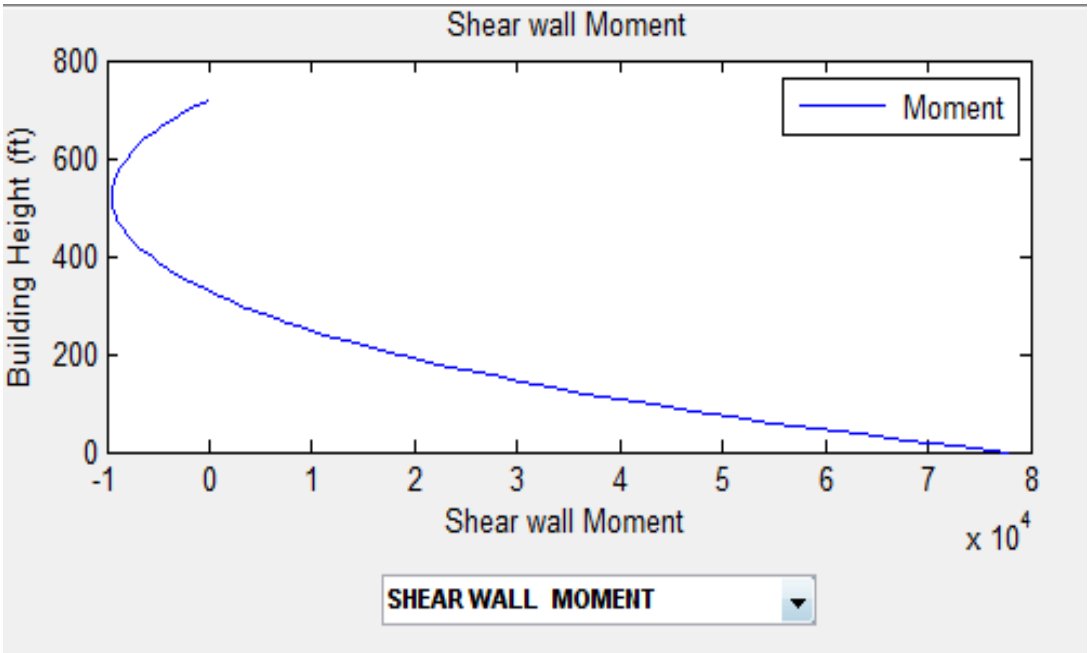

Figure 29: Example 2-2 Shear Wall Moment vs. Height Wall_Frame_2D Graphics

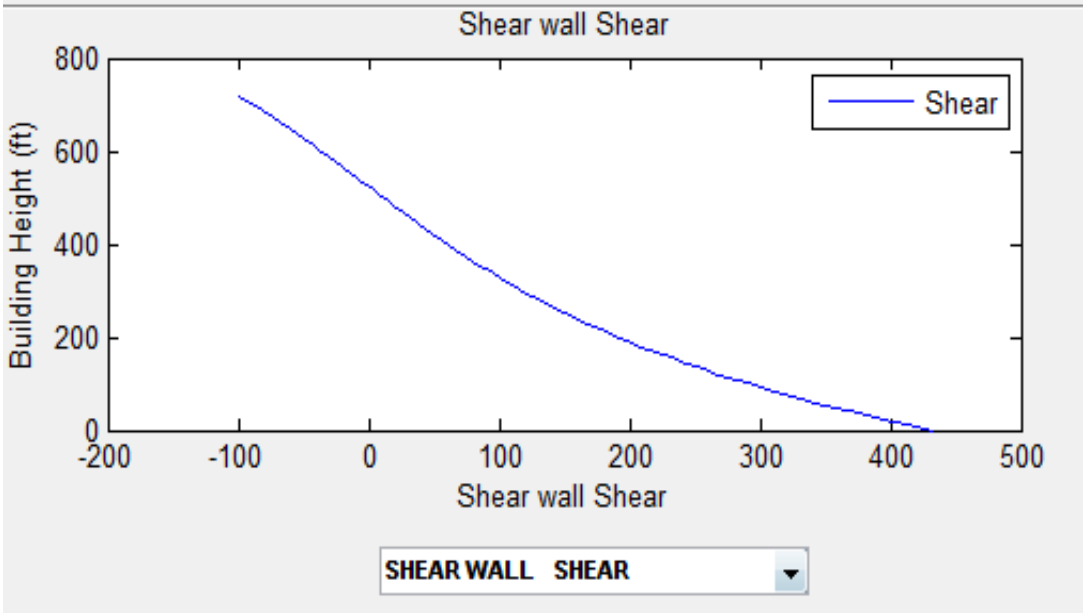

Figure 30: Example 2-2 Shear Wall Shear vs. Height Wall_Frame_2D Graphics

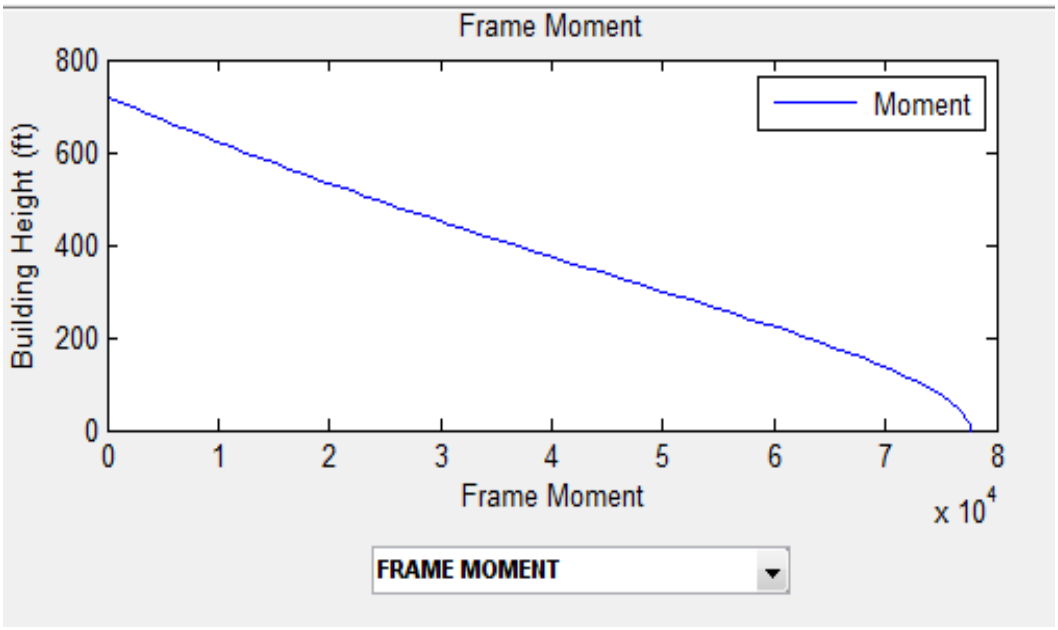

Figure 31: Example 2-2 Frame Moment vs. Height Wall_Frame_2D Graphics

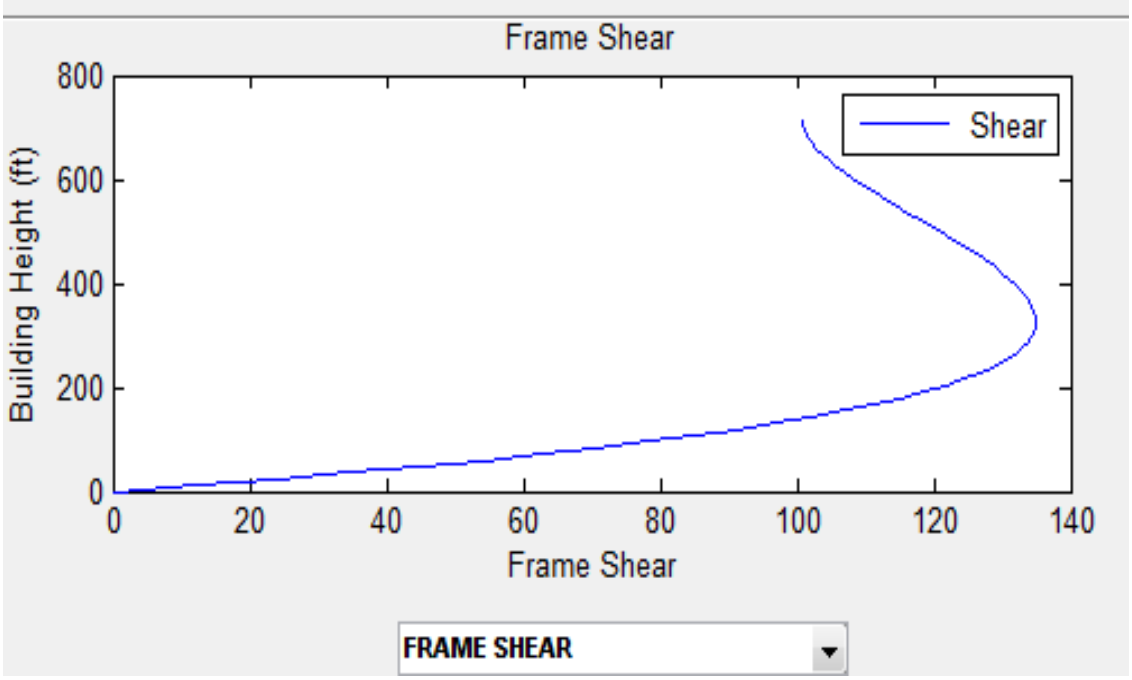

Figure 32: Example 2-2 Frame Shear vs. Height Wall_Frame_2D Graphics

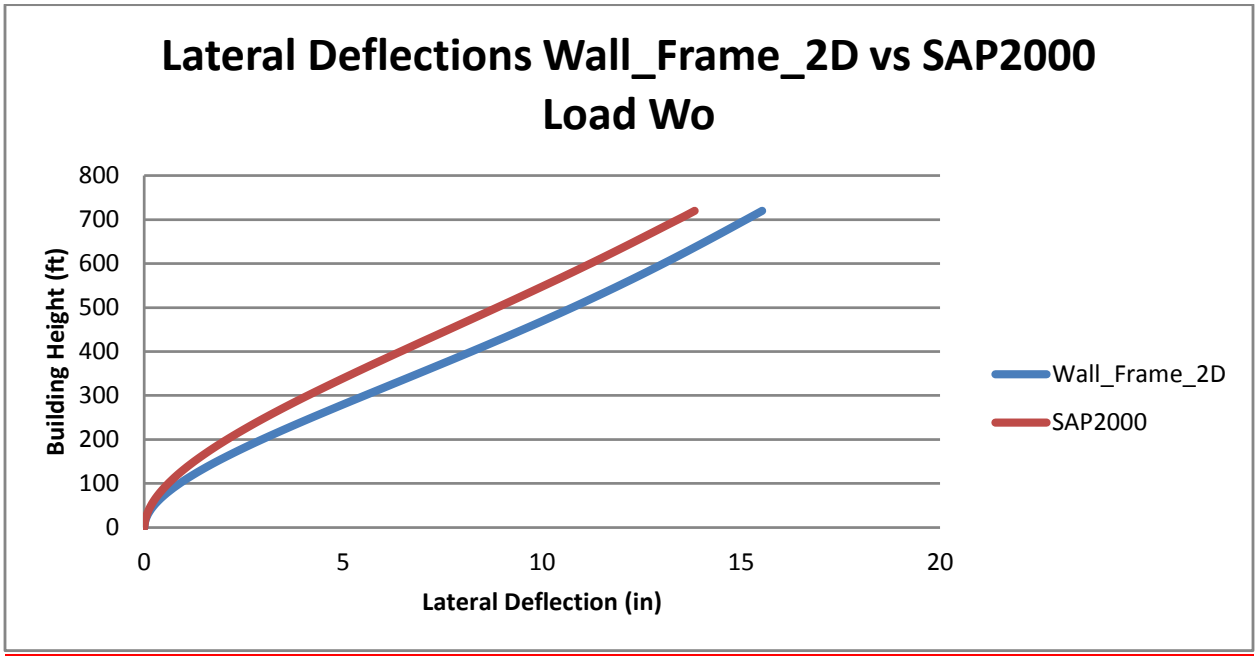

Figure 33 Example 2-2: 60 Story Composite Building, Lateral Deflections Wall_Frame_2D vs. SAP2000

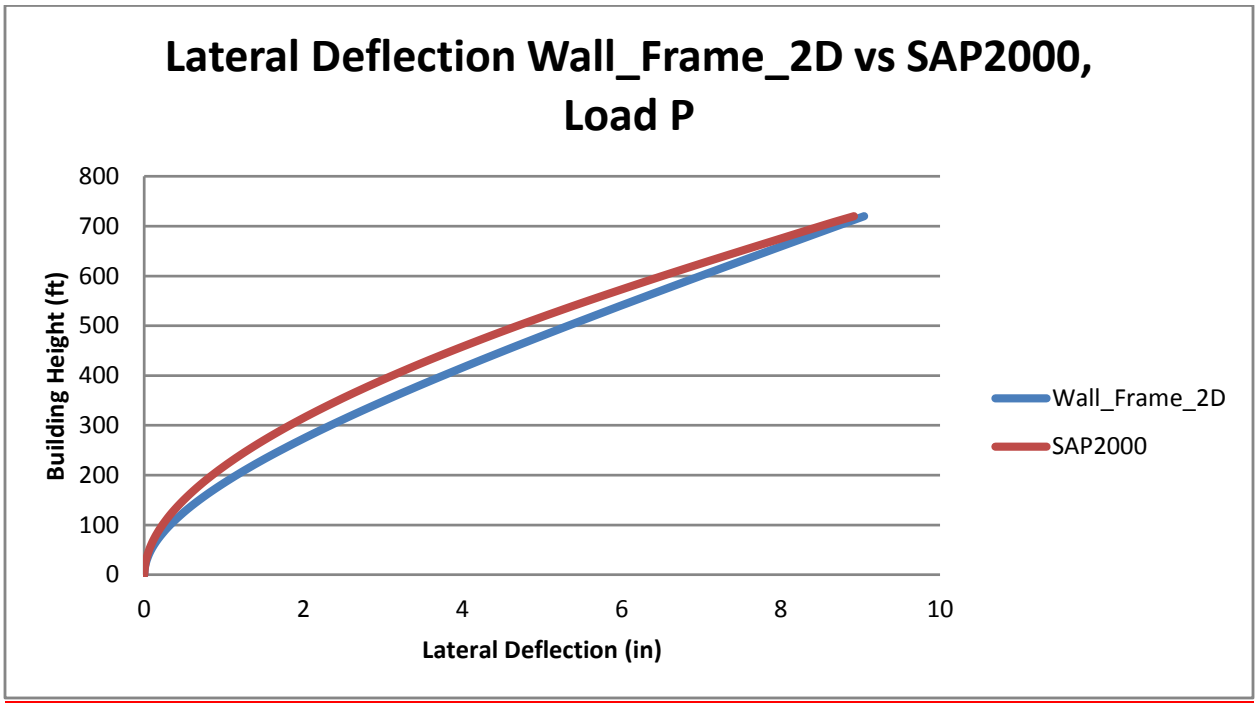

Figure 34 Example 2-3: 60 Story Composite Building, Lateral Deflections Wall_Frame_2D vs. SAP2000

2.5 Discussion of Results

Based on the previous three examples it can be stated that the shear-flexural cantilever approach for analyzing shear wall-frame interactive structures is fast. Simple to apply, and accurate enough for preliminary analysis. However the user should also be aware of its shortcomings.

Figure 22 illustrates the very close agreement between the six, four, two, and single segment model lateral deflections for a uniformly distributed load case. Observe that the six, four, and two segment models provide exact correlation near the base of the structure and there is little deviation near the top of the building. The triangular and concentrated load cases result in greater deflections throughout the structure. This is expected because although base moments are identical the moment at any location away from the free end is greater for these cases than for the uniformly distributed load case. This is verified by Figure 23.

The uniform segment approximation should result in greater deflection than a more accurate representation of the non-uniform building properties due to the reduced shear wall stiffness near the base and the reduced frame/shear wall stiffness ratio near the top of the building. For normally proportioned buildings this should not create any substantial variation between the approximate and the actual lateral deflections.

Figure 23 illustrates results similar to those for lateral deflection. In this case though the uniform segment model provided exact correlation with the six, four, and two segment models. This can be expected for structures with a gradual tapering of stiffness with height The triangular load case provides a reasonable approximation and the correlation with the uniform

load case is good near the 'boundaries. Good correlation is also obtained in the shear force comparison of Figure 24 for all model configurations. The P load case results in greater relative frame shear throughout the structure. This can be attributed to the constant shear force (V= P at all x) in the shear-flexure cantilever for this loading case. Program NUSWFS does not accept triangular or concentrated load cases but since it is based on the same theory as Wall Frame 2D and only provides a venue for exact representation of non-uniform buildings, we could expect similar correlation between the WI and P load cases of Wall Frame 2D and NUSWFS.

For example 2-2 and 2-3 the SAP2000 results shown in Figures 33 and 34 do not include effects due to member self-weight or P-Δ(second order) effects. These effects would have to be superimposed on the Wall_Frame_2D analysis. Herein a "purer" lateral load comparison can be made.

Lateral deflections of the 60 story building for a W_O and P load are compared in Figure 33, and 34. The maximum lateral deflection of the Wall_Frame_2D analysis is within 10.92% and 1.4% respectively of the SAP2000 result. Note the shear-flexural deflection mode of the SAP2000 analysis. The deflected shapes show reasonable correlation near the base. One would normally expect smaller deflections for a continuum analysis, (as opposed to a discrete element method) because it is a more constrained model.

The results for moment in the core and frame are very good. Since the shear-flexural theory underestimates frame stiffness at the base the Wall_Frame_2D results for core moment are greater than those for the SAP2000 analysis. This results in a greater shear cantilever moment in the real structure. The same holds true for the shear results. Observe that since the slope at the base is assumed equal to zero for a rigid foundation (dy/dx=0), the frame shear

force, $S_S(x)$, will be always be zero at the base because from beam theory $S_S(x) = GA(dy_S/dx)$ for the shear cantilever. It is suggested that the shear force at a lower level be assumed equal to the actual base shear in the frame.

The graphics of Wall Framed 2D in Figures 28, 29, 30, 31 and 32 are shown for illustration and comparison purposes.

The approximate analysis is "infinitely" faster to use than the exact analysis. The SAP2000 analysis utilized approximately 10 seconds of central processing unit (cpu) time whereas the Wall_Frame_2D analyses execute in a fraction of a second.

III. OUTRIGGER BRACED TALL BUILDING STRUCTURES

3 Introduction

For structures that don't rely on shear wall-frame interaction to resist lateral loads, in which the girders are essentially pin-connected to the columns, a substantial increase in stiffness and subsequent decrease in lateral drift can result from "tying" the exterior columns to the core at one or several levels with one or two story stiff horizontal outrigger trusses. Outrigger trusses are usually located for architectural purposes at mechanical levels near the middle or top of the building. In order to mobilize the additional axial stiffness of several columns and provide for torsional stiffness a belt truss can be used at the outrigger levels. Figure 8 shows a schematic of a two outrigger-belt truss system. The outriggers may be linked to a vertical truss or shear wall core although special connection details will be required for the latter.

Outrigger systems can be used in one or two directions in the building. If the building plan is rectangular outriggers may be necessary in the short direction only as in Figure 9. Normally an increase in stiffness of 30% can be realized with the addition of an outrigger-belt truss system ref (19).

This chapter will discuss the analysis of outrigger braced tall buildings in two dimensions. In this case a representative bent of the symmetric structure is analyzed for a tributary percentage of the lateral load. Section 3.2 will present the rigid outrigger approach whereby the horizontal outrigger truss (es) is considered an infinitely rigid arm ref (47). Using this approach the author derived equations for a triangular distributed load and a concentrated load at the top of the building. Design equations are also given for a uniformly distributed load. Section 3.2.4 briefly discusses the incorporation of outrigger flexibility into the analysis.

Computer program Outrigger_Program developed from the equations in Section 3.2 is introduced in Section 3.3. Two examples are presented, one to compare the Outrigger_Program results for different load types and the second to compare Outrigger_Program results to those of a SAP2000 analysis for various configurations of outrigger bracing.

3.1 Review of Research

The outrigger bracing system is a relatively new approach having been introduced in 1961 ref (45). Therefore research is somewhat limited. The majority of research conducted on the outrigger bracing system consists of preliminary analysis by means of the rigid outrigger approach ref (13), (47), (46), (97), (98), and (99). Later work studied incorporation of flexible outriggers ref (100), and (45).

In 1972, Pancewicz and Arciszewski ref (101) introduced an approximate method for determining internal forces in a pin jointed skeletqn with a vertical truss core and a horizontal truss at the top story. The trusses are replaced with bars of equivalent flexural stiffness. Pancewicz uses eq. (13). with a universal efficiency factor of 0.8 to calculate the flexural stiffness of the vertical truss. Several statically patterns based on varied horizontal truss and exterior column rigidities are proposed. The axial forces in the outer and inner columns are solved for by considering equilibrium of the horizontal truss under balanced couples produced by the horizontal load and the column axial forces ref (101).

An early study by Fleming ref (95) illustrated lateral drift reductions for various locations of a single outrigger in two steel structures. He performed STRUDL analyses of 40 and 60 story steel bents subjected to a uniformly distributed lateral load for various combinations of outrigger location and stiffness. He concluded that the optimum location for the horizontal truss was at approximately two thirds to three quarters of the height of the structure from the base and that the stiffness of the outrigger truss is affected not only by the bracing members within the truss but also the stiffnesses of the columns and girders surrounding the truss.

Contributions to the rigid outrigger approach are briefly discussed below. Taranath Ref (13) introduced the rigid outrigger approach as it is applied in this chapter. He showed that the optimum location for minimizing drift of a single outrigger is near mid-height of a building subjected to a uniformly distributed load. McNabb and Muvdiref (97) verified Taranath's results for a single outrigger. They observed that the important design parameters are location of the outrigger, the core flexural stiffness, and the exterior column spacing in the direction parallel to the applied load. In a later discussion ref (98) of this paper they extended

the theory to double outrigger structures and provided a useful method for solving the simultaneous non-'linear algebraic equations that govern the optimization of outrigger location. McNabb and Muvdi realized that the benefit of adding additional outriggers diminishes with the addition of each outrigger.

Rutenbergref (99) applied the rigid outrigger approach to dynamic analysis of an outrigger-belt truss supported structure.

In 1980 Stafford Smith and Nwaka ref (47) extended the theory to multi-outrigger structures. Relative performance of different outrigger arrangements are studied and general formulae for determining optimum outrigger locations, core moments, and outrigger resisting moments are provided for structures subjected to a uniformly distributed load. The following sections will discuss the rigid outrigger approach in detail.

3.2 The Rigid Outrigger Approach

3.2.1 Introduction

The behavior of outrigger braced tall buildings was previously discussed in Section 1.2.3. Without the outriggers the building resists lateral load primarily through core flexural stiffness. With the addition of an outrigger truss the resistance to rotation of the core at the outrigger level can be idealized as that due to outrigger flexural stiffness and that due to exterior column axial stiffness. The resisting moment provided by the outriggers can be determined by compatibility of the core rotations at the outrigger level. Subsequently the reduction in core moment below the outrigger is determined and the drift reduction due to the outrigger resisting moment can be determined for any number of outriggers at any locations.

Minimizing the drift equations will provide the optimum outrigger location(s) for drift reduction.

The following assumptions apply ref (77):

1. The connection between the perimeter columns and the outrigger arms is such that the exterior columns are subjected to axial forces only (incidental bending is neglected).
2. Steel cores are assumed heavily braced so that rotation due to bracing deformations can be considered negligible.
3. The girders within the outrigger truss are fixed to the core and all other girders are simply supported to the core and the exterior columns.
4. The belt trusses, if present, are infinitely rigid.
5. The perimeter columns and core have constant properties with height.
6. The structure is symmetric in the plane parallel to the applied load.
7. Interior columns not within the braced core are assumed not to be tied to the outrigger system.
8. The building is fixed at the base.
9. All material behaves linearly elastically.

Since the outriggers are considered infinitely rigid herein, the rotation of the core at the outrigger level will consist of that due to the exterior load, that due to the outrigger resisting moment, and that due to exterior column deformation only. Figure 32 shows the restraining moments and the resulting core bending moment diagrams for one, two, and three outrigger systems subjected to a uniformly distributed load of magnitude W_O .Figure 33illustrates the

axial deformation (Δ) of the perimeter columns linked to an infinitely rigid outrigger i for any lateral load. The exterior columns have cross sectional area A, modulus of elasticity Ec, and an effective length H-X_i where H is the total building height and X_i is the distance from the top of the building to the i^{th} outrigger.

For the single outrigger system of Figure 32a the core rotation due to W_O and M_1 at X_1 per the First Moment Area Theorem is given by:

$$\theta = \frac{1}{\mathrm{EI}} \int_{X_1}^{\mathrm{H}} \left(\frac{W_O X_1^{\,2}}{2} - \mathrm{M}_1 \right) dx$$

Or

$$\theta = \frac{W_O}{6\mathrm{EI}} \left(\mathrm{H}^3 - X_1^{\,3} \right) - \frac{\mathrm{M}_1}{\mathrm{EI}} \left(\mathrm{H} - X_1 \right) \quad \text{Equation 40}$$

Where: E= Modulus of elasticity of core material

I= Moment of inertia of the core about an axis perpendicular to the load direction

M_1= Resisting moment of outrigger 1.

Positive moment is defined as that which produces tension on the windward side of the structure.

Referring to Figure 33 and assuming small angle θ_{col} gives:

$$\theta_{col} = \frac{\Delta}{d/2} \quad \text{Equation 41}$$

Where θ_{col} represents core rotation due to the perimeter column axial deformation.

From elementary mechanics we can state that:

$$\Delta = \frac{\mathrm{P}\left(\mathrm{H} - X_1\right)}{\mathrm{AE}_C} \quad \text{Equation 42}$$

Substituting P= M_1/d into eq. 42 and then substituting the result into eq. (41) yields:

$$\theta_{col} = \frac{2\mathrm{M}_1}{\mathrm{AE}_C d^2}\left(\mathrm{H} - X_1\right) \quad \text{Equation 43}$$

Eq. 43 can represent the rotation of the core at any outrigger level i due to perimeter column deformation by substituting i for 1. Rotational compatibility is expressed by equating eq. (40) and (43) to give:

$$\frac{W_O}{6\mathrm{EI}}\left(\mathrm{H}^3 - X_1^{\,3}\right) - \frac{\mathrm{M}_1}{\mathrm{EI}}\left(\mathrm{H} - X_1\right) = \frac{2\mathrm{M}_1}{\mathrm{AE}_C d^2}\left(\mathrm{H} - X_1\right) \quad \text{Equation 44}$$

Solving eq. (44) for Ml gives:

$$\mathrm{M}_1 = \frac{W_O}{6\mathrm{EIS}}\left(\mathrm{H}^2 + X_1\mathrm{H} + X_1^{\,2}\right) \quad \text{Equation 45}$$

Where $S = \left(\frac{1}{\mathrm{EI}} + \frac{2}{\mathrm{AE}_C d^2}\right)$ Equation 46

To solve for the maximum drift, Y_{max} at x=0, the Second Moment Area Theorem is applied to Figure 32a yielding:

$$y_{\max} = \frac{1}{\mathrm{EI}}\left(\int_0^{X_1} \frac{W_O x^2}{2} x dx + \int_0^{H} \left(\frac{W_O x^2}{2} - \mathrm{M}_1 \right) x dx \right)$$

Or

$$y_{\max} = \frac{W_O \mathrm{H}^4}{8\mathrm{EI}} - \frac{\mathrm{M}_1 \left(\mathrm{H}^2 - X_1^{\,2} \right)}{2\mathrm{EI}} \quad \text{Equation 47}$$

Observe that the first term of eq. (47) is the maximum deflection of a pure flexural cantilever. Therefore the second term is the drift reduction due to outrigger 1. The optimum location for outrigger 1 is found by minimizing eq. (47) Substituting eq. (45) into eq. (47) differentiating with respect to X_1, and setting the result equal to zero the optimum location for drift reduction for a single outrigger in a structure subjected to W_O is found to be X_1= 0.455H. The deflection at any x, y(x), for this system is given by:

$$y(x) = \frac{W_O}{24\mathrm{EI}} \left(x^4 - 4\mathrm{H}^3 x + 3\mathrm{H}^4 \right) - y_{out} \quad \text{Equation 48}$$

Where: $y_{out} = \frac{\mathrm{M}_1 \left(\mathrm{H}^2 - X_1^{\,2} \right)}{2\mathrm{EI}}$ at x=0 Equation 49

$$y_{out} = \frac{M_1}{2EI}\left(\left(H^2 - X_1^{\,2}\right) + 2\left(H - X_1\right)\left(X_1 - x\right)\right) 0<x\leq X_1$$ Equation 50

$$y_{out} = \left(\frac{M_1}{2EI}\right)\left(H^2 - x^2\right) X_1<x\leq H$$ Equation 51

The equation for core moment at any x, M(x), referring to Figure 32a is:

$$M\left(x\right) = \frac{W_O x^2}{2} - M_1$$ Equation 52

Where: $M_1=0$ $0\leq x<X_1$

M_1= eq. (45) $X_1\leq x\leq H$

This approach is extend to multi-outrigger braced structures subjected to W_O in Section 3.2.2 and single and multi-outrigger braced structures subjected to a triangular (W_1) or concentrated load (P at x=0) case in Sections 3.2.3 and 3.2.4 respectively.

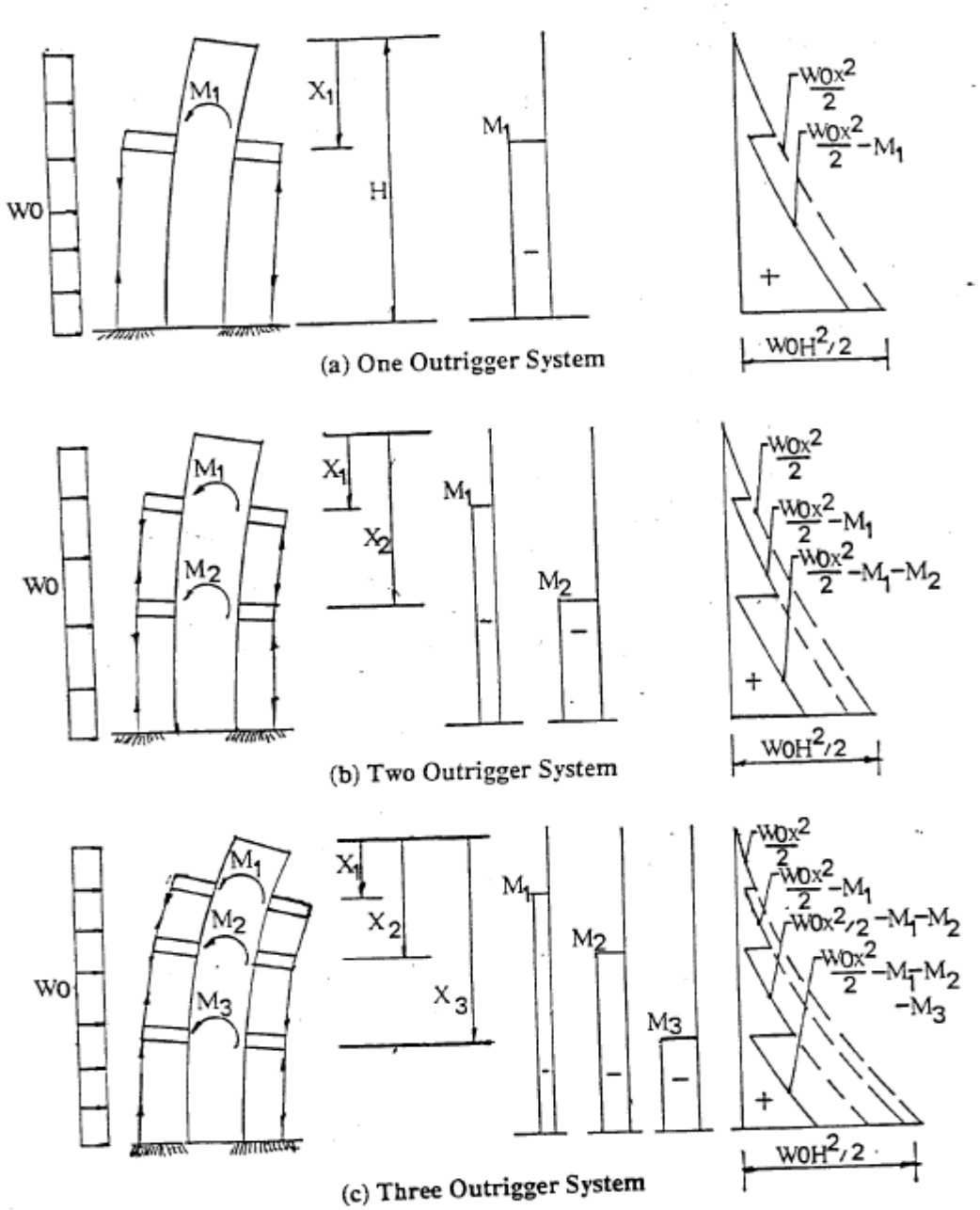

Figure 35: Multi-Outrigger Core Moment (Uniform Load)

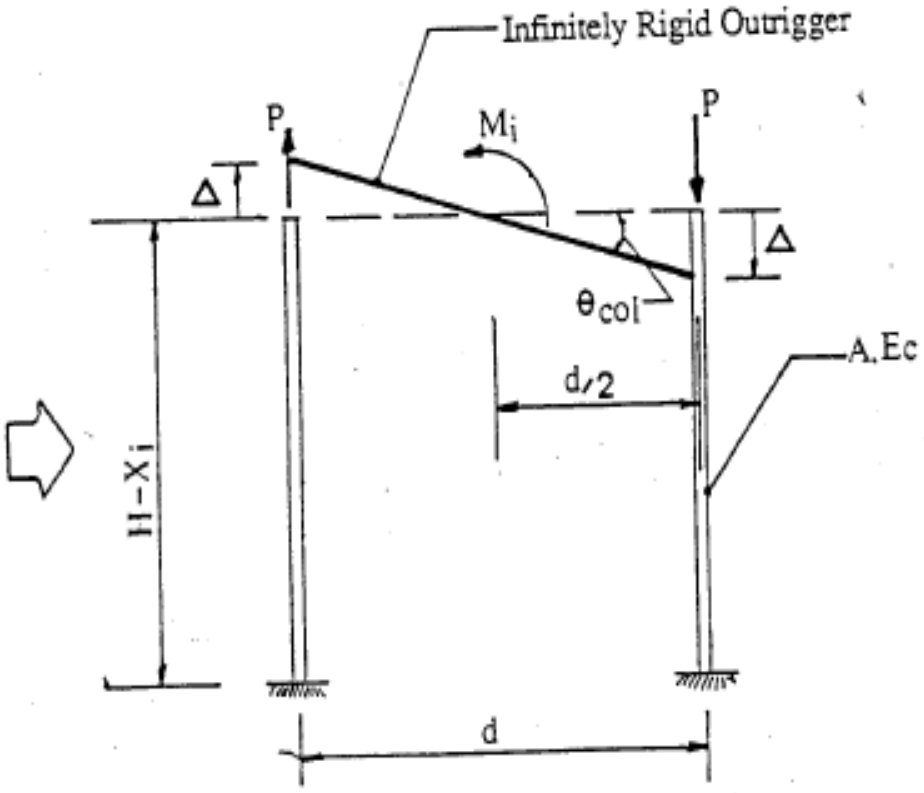

Figure 36: Axial Deformation of Perimeter Columns

3.2.2 Uniformly Distributed Load: Multi-Outrigger Systems

The rigid outrigger approach for W_O load is now extended to multi-outrigger structures. The addition of each outrigger adds another degree of redundancy to the system. For the two outrigger system of Figure 36 b the rotation compatibility equations reduce to:

$$\mathrm{M}_1\left(\mathrm{H}-X_1\right)+\mathrm{M}_2\left(\mathrm{H}-X_2\right)=\frac{W_O\left(\mathrm{H}^3-{X_1}^3\right)}{6\mathrm{EI}S} \quad \text{At } x=X_1 \quad \text{Equation 53}$$

$$\mathrm{M}_1\left(\mathrm{H}-X_2\right)+\mathrm{M}_2\left(\mathrm{H}-X_2\right)=\frac{W_O\left(\mathrm{H}^3-{X_2}^3\right)}{6\mathrm{EI}S} \quad \text{At } x=X_2 \quad \text{Equation 54}$$

Solving equations (53) and (54) simultaneously for the redundant M_1 and M_2yields:

$$\mathrm{M}_1=\frac{W_O}{6\mathrm{EI}S}\left({X_2}^2+X_2X_1+{X_1}^2\right) \quad \text{Equation 55}$$

$$\mathrm{M}_2=\frac{W_O}{6\mathrm{EI}S}\left(\mathrm{H}^2+\mathrm{H}X_2-X_2X_1-{X_1}^2\right) \quad \text{Equation 56}$$

The core moment at any x is thus given by:

$$\mathrm{M}(x)=\frac{W_O x^2}{2} \quad 0\le x<X_1 \quad \text{Equation 57}$$

$$\mathrm{M}(x)=\frac{W_O x^2}{2}-\mathrm{M}_1 \quad X_1\le x\le X_2 \quad \text{Equation 58}$$

$$\mathrm{M}(x)=\frac{W_O x^2}{2}-\mathrm{M}_1-\mathrm{M}_2 \quad X_2\le x\le H \quad \text{Equation 59}$$

By applying the second moment area theorem to the moment diagram in Figure 36b the maximum lateral deflection becomes:

$$y_{\max}=\frac{W_O \mathrm{H}^4}{8\mathrm{EI}}-\frac{1}{2\mathrm{EI}}\left(\mathrm{M}_1\left(\mathrm{H}^2-X_1^{\,2}\right)+\mathrm{M}_2\left(\mathrm{H}^2-X_2^{\,2}\right)\right) \quad \text{Equation 60}$$

And subsequently at any location x:

$$y(x)=\frac{W_O \mathrm{H}^4}{24\mathrm{EI}}\left(x^4-4\mathrm{H}^3 x+3\mathrm{H}^4\right)-\sum_{i=1}^{2} y_{out} \quad \text{Equation 61}$$

Where y_{out} is as given in eq. (49) for the i^{th} outrigger.

For a three outrigger structure (Figure 35c) the outrigger resisting moments are given by ref (47):

$$M_1 = \frac{W_O}{6EIS}\left(X_2{}^2 + X_2X_1 + X_1{}^2\right)$$ Equation 62

$$M_1 = \frac{W_O}{6EIS}\left(X_3{}^2 + X_3X_2 - X_2X_1 - X_1{}^2\right)$$ Equation 63

$$M_1 = \frac{W_O}{6EIS}\left(H_2{}^2 + HX_3 - X_3X_2 - X_2{}^2\right)$$ Equation 64

And the maximum drift by:

$$y_{\max} = \frac{W_O H^4}{8EI} - \frac{1}{2EI}\left(M_1\left(H^2 - X_1{}^2\right) - M_2\left(H^2 - X_2{}^2\right) - M_3\left(H^2 - X_3{}^2\right)\right)$$ Equation 65

The equations for core moment at any x follow from Figure 35c:

$$M(x) = \frac{W_O x^2}{2}$$ $0 \le x < X_1$ Equation 66

$$M(x) = \frac{W_O x^2}{2} - M_1$$ $X_1 \le x < X_2$ Equation 67

$$M(x) = \frac{W_O x^2}{2} - M_1 - M_2$$ $X_2 \le x < X_3$ Equation 68

$$M(x) = \frac{W_O x^2}{2} - M_1 - M_2 - M_3$$ $X_3 \le x \le H$ Equation 69

And the lateral drift of the structure at any x can be found from:

$$y(x) = \frac{W_O H^4}{24EI}\left(x^4 - 4H^3x + 3H^4\right) - \sum_{i=1}^{3} y_{out}$$ Equation 70

Where y_{out} is as given in eq. (49) for the i^{th} outrigger.

In an N-outrigger system, where N equals some number of outriggers greater than one, the equations for the outrigger resisting moments and the structures lateral drift can be expressed based on the recursive relationships determined from inspection of the equations for the single, double, and triple outrigger braced systems.

For an N-outrigger system the outrigger resisting moments are given by ref (47):

$$\mathrm{M}_1 = \frac{W_O}{6\mathrm{EIS}}\left({X_2}^2 + X_2 X_1 + {X_1}^2 \right) \quad \text{Equation 71}$$

$$\mathrm{M}_1 = \frac{W_O}{6\mathrm{EIS}}\left({X_{i+1}}^2 + X_{i+1} X_i - X_i X_{i-1} - {X_{i-1}}^2 \right) \quad \text{Equation 72}$$

(i=2,N) and (X_{i+1} = H when i = N)

And the maximum lateral deflection by:

$$y_{\max} = \frac{W_O \mathrm{H}^4}{8\mathrm{EI}} - \frac{1}{2\mathrm{EI}} - \sum_{i=1}^{N} \mathrm{M}_i \left(\mathrm{H}^2 - {X_i}^2 \right) \quad \text{Equation 73}$$

The equations for M(x) and y(x) take forms similar to those of eq. (66) and (70) respectively. However, eq. (69) would become:

$$\mathrm{M}(x)=\frac{W_O x^2}{2}-\sum_{i=1}^{N}\mathrm{M}_i \qquad \mathrm{X_N} \le \mathrm{x} \le \mathrm{H} \quad \text{Equation 74}$$

And, $\sum_{i=1}^{N} y_{out}$ would replace $\sum_{i=1}^{3} y_{out}$ in eq. (70)

Location of the optimum outrigger locations for drift reduction is discussed in Section 3.2.5.

3.2.3 Analysis for Triangularly Distributed Load

The triangular load case (W_1) is defined as that of a linearly distributed load of magnitude WI at the top of the building and zero at the base. The outrigger restraining moments and the resulting bending moment diagrams for a single, double, and triple outrigger structure subjected to the WI load case are shown in Figure 37. The systems act identically to those of Figure 37 The basic moment equation now reflects that for the W_1load. The procedure for obtaining the design equations is identical regardless of load type. For a single outrigger system the rotation compatibility equation at X_1 is given by:

$$\frac{W_1}{24\mathrm{HEI}}\left(3\mathrm{H}^4-4\mathrm{H}X_1^{\,3}+X_1^{\,4}\right)-\frac{\mathrm{M}_1}{\mathrm{EI}}\left(\mathrm{H}-X_1\right)=\frac{2\mathrm{M}_1\left(\mathrm{H}-X_1\right)}{\mathrm{AE}_C d^2} \quad \text{Equation 75}$$

Solving for M_1 gives:

$$M_1 = \frac{W_O}{6EIS}\left(3H\left(H^2 + HX_1 + X_1^{\,2}\right) - X_1^{\,3}\right)$$ Equation 76

Where S is defined by eq. (46).

The maximum drift in this case is given by:

$$y_{max} = \frac{11W_1H^4}{120EI} - \frac{M_1}{2EI}\left(H^2 - X_1^{\,2}\right)$$ Equation 77

The equations for M(x) and y(x) take similar forms as those for the uniformly distributed load case previously presented. For the triangular load case with one outrigger:

$$M(x) = \frac{W_1x^2}{2}\left(1 - \frac{x}{3H}\right) - M_1$$ Equation 78

Where: M_1=0 $0 \le x < X_1$

M_1 = eq. [3.2.3-2] $X_1 \le x \le H$

And

$$y(x) = \frac{W_1}{120HEI}\left(H^4\left(11H - 15x\right) - x^4\left(x - 5H\right)\right) - y_{out}$$ Equation 79

Where y_{out} is defined by eq. (49).

For the double outrigger case shown in Figure 37b the compatibility equations at

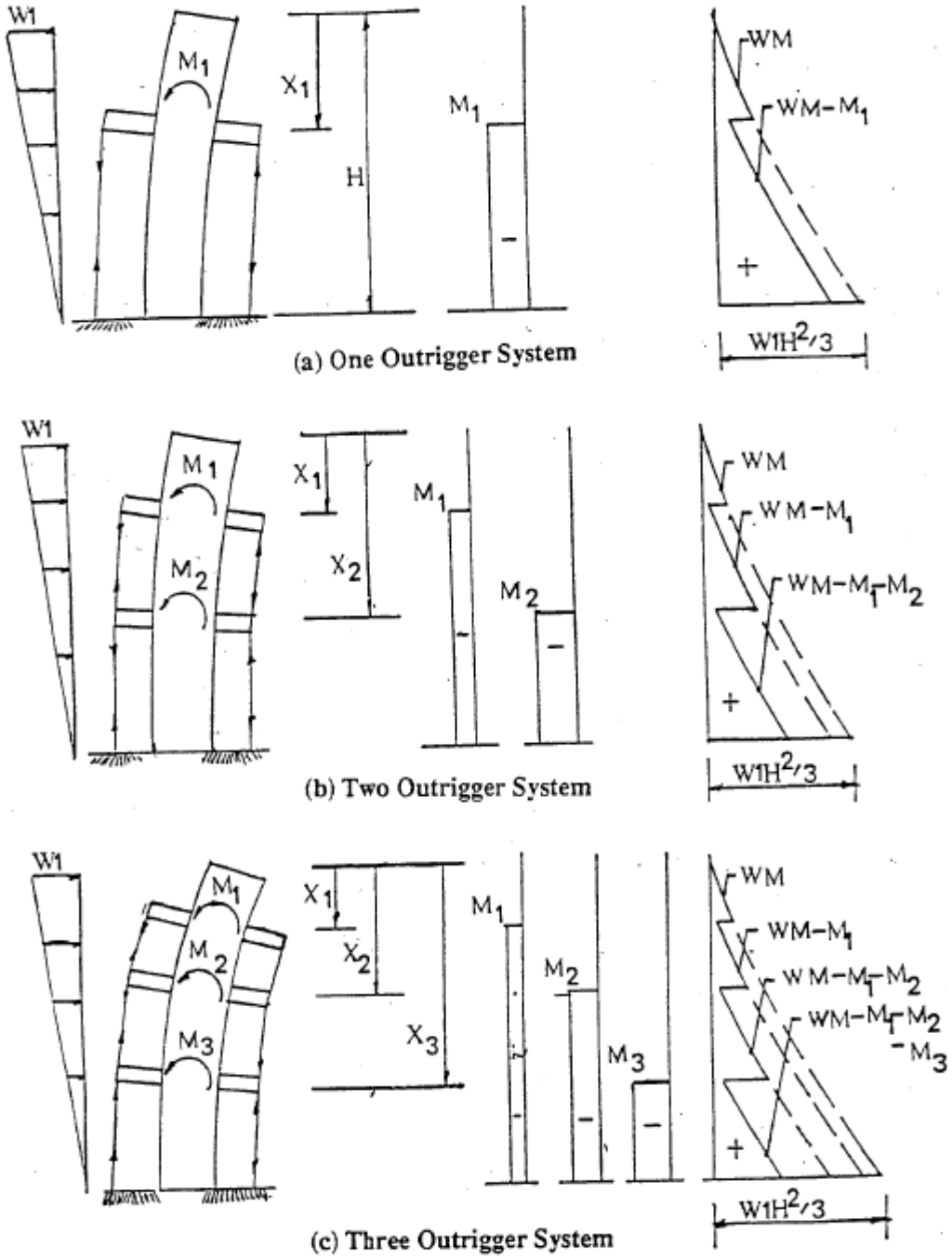

Figure 37: Multi-Outrigger Core Moments (Triangular Load)

X_1 and X_2 respectively reduce to:

$$\mathrm{M}_1\left(\mathrm{H}-X_1\right)+\mathrm{M}_2\left(\mathrm{H}-X_2\right)-\frac{W_1}{24\mathrm{HEIS}}\left(3\mathrm{H}^4-4\mathrm{H}{X_1}^3+{X_1}^4\right)=0 \text{ Equation 80}$$

$$\mathrm{M}_1\left(\mathrm{H}-X_2\right)+\mathrm{M}_2\left(\mathrm{H}-X_2\right)-\frac{W_1}{24\mathrm{HEIS}}\left(3\mathrm{H}^4-4\mathrm{H}{X_2}^3+{X_2}^4\right)=0 \text{ Equation 81}$$

Solving these equations simultaneously leads to:

$$\mathrm{M}_1=\frac{W_1}{24\mathrm{HEIS}}\left(\left(4\mathrm{H}-X_2\right)\left({X_2}^2+X_1X_2+{X_1}^2\right)-{X_1}^3\right) \text{ Equation 82}$$

$$\mathrm{M}_1=\frac{W_1}{24\mathrm{HEIS}}\left(3\mathrm{H}\left(\mathrm{H}^2+\mathrm{H}X_2+{X_2}^2\right)-{X_2}^3\right)-\mathrm{M}_1 \text{ Equation 83}$$

The equation for maximum deflection is:

$$y_{\max}=\frac{11W_1\mathrm{H}^4}{120\mathrm{EI}}-\frac{1}{2\mathrm{EI}}\sum_{i=1}^{2}\mathrm{M}_i\left(\mathrm{H}^2-{X_i}^2\right) \text{ Equation 84}$$

Observe again that the first term in the deflection equation is that for a pure flexural cantilever beam. The core moment at any at x can be expressed as:

$$\mathrm{M}\left(x\right)=\frac{W_1x^2}{3\mathrm{H}^2}\left(3\mathrm{H}-x\right) 0\leq x<X_1 \text{ Equation 85}$$

$$\mathrm{M}\left(x\right)=\frac{W_1x^2}{3\mathrm{H}^2}\left(3\mathrm{H}-x\right)-\mathrm{M}_1 X_1\leq x<X_2 \text{ Equation 86}$$

$$\mathrm{M}(x)=\frac{W_1 x^2}{3\mathrm{H}^2}(3\mathrm{H}-x)-\mathrm{M}_1-\mathrm{M}_2 \quad \mathrm{X}_2 \le x < \mathrm{H}$$ Equation 87

and the lateral drift at any x as:

$$y_{\max}=\frac{W_1}{120\mathrm{HEI}}\left(\mathrm{H}^4(11\mathrm{H}-15x)-x^4(x-5\mathrm{H})\right)-\sum_{i=1}^{2} y_{out}$$ Equation 88

Where y_{outi} is as given in eq. (49) for outrigger i.

For a triple outrigger structure, the outrigger resisting moments M_1, M_2, M_3in Figure 45c are as follows:

$$\mathrm{M}_1=\frac{W_1}{24\mathrm{HEIS}}\left((4\mathrm{H}-X_2)\left(X_2{}^2+X_1X_2+X_1{}^2\right)-X_1{}^3\right)$$ Equation 89

$$\mathrm{M}_2=\frac{W_1}{24\mathrm{HEIS}}\left((4\mathrm{H}-X_3)\left(X_3{}^2+X_2X_3+X_2{}^2\right)-X_2{}^3\right)-\mathrm{M}_1$$ Equation 90

$$\mathrm{M}_3=\frac{W_1}{24\mathrm{HEIS}}\left(3\mathrm{H}\left(\mathrm{H}^2+\mathrm{H}X_3+X_3{}^2\right)-X_3{}^3\right)-\mathrm{M}_2-\mathrm{M}_1$$ Equation 91

Maximum drift is now reduced by the resistance of a third outrigger therefore:

$$y_{\max}=\frac{11W_1\mathrm{H}^4}{120\mathrm{EI}}-\frac{1}{2\mathrm{EI}}\sum_{i=1}^{3}\mathrm{M}_i\left(\mathrm{H}^2-X_i{}^2\right)$$ Equation 92

The equation for core moment at any x can be expressed as eq. (66) by replacing $W_O x^2/2$ with $(W_1 x^2/2)(1 - x/3H)$ and the lateral drift at any x can be expressed as eq. (85) by replacing the first term on the right hand side with the corresponding term of eq. (79) .

By studying the equations is previously given for outrigger resisting moments in the single, double, and triple outrigger system recursive relationships were observed. Consequently the outrigger resisting moments in the N-outrigger system subjected to W_1 can Be expressed as:

$$\mathrm{M}_1 = \frac{W_1}{24\mathrm{HEIS}}\left(\left(4\mathrm{H} - X_2\right)\left(X_2{}^2 + X_1 X_2 + X_1{}^2\right) - X_1{}^3\right) \quad \text{Equation 93}$$

$$\mathrm{M}_i = \frac{W_1}{24\mathrm{HEIS}}\left(\left(4\mathrm{H} - X_{i+1}\right)\left(X_{i+1}{}^2 + X_i X_{i+1} + X_i{}^2\right) - X_i{}^3\right) - \sum_{j=1}^{i-1}\mathrm{M}_j \quad \text{Equation 94}$$

(i=2,N) and (X_{i+1} = H when i= N)

The maximum drift in the N-outrigger structure is given by:

$$y_{\max} = \frac{11W_1\mathrm{H}^4}{120\mathrm{EI}} - \frac{1}{2\mathrm{EI}}\sum_{i=1}^{N}\mathrm{M}_i\left(\mathrm{H}^2 - X_i^2\right) \quad \text{Equation 95}$$

The equations for M(x) and y(x) are as for the uniform load case for an N-outrigger system when the pure flexure cantilever terms are replaced with those for the W_1 case.

3.2.4 Analysis for Concentrated Load Case

The concentrated load case (P) is defined as that of a concentrated lateral load of magnitude P applied at the top of the structure (x=0). This loading case is useful when code required load cases have to be simulated. The outrigger restraining moments and resulting bending moment diagrams for the single, double, and triple outrigger structure subjected to the P loading case are shown in Figure 38. The core moment is now of a linear variation with x.

The procedure for obtaining the governing equations follows directly from those loading cases previously presented. The reader is referred to Section 3.2.1 for details of the approach and explanation of terms. For a single outrigger case (Figure 38a):

$$M_1 = \frac{P}{2EIS}\left(H + X_1\right)$$ Equation 96

$$y_{max} = \frac{PH^3}{3EI} - \frac{M_1}{2EI}\left(H^2 - X_1^2\right)$$ Equation 97

$$M\left(x\right) = PH - M_1$$ Equation 98

Where: $M_1 = 0$ $0 \le x < X_1$

$$M_1 = \frac{P}{2EIS}\left(H + X_1\right)$$ $X_1 \le x \le H$

And

$$y(x)=\frac{\mathrm{P}}{6\mathrm{EI}}\left(2\mathrm{H}^3-3\mathrm{H}^2x+x^3\right)-y_{out}$$ Equation 99

Where y_{out} is given by eq. (49).

For the double outrigger case (Figure 38b):

$$\mathrm{M}_1=\frac{\mathrm{P}}{2\mathrm{EIS}}\left(X_2+X_1\right)$$ Equation 100

$$\mathrm{M}_2=\frac{\mathrm{P}}{2\mathrm{EIS}}\left(\mathrm{H}-X_1\right)$$ Equation 101

$$y_{\max}=\frac{\mathrm{PH}^3}{3\mathrm{EI}}-\frac{1}{2\mathrm{EI}}\sum_{i=1}^{2}\mathrm{M}_i\left(\mathrm{H}^2-X_i^2\right)$$ Equation 102

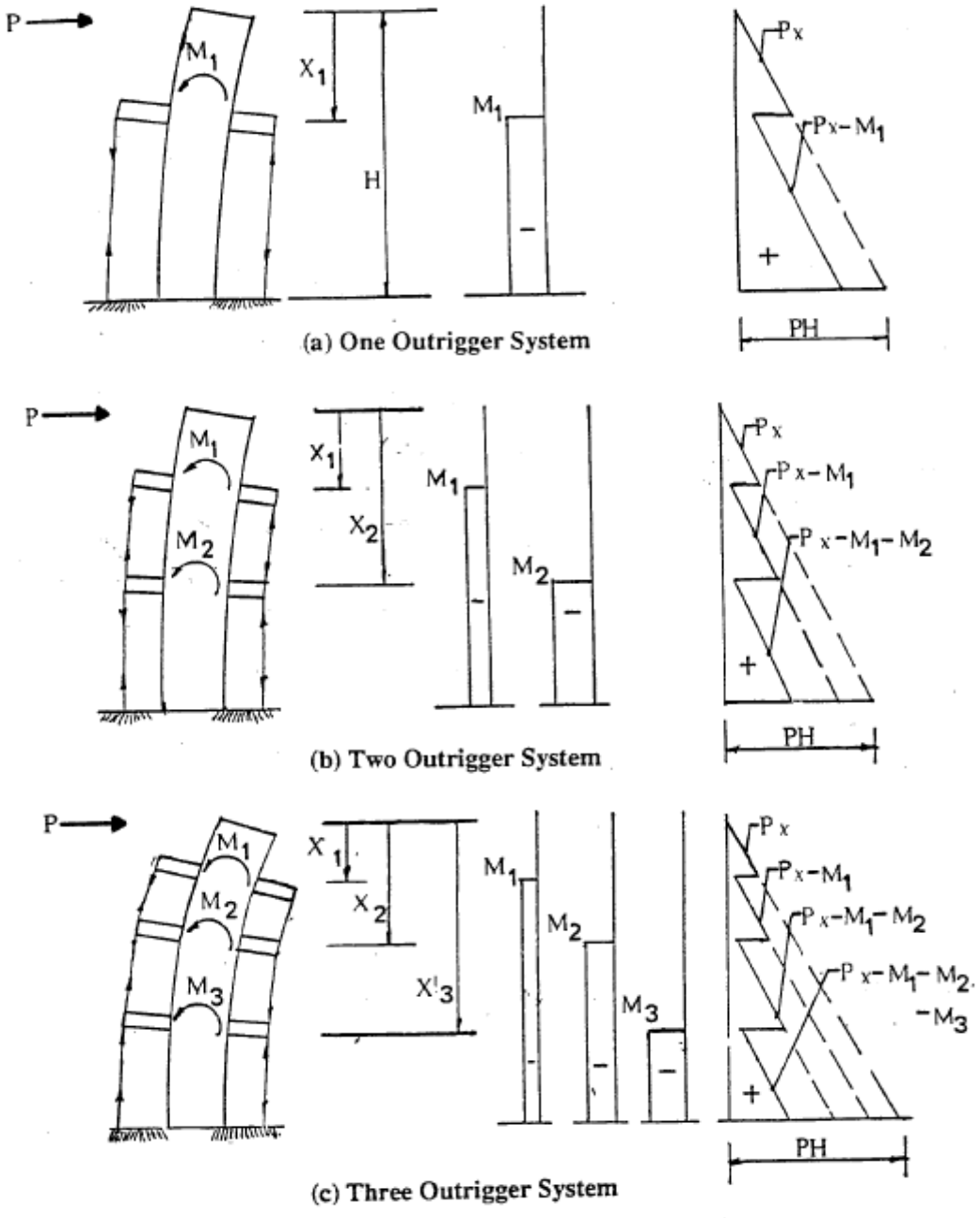

Figure 38: Multi-Outrigger Core Moments (Concentrated Load)

$$M(x) = PH \quad 0 \le x < X_1 \quad \text{Equation 103}$$

$$M(x) = PH - M_1 \quad X_1 \le x < X_2 \quad \text{Equation 104}$$

$$M(x) = PH - M_1 - M_2 \quad X_2 \le x \le H \quad \text{Equation 105}$$

And

$$y(x) = \frac{P}{6EI}\left(2H^3 - 3H^2 x + x^3\right) - \sum_{i=1}^{2} y_{out} \quad \text{Equation 106}$$

Where Y_{outi} is given by eq. (49) for outrigger i.

The governing equations for the triple outrigger case shown in Figure 38c are as follows:

$$M_1 = \frac{P}{2EIS}\left(X_2 + X_1\right) \quad \text{Equation 107}$$

$$M_2 = \frac{P}{2EIS}\left(X_3 - X_1\right) \quad \text{Equation 108}$$

$$M_3 = \frac{P}{2EIS}\left(H - X_2\right) \quad \text{Equation 109}$$

$$y_{max} = \frac{PH^3}{3EI} - \frac{1}{2EI}\sum_{i=1}^{3} M_i \quad \text{Equation 110}$$

$$M(x) = PH \quad 0 \le x < X_1 \quad \text{Equation 111}$$

$$M(x) = PH - M_1 \quad X_1 \le x < X_2 \quad \text{Equation 112}$$

$$M(x) = PH - M_1 - M_2 \quad X_2 \le x < X_3 \quad \text{Equation 113}$$

$$M(x) = PH - M_1 - M_2 - M_3 \quad X_3 \le x \le H \quad \text{Equation 114}$$

And

$$y(x) = \frac{P}{6EI}\left(2H^2 - 3H^2 x + x^3\right) - \sum_{i=1}^{3} y_{out} \quad \text{Equation 115}$$

For an N-outrigger structure subjected to P loading:

$$M_1 = \frac{P}{2EIS}\left(X_2 + X_1\right) \quad \text{Equation 116}$$

$$M_i = \frac{P}{2EIS}\left(X_{i+1} - X_{i-1}\right)$$ With (i=2, N) and (X_{i+1} = H when i=N) **Equation 117**

$$y_{max} = \frac{PH^3}{3EI} - \frac{1}{2EI}\sum_{i=1}^{N} M_i\left(H^2 - X_i^{\,2}\right)$$ **Equation 118**

M(x) for this case is given per eq. [3.2.4-11] where the N+ 1st equation would be:

$$M(x) = PH - \sum_{i=1}^{N} M_i \quad X_N \le x \le H$$ **Equation 119**

y(x) is given by eq. (115) when the last term is replaced by $\sum_{i=1}^{N} y_{out}$

These equations and those of Sections 3.2.1, 2, and 3 were used to create program Outrigger_Program presented in Section 3.3. Section 3.2.5 discusses optimization for minimum drift and gives guidelines for expected outrigger performance based on load type and equidistant outrigger spacing.

3.2.5 Discussion of Optimization and Performance

In order to determine the best location for the outriggers in terms of drift reduction the equations for maximum drift are minimized with respect to the outrigger locations X_i. The benefits of multi-outrigger structures must be balanced against the economics of the additional material and construction costs. It will be shown that each additional outrigger provides less and less benefit to the structure. Four outriggers is considered a practical limit.

To calculate the optimum outrigger locations in terms of drift reduction the equations for maximum drift are differentiated with respect to each unknown Xi. The resulting non-linear algebraic equation(s) are set equal to zero and solved simultaneously (if necessary) for the roots Xi.

The equations used by the author to solve for the outrigger locations shown in Table 10 are presented in Tables7, 8 and 9 for the uniform, triangular, and concentrated load cases respectively. The method of solution is indicated in the right most columns. Ref (98) refers to the approach introduced by Muvdi and McNabb. Ref (47) refers to the work by Stafford Smith and Nwaka. Table 11 is included because program Outrigger_Program requires input of the outrigger locations based on Di and not Xi for user convenience. Study of Table 11 shows that when the structure is subject to greater core rotation and lateral drift the optimum locations for the rigid outrigger are closer to the top of the building. The $W_1$and P cases will result in greater maximum drift and rotation, (for a given base overturning moment), than the W_O case. The values for P are only of academic interest as this load is unlikely to occur independently.

Based on the equations for outrigger resisting moment it can be seen that the lower the outrigger is placed the greater will be its resisting moment But the moment reduction will not only act over a smaller segment of the structure but the lower outrigger location will sacrifice

drift reduction benefits. It is possible to get cases where the moment at the outrigger will be greater than the moment at the base of the structure.

If outriggers were placed at an infinite number of locations in the structure as shown in

Table 9 :Outrigger Optimization Equations-Concentrated Load

Number of Outriggers	Optimization Equation(s) (H=1)	Method of Solution
1	$3X_1^2+2X_1-1=0$	Quadratic Formula
2	$3X_1^2+2X_2X_1-X_2^2=0$ $X_1^2-2X_1X_2+2X_2-1=0$	Ref (98)
3	$3X_1^2+2X_2X_1-X_2^2=0$ $X_1^2-2X_1X_2+2X_2X_3-X_3^2=0$ $X_2 3-2X_2X_3+2X_3-1=0$	Ref (98)
N	$3X_1^2+2X_2X_1-X_2^2=0$ $X_{j-1}^2-2X_{j-1}X_j+2X_jX_j+1-X_{j+1}^2=0$ (N total Eqs., J=equation number, $X_{N+1}=H$	Ref (98)

Table 10 :Optimum location(s) of Outrigger truss(es) Xi

Optimum Location(s) of Outrigger Truss(es) Xi					
	Optimum Location(s) Xi, for the i^{th}Outrigger (%H)				
Load Type	Total No. of Outrigger Levels	X_1	X_2	X_3	X_4
P	1	0.333			
	2	0.199	0.599		
	3	0.142	0.427	0.713	
	4	0.105	0.314	0.524	0.735
W_o	1	0.455			
	2	0.312	0.686		
	3	0.243	0.534	0.779	
	4	0.202	0.443	0.646	0.829
W_1	1	0.43			
	2	0.288	0.661		
	3	0.226	0.509	0.76	

X_i= Distance from top of the building to the i^{th} Outrigger level

Table 11: Optimum location(s) of Outrigger truss (es) Di

Optimum Location(s) of Outrigger Truss(es) Di					
	Optimum Location(s) Xi, for the i^{th} Outrigger (%H)				
Load Type	Total No. of Outrigger Levels	D_1	D_2	D_3	D_4
P	1	0.667			
	2	0.401	0.801		
	3	0.287	0.573	0.858	
	4	0.265	0.476	0.686	0.895
W_o	1	0.545			
	2	0.314	0.688		
	3	0.221	0.466	0.757	
	4	0.171	0.354	0.557	0.798
W_1	1	0.57			
	2	0.339	0.712		
	3	0.24	0.491	0.774	

D_i= Distance from base of the building to the ith Outrigger level

Figure 36 the columns would behave fully compositely with the core and contribute a resisting moment equal to ref (47):

$$M_{fc} = \left(\frac{\frac{AE_C d^2}{2}}{EI + \frac{AE_C d^2}{2}} \right) M_{total} \quad \text{Equation 120}$$

Where $M_{total}= W_O H^2/2$, $W_1 H^2/3$, or PH for the three standard load cases discussed herein.

M_{fc} can be used as a measure of efficiency ref (47). By taking M_i, the actual resisting moment of outrigger i from eq. (72) and expressing it as a percentage of M_{fc} give:

$$M_i^* = \frac{M_i}{M_{fc}} * 100 = \frac{100W_0}{6EIS}\left(X_{i+1}^2 + X_{i+1}X_i - X_iX_{i-1} - X_{i-1}^2\right)\left(\frac{2EI}{W_0H^2}\right)$$ Equation 121

Or

$$M_i^* = \frac{33.3\left(X_{i+1}^2 + X_{i+1}X_i - X_iX_{i-1} - X_{i-1}^2\right)}{H^2}$$ Equation 122

Where M_i^* is the "percentage of efficiency" of the i^{th} outrigger and $M_i^* = 100$ represents perfect composite core and column action. The M_i^* values were calculated for the WO load case by Stafford Smith and Nwaka ref (47). They are presented in Table 3.2.5.6 for equi-spaced outrigger braced structures with a top outrigger. The values of M_i^* are useful because they can be used to calculate the actual resisting moment in any structure of similar outrigger spacing by using:

$$M_i = \frac{M_i^*}{100EIS}\left(M_{total}\right)$$ Equation 123

The author calculated the M_i^* values for the W_1 and P load cases in the same manner. They are presented in Tables 13 and 14 respectively for equi-spaced outrigger structures with a top outrigger. These arrangements are considered those most likely to occur in a real structure.

Based on eq. (122) it can be seen that the efficiency of the outrigger system based on full composite action between the core and columns as being 100% efficient is based only on the number and location of the outriggers. Tables 13 and 14, show that the load type also affects the system efficiency.

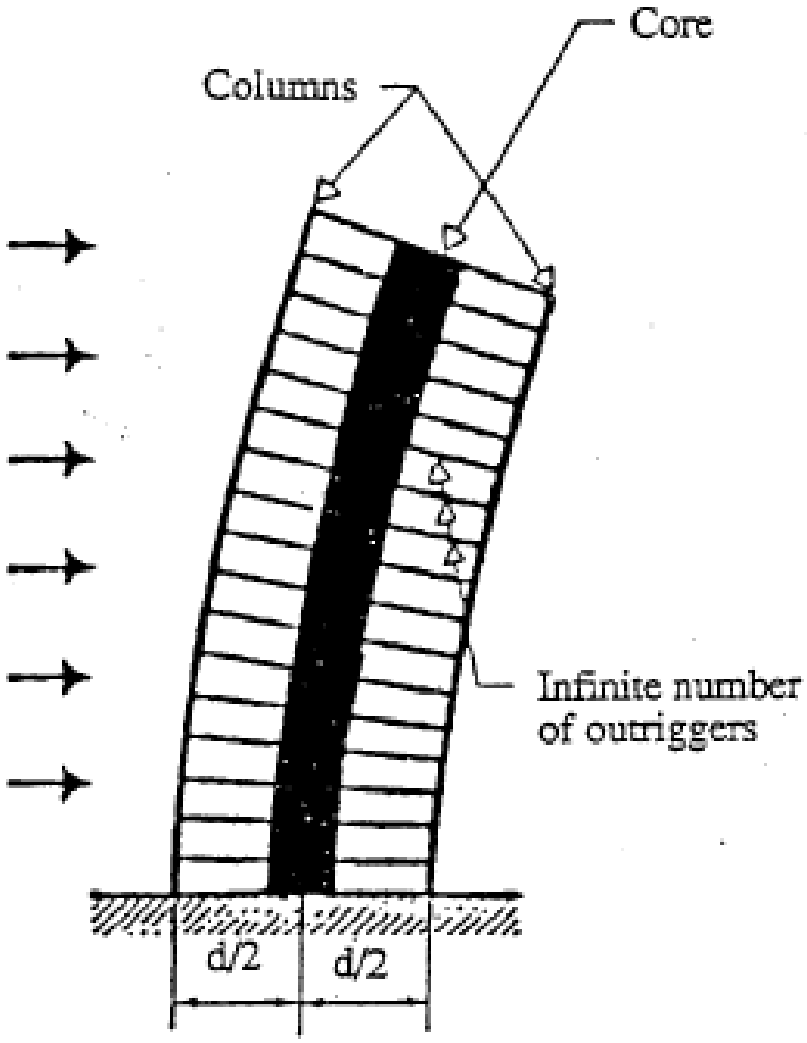

Figure 39: Fully Composite Outrigger Braced Structure ref (47)

Table 12: Performance of Equi-sapced Outrigger with a Top Outrigger- Uniform Load ref (47)

Number of Outriggers	Distance From Top H				M_i as % of M_{fc}				
	X_1	X_2	X_3	X_4	M_1*	M_2*	M_3*	M_4*	∑M*
1	0				33.2				33.2
2	0	0.5			8.3	50			58.3
3	0	0.33	0.67		3.6	23.1	43.9		70.6
4	0	0.25	0.5	0.75	2.1	12.5	25	37.5	77.1

Table 13: Performance of Equi-sapced Outrigger with a Top Outrigger- Triangular Load

Number of Outriggers	Distance From Top H				M_i as % of M_{fc}				
	X_1	X_2	X_3	X_4	M_1*	M_2*	M_3*	M_4*	∑M*
1	0				37.5				37.5
2	0	0.5			10.94	53.12			64.06
3	0	0.33	0.67		4.99	26.98	43.72		75.69
4	0	0.25	0.5	0.75	2.92	16.03	27.73	34.77	81.45

Table 14: Performance of Equi-sapced Outrigger with a Top Outrigger- Concentrated Load

Number of Outriggers	Distance From Top H				M_i as % of M_{fc}				
	X_1	X_2	X_3	X_4	M_1*	M_2*	M_3*	M_4*	∑M*
1	0				50				50
2	0	0.5			25	50			75
3	0	0.33	0.67		16.67	33.33	33.33		83.27
4	0	0.25	0.5	0.75	12.5	25	25	25	87.5

The $\sum M_i^*$ values show that the outriggers subjected to the W_1 and P load cases are more efficient (relative to those subjected to the W_O load) in providing cantilever action. This is a result of the greater individual M_i* values for these cases. Because the analysis is based on rotational compatibility of the core and exterior column "spring" load cases that cause greater core rotation will yield greater M_i values. The $\sum M_i^*$ values also illustrate the "diminishing returns" of adding additional outriggers. A graph of number of outriggers vs. $\sum M_i^*$ would yield a curve whose slope (the measure of the benefit of additional outriggers) which would quickly diminish beyond 4 outriggers and eventually go to zero at i =INF. Also of interest are the M_i^* values for the P load case in Table 14.Inspection of eqs.(62), (89), and (107) reveals that the magnitude of the outrigger resisting moments are only a function of the number and spacing of the outriggers times a constant which involves core and column rigidities. Therefore it is possible based on the linear equations that govern the M_i values for the P load case to arrange the outriggers from i =2 to N so that they provide equal resistance. However, this can only be accepted mathematically.

The greater resistance provided by the top outrigger in the WI and P load cases can be explained per the principles of mechanics. If a structure with a single outrigger structure at the top of the building were subjected to P, W_1, and W_O load cases that produce equal base moment, the resulting M_i values would be in the proportion 0.5: 0.375: 0.333 for the three cases respectively. This is the same proportion that the maximum free rotations of a cantilever beam subjected to the same loading scenario would exhibit.

3.2.6 Incorporating Outrigger Flexibility

In the real structure infinite flexural rigidity of the outrigger(s) would be practically impossible to achieve. In this section a method for introducing outrigger flexibility will be presented and some indication of outrigger flexibility on system performance will be discussed.

Previously the rotation of the core at any location X_i of an outrigger was determined from the effects of external load, the outrigger resisting moment M_i and the perimeter column axial deformation. Figure 40a is a beam model of an outrigger i. M_i is the outrigger resisting moment and the pinned connection represents the connections to the exterior columns. The static reactions due to a moment M_i applied at the center (c) of the "beam" are shown. The resulting conjugate beam loading and reactions are shown in Figure 40. The slope at any point is equal to the shear at that location in the conjugate beam. Therefore the rotation at c becomes:

$$\theta_c = \frac{M_1 d}{12(EI)_o}$$ Equation 124

Where $(EI)_o$ is the effective flexural rigidity of the outrigger as shown in Figure 38b.

The effective flexural rigidity of the actual wide-column arrangement shown in Figure 41a is ref (100):

$$(EI)_o = (1+(a/b))^3 (EI')_o$$ Equation 125

Where: a= core width/2

b= distance from the perimeter column to the "face" of the core.

I'= the actual outrigger moment of inertia

Eq. (124) can be incorporated into the rotation compatibility equations for any loading. Stafford Smith and Salim ref (100) have done this and studied the effects of outrigger flexibility for the uniformly distributed load case. In doing so the following dimensionless parameter was established:

$$\omega = \frac{\beta}{12(1+\alpha)}$$ Equation 126

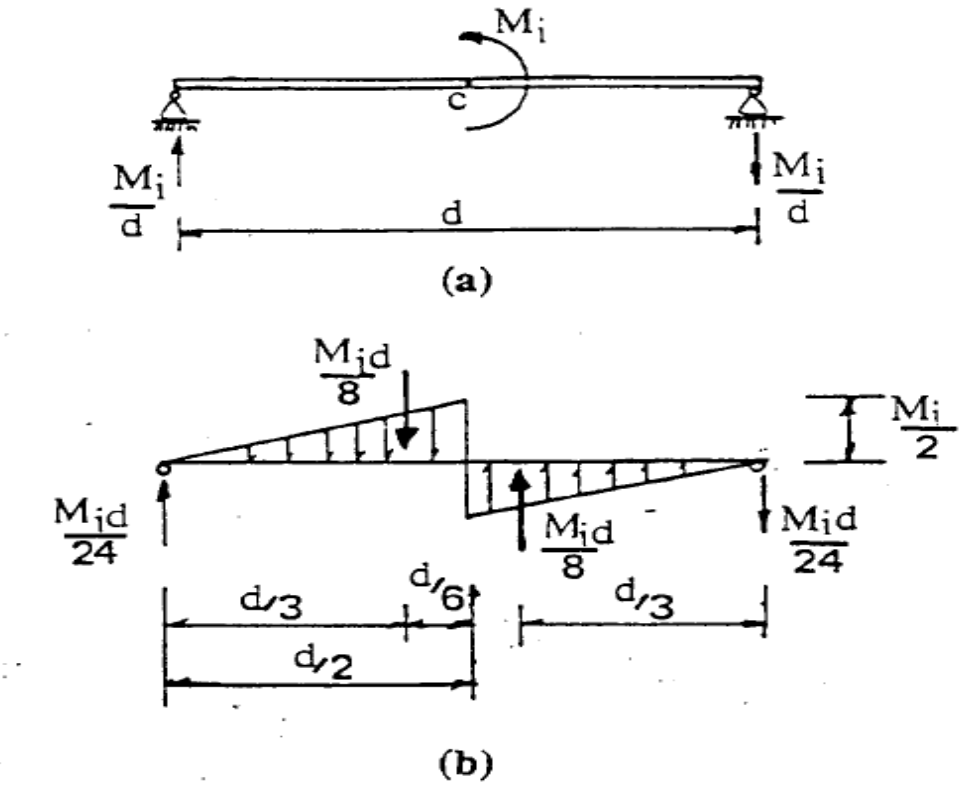

Figure 40: Outrigger Conjugate Beam Model ref (100)

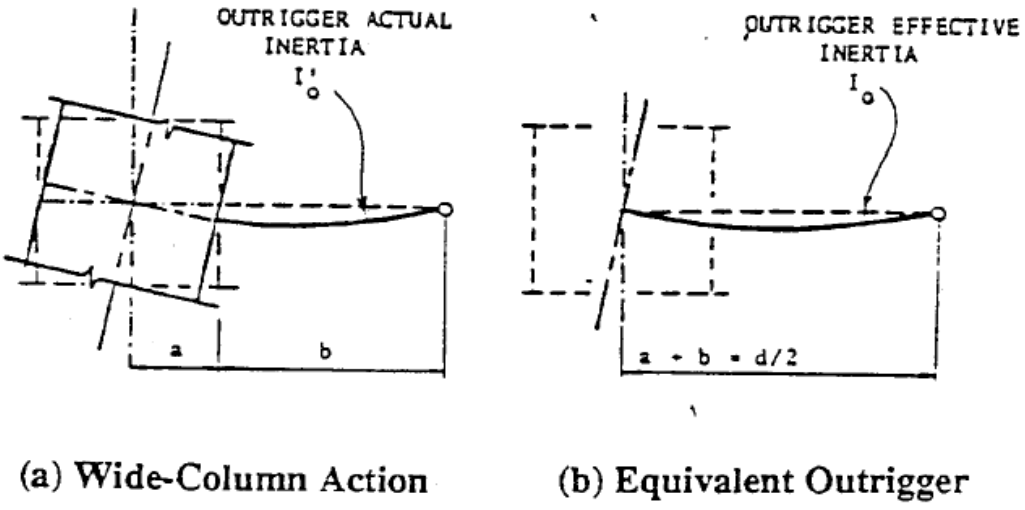

Figure 41: Outrigger Wide-Column Analogy ref (100)

Where: $\alpha = \frac{2EI}{d^2 AE_c}$ and $\beta = \frac{EI}{(EI)_o}\frac{d}{H}$

Figures 43 and 44 show how the parameter ω effects drift and moment reduction efficiencies for optimum located outrigger systems subjected to the W_O load case. (See Table 3.2.5.4 for the optimum outrigger locations). Figure39 illustrates the change in optimum location for a single outrigger system due to outrigger flexibility. The figure shows that increased outrigger flexibility results in an optimum location higher up in the structure. The best location ranges from approximately 55% to 78% of the building height from the base. Tables for double, triple, and quad-braced systems are of similar form ref (100).

From Figures 43 and 44 it is observed that increased outrigger flexibility will reduce drift and moment reduction efficiencies. Figure 43 shows that the drift reduction efficiency is affected less and less by outrigger flexibility with each additional outrigger added to the system. Efficiency reduction is more prominent for systems with greater perimeter column stiffness and less so for systems with a lower core to outrigger stiffness ratio. This implies that outrigger systems that employ belt trusses (subsequently increasing the mobilized column area per outrigger) are more susceptible to reduced outrigger effectiveness for flexible outriggers. The ω parameter can be used as a guide to the accuracy of the rigid outrigger results as compared to those of a matrix type analysis.

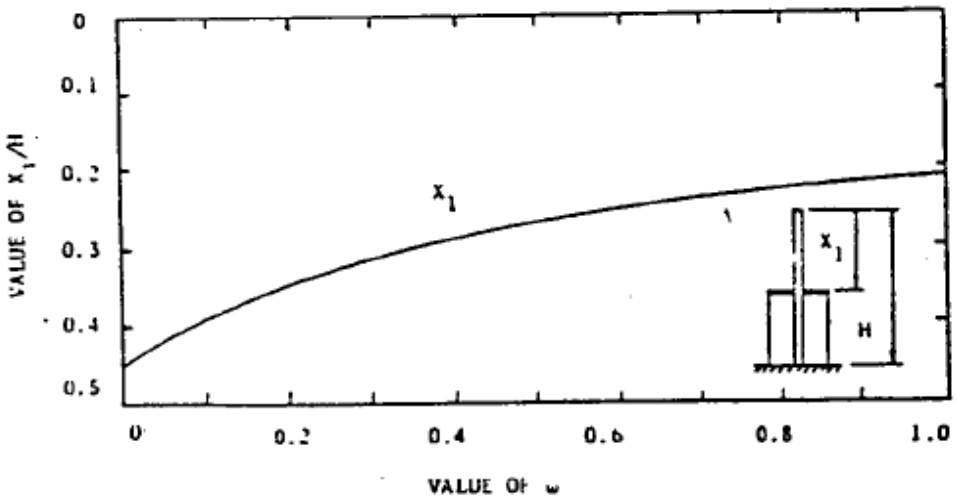

Figure 42: Optimum Outrigger Location vs. ω ref (100)

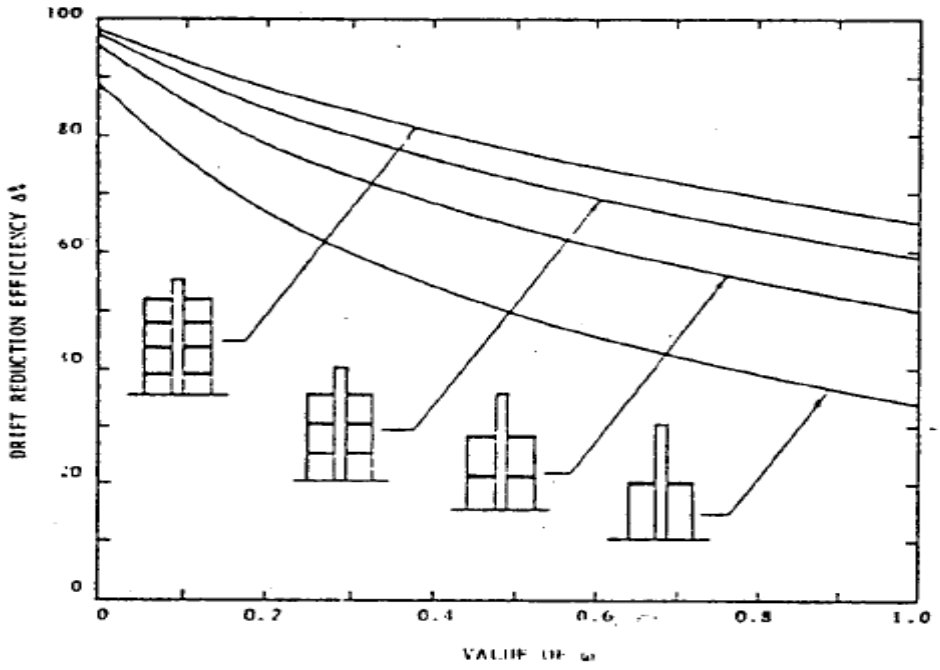

Figure 43: Drift Reduction Efficiency Optimum Location Outriggers ref (100)

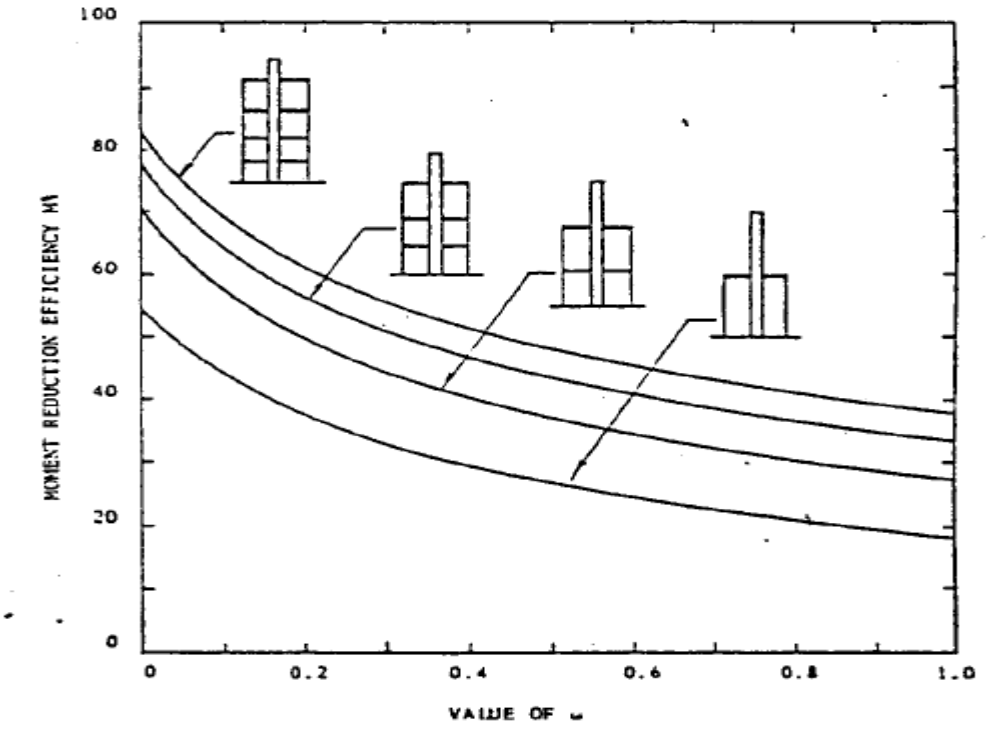

Figure 44: Moment Reduction Efficiency Optimum Location Outriggers ref (100)

3.3 Computer Program Outigger_Program

3.3.1 Program Description and Use

Program Outrigger_Program was written to apply the equations of Sections 3.2.1, 2, 3, and 4 for Multi-Outrigger Braced Tall Building Structures. The program was written in in Matlab® graphical user interface and compiled with version2009a. The linker used to create the executable file was version 7.8.0. The computer requirements are identical for MOBTBS to those described for program Wall_Frame_2D in Section 2.3.1.

The analysis assumes no twisting of the building is allowed i.e., the bent is considered a section of a symmetrical structure. The building material is assumed to behave linear elastically; therefore gravity load effects can be superimposed. The shear core and frame must be of uniform properties and extend the full height of the structure. Horizontal outrigger trusses must be considered fixed to the core and pinned to the perimeter columns. Incidental bending resulting from fixed connections at the

exterior columns can be neglected at the designer's discursion. The foundation is assumed to provide full fixity. Any foundation translation or rotation will violate the results of the moment area formulations for rotation and lateral deflection.

Program structure consists of a main program called Outrigger_Program and subroutines. The graphics subroutine to be discussed in Section 3.3.2. The executable version of Outrigger_Program is included in a CD in the back of this thesis. A condensed variable list is included in Section 3.3.1.1.

To start the program the user simply double clicks Outrigger_Program.EXE at the appropriate PC prompt, then select from the drop up menu bottom the load case to be study. In this program the input values can be change at any time in the screen. The required input variables are E, XI, EC, AC, DC, H, LOAD, and the applicable load type W_O, P, or W_1. Only one type of load is allowed per analysis. Average values can be used for XI and AC for non-uniform structures. Subsequent input includes the location(s) of the outrigger(s) with respect to the base of the structure. The outriggers should be labeled from lowest to highest. After each section the input is echoed and the user has the option of retyping erroneous data.

The user has two output options. The output consists of a full input echo, the outrigger resisting moments, and the core moment and lateral deflections at equally spaced intervals along H. At each outrigger level two output points are required to property show the core moment diagram. The number of output points does not affect numerical accuracy but twenty to thirty points is suggested for analysis of structures with several outriggers for graphical purposes. Repeated analyses can be performed without leaving the program environment. Two examples utilizing this program are presented in Section 3.4.

3.3.1.1 Condensed Variable List – Outrigger_Program

Listed below is a condensed variable list for program Outrigger_Program:

- Modulus of elasticity of core material (E)
- Moment of inertia of core about an axis perpendicular to the load direction (IX)
- Modulus of elasticity of exterior column material (EC)
- Exterior column cross-sectional area (AC)
- Distance between exterior columns parallel to the load
- Total building height (H)
- Outrigger locations with respect to the base (D)
- The Load type: uniform Distribute (W_o), Triangular (W_1), Concentrated (P)
- Uniform (W_o): Value of distributed lateral load
- Concentrated (P): Value of distributed lateral load
- Triangular (W_1): Maximum value of a linearly distributed load which has a magnitude of W_1 at the top of the building and zero at the base of the building

3.3.2 Description of Graphics

The description of graphics for program Outrigger_Program is identical to that for program Wall_Frame_2D discussed in Section 2.3.3. MOBTBS however, displays lateral deflection vs. height and the core moment vs. height only. The requirements and procedure for obtaining graphic hardcopy is also described in Section 2.3.3.

3.4 Example Analyses

In this section two examples will be presented using program Outrigger_Program. The first example is a 40 story composite structure consisting of a reinforced concrete core and steel exterior. It will be analyzed using MOBTBS and three load cases of equal overturning moment for one, two, and three outrigger systems.

The second example is the 60 story composite structure previously analyzed in Section 2.4.2. Here the building will be reanalyzed for one, two, and three outrigger arrangements to compare outrigger_Program results to those of a SAP2000 analysis for a uniformly distributed load.

3.4.1 Example 3-1: 40 Story Composite Building

3.4.1.1 Statement of the Problem

A typical braced bent from a 40 story structure consisting of a reinforced concrete shear wall core and a steel exterior frame and outrigger truss (es) will be analyzed. The Outrigger_Program and three loading conditions of equal base overturning moment will be "used to show a comparison of the results for one, two, and three outrigger systems. The input data for these analyses is shown in Table 15.

The exterior column area is the sum of that for six columns of cross-sectional area equal to 125.25 square inches (sq. in.) due to the assumed engagement of a rigid belt truss at each outrigger level. Units for the analyses are kips (k) and feet (ft.).

3.4.1.2 Method of Analysis

The 40 story structure will be analyzed for nine different configurations of varied load type and number of outriggers. The structure will be analyzed for outrigger configurations of one at the 40^{th} story, one at the 40^{th} and 20^{th} stories, and one at the 40^{th}, 27^{th}, and 15^{th}stories. These locations are considered practical locations for the given number of outriggers. Results of these analyses are presented in Section 3.4.1.3.

Table 15 Example 3-1: Input Data for Outrigger_Program -40 Story Composite Building

E=518400 k/ft^2	1: D1=480 ft.
XI=1302.0 ft^4	2: D1=240 ft., D2= 480 ft.
EC=4176000 k/ft^2	3: D1=180 ft., D2=324 ft., D3=480 ft.
AC=5.22 ft^2	Load 1, 2, and 3
DC=75 ft.	1: W_o=0.1042 k/ft.
H=480 ft.	2: P=25 k
N= Any value greater than cero	3: W_1=0.1563 k/ft.

Note:

1. Three load cases (W_o, W_1, P) used for each outrigger arrangement
2. Story height= 12 ft.
3. AC= 6*125.25 in^2
4. Concrete core wall: width= 25 ft., thickness= 1 ft.

3.4.1.3 Results

The Outrigger_Program output files for the single, two and three outrigger analyses are shown in Tables 16, 17 and 18 for the uniform, triangular, and concentrated load cases respectively.

Figure 45 and Figure 46 show the lateral deflection and normalized core moment vs. height for the single outrigger case. The lateral deflections and normalized core moment for the two outrigger case are presented in Figures 47 and 48 respectively. For the three outrigger case lateral deflections and normalized core moment vs. height are given in Figures 49 and 50.

Table 16: Example 3-1: 40 Story Composite Building, Outrigger_Program Output, Uniform, Triangular, and Concentrated Load. One Outrigger

One Outrigger						
	W_0=0.1042 k/ft.		W_1=0.1563 k/ft.		P=25 kips	
	M_1=3957.71 k/ft.		M_1=4452.42 k/ft.		M_1=5934.66 k/ft.	
	D_1=480.0 ft.		D_1=480.0 ft.		D_1=480.0 ft.	
Height (ft.)	Lateral Deflection (ft.)	Core Moment (K/ft.)	Lateral Deflection (ft.)	Core Moment (K/ft.)	Lateral Deflection (ft.)	Core Moment (K/ft.)
0	0	8.46100E+03	0	7.5514E+03	0	6.0653E+03
48	0.012401	5.76540E+03	0.011865	5.7568E+03	0.009669	4.8653E+03
96	0.044551	3.72470E+03	0.043392	3.9983E+03	0.035947	3.6653E+03
144	0.089484	1.92420E+03	0.088588	2.3117E+03	0.074736	2.4653E+03
192	0.141054	3.63670E+02	0.141705	7.3324E+02	0.121941	1.2653E+03
240	0.193933	-9.56750E+02	0.197367	-7.0122E+02	0.173465	6.5335E+01
288	0.243614	-2.03710E+03	0.250686	-1.9556E+03	0.225213	-1.1347E+03
336	0.286411	-2.87740E+03	0.29739	-2.9940E+03	0.273087	-2.3347E+03
384	0.319453	-3.47760E+03	0.333947	-3.7802E+03	0.312991	-3.5347E+03
480	0.348901	0.00000E+00	0.366904	0.0000E+00	0.352507	0.0000E+00

Table 17: Example 3-1: 40 Story Composite Building, Outrigger_Program Output, Uniform, Triangular, and Concentrated Load. Two Outriggers

Two Outrigger						
	W_0=0.1042 k/ft.		W_1=0.1563 k/ft.		P=25 kips	
	M_1=5936.56 k/ft.		M_1=6307.60 k/ft.		M_1=5934.66 k/ft.	
	M_2=989.43k/ft.		M_2=1298.62k/ft.		M_2=2967.33 k/ft.	
	D_1=240.0 ft.		D_1=240.0 ft.		D_1=240.0 ft.	
	D_2=480.0 ft.		D_2=480.0 ft.		D_2=480.0 ft.	
Height (ft.)	Lateral Deflection (ft.)	Core Moment (K/ft.)	Lateral Deflection (ft.)	Core Moment (K/ft.)	Lateral Deflection (ft.)	Core Moment (K/ft.)
0	0	5.08E+03	0	4.40E+03	0	3.10E+03
32	0.003454	3.53E+03	0.003032	3.20E+03	0.002148	2.30E+03
64	0.012278	2.09E+03	0.01092	2.01E+03	0.007782	1.50E+03
96	0.024286	7.56E+02	0.021861	8.44E+02	0.015689	6.98E+02
128	0.037456	-4.71E+02	0.034087	-2.90E+02	0.024654	-1.02E+02
160	0.049926	-1.59E+03	0.045878	-1.38E+03	0.033466	-9.02E+02
240	0.067278	2.01E+03	0.062796	2.45E+03	0.046851	3.03E+03
256	0.068069	1.62E+03	0.063709	2.01E+03	0.047959	2.63E+03
288	0.071364	9.31E+02	0.067669	1.20E+03	0.053017	1.83E+03
320	0.076086	3.44E+02	0.073459	4.80E+02	0.060856	1.03E+03
352	0.081343	-1.36E+02	0.079991	-1.32E+02	0.070262	2.33E+02
384	0.086408	-5.09E+07	0.086337	-6.26E+02	0.080021	-5.67E+02
416	0.090714	-7.76E+02	0.091749	-9.93E+02	0.088919	-1.37E+03
480	0.095591	0	0.097762	0	0.099278	0

Table 18: Example 3-1: 40 Story Composite Building, Outrigger_Program Output, Uniform, Triangular, and Concentrated Load. Three Outriggers

Three Outrigger						
	W0=0.1042 k/ft.		W1=0.1563 k/ft.		P=25 kips	
	M1=5209.33 k/ft.		M1= 5159.87k/ft.		M1=4005.90 k/ft.	
	M2=2359.89k/ft.		M2=2876.10k/ft.		M2= 3709.17k/ft.	
	M3=418.03K/ft.		M3=576.10K/ft.		M3=1928.77K/ft.	
	D1=180.0 ft.		D1=180.0 ft.		D1=180.0 ft.	
	D2=324.0 ft.		D2=324.0 ft.		D2=324.0 ft.	
	D3=480ft.		D3=480ft.		D3=480ft.	
Height (ft.)	Lateral Deflection (ft.)	Core Moment (K/ft.)	Lateral Deflection (ft.)	Core Moment (K/ft.)	Lateral Deflection (ft.)	Core Moment (K/ft.)
0	0	4.03E+03	0	3.39E+03	0	2.36E+03
24	0.00155	2.86E+03	0.001319	2.49E+03	0.00092	1.76E+03
48	0.005541	1.75E+03	0.004766	1.60E+03	0.003339	1.16E+03
72	0.011026	6.96E+03	0.009576	7.11E+02	0.006744	5.56E+02
96	0.017109	-2.95E+02	0.014994	-1.61E+02	0.010624	-4.38E+01
120	0.022945	-1.23E+03	0.020275	-1.02E+03	0.014467	-6.44E+02
180	0.031369	1.92E+03	0.028146	2.12E+03	0.020549	1.86E+03
192	0.031842	1.55E+03	0.028662	1.73E+03	0.021077	1.56E+03
216	0.033707	8.63E+02	0.030723	9.96E+02	0.023068	9.62E+02
240	0.036314	2.33E+02	0.033637	2.99E+02	0.025881	3.62E+02
264	0.039123	-3.37E+02	0.03681	-3.53E+02	0.029002	-2.38E+02
324	0.043968	8.50E+02	0.042327	1.12E+03	0.034797	1.97E+03
336	0.044411	6.62E+02	0.042838	8.82E+02	0.035495	1.67E+03
360	0.045685	3.32E+02	0.04438	4.55E+02	0.037897	1.07E+03
384	0.047247	6.21E+01	0.046315	9.61E+01	0.041214	4.71E+02
408	0.048865	-1.48E+02	0.048337	-1.91E+02	0.044932	-1.29E+02
432	0.050362	-2.98E+02	0.050201	-4.02E+02	0.048541	-7.29E+02
480	0.052529	0	0.052808	0	0.05338	0

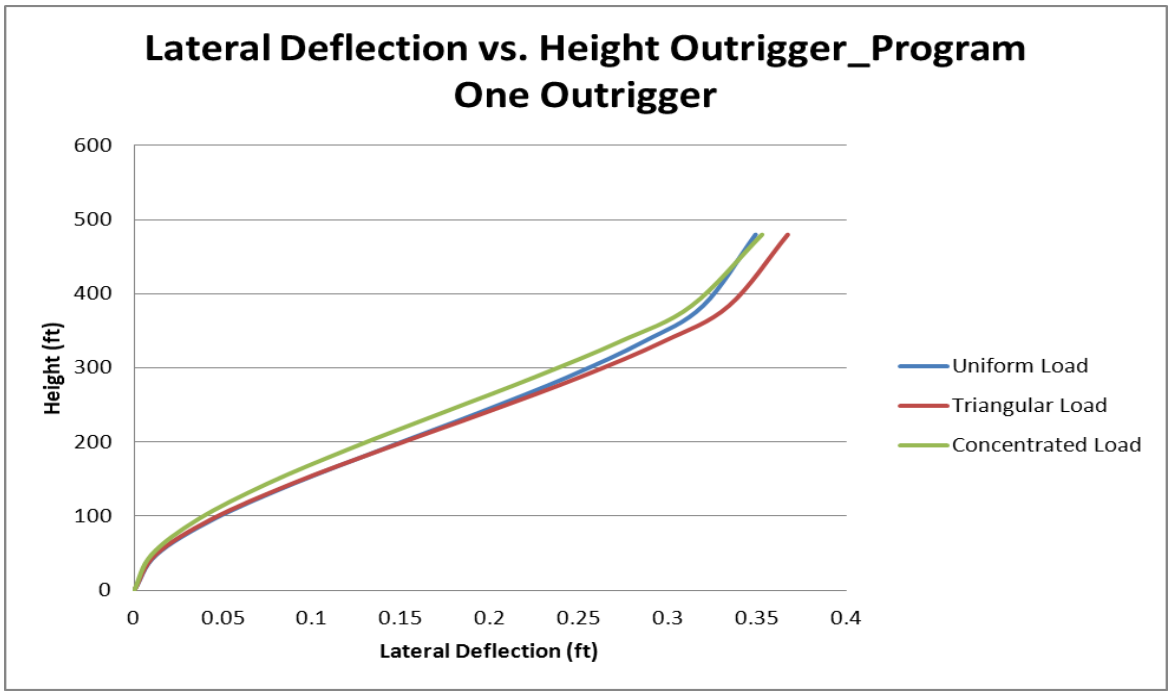

Figure 45: Example 9-1: 40 Story Composite Building, Lateral Deflection Outrigger Program, One Outrigger

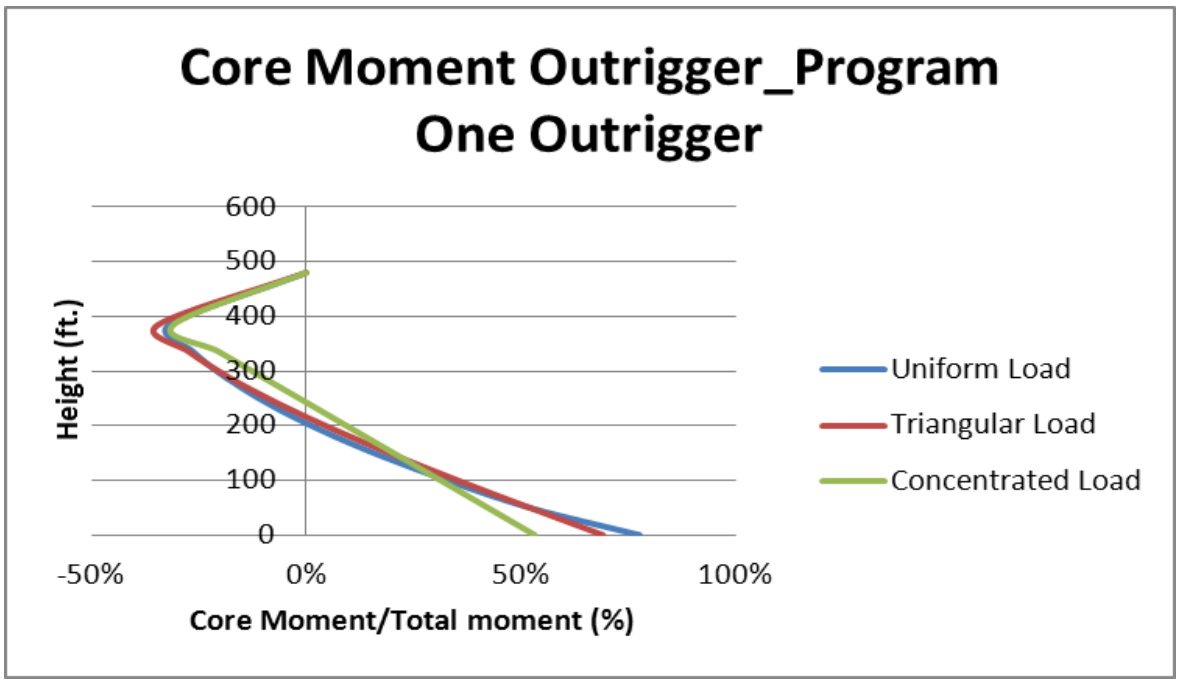

Figure 46: Example 9-1: 40 Story Composite Building, Core Moment Outrigger Program, One Outrigger

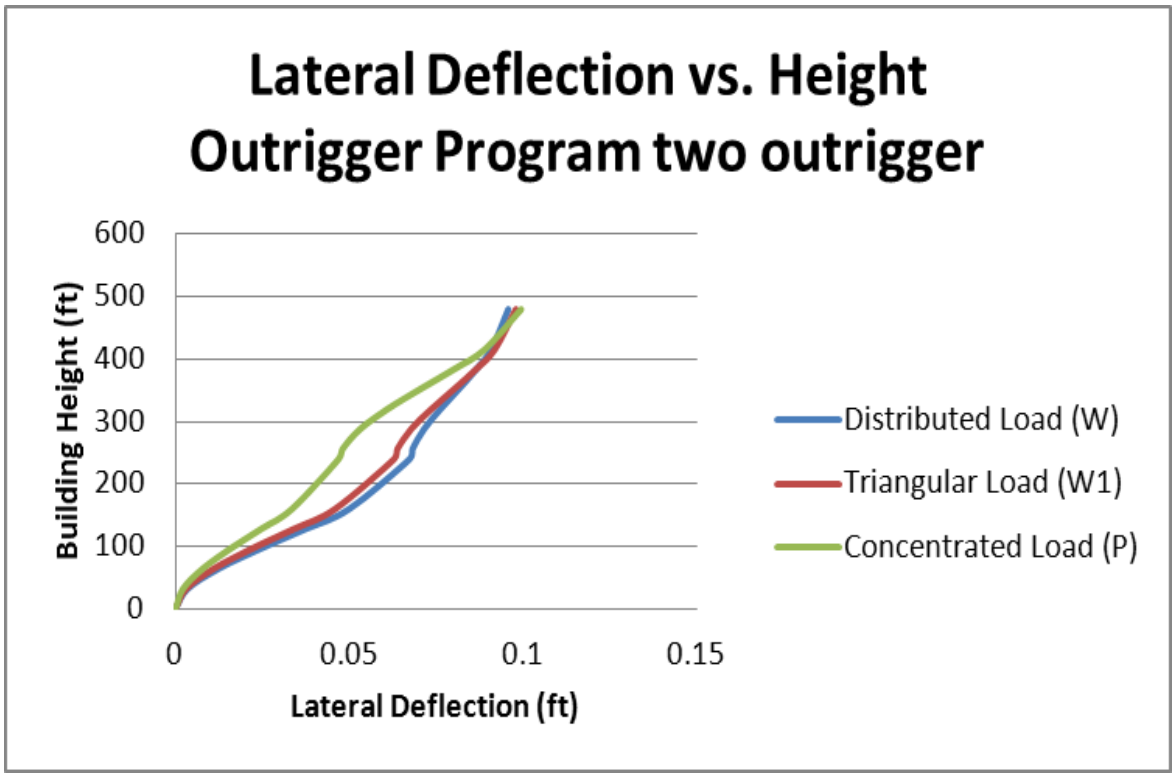

Figure 47: Example 9-1: 40 Story Composite Building, Lateral Deflection Outrigger Program, Two Outriggers

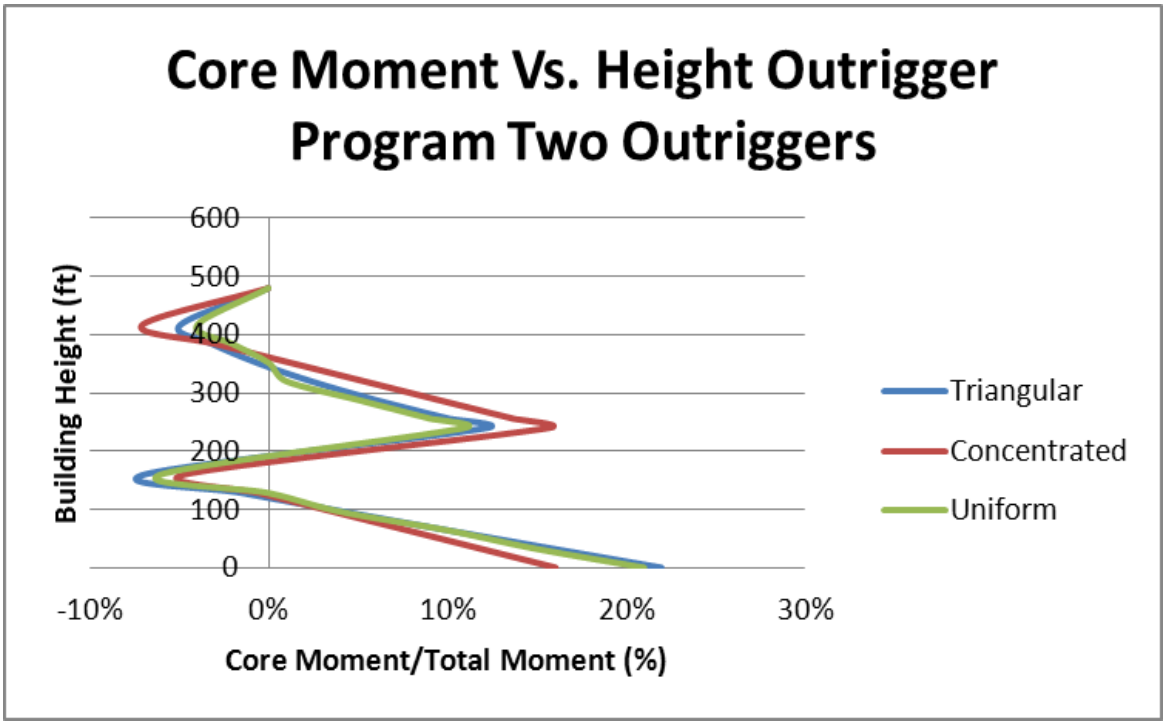

Figure 48 : Example 9-1: 40 Story Composite Building, Core Moment Outrigger Program, Two Outriggers

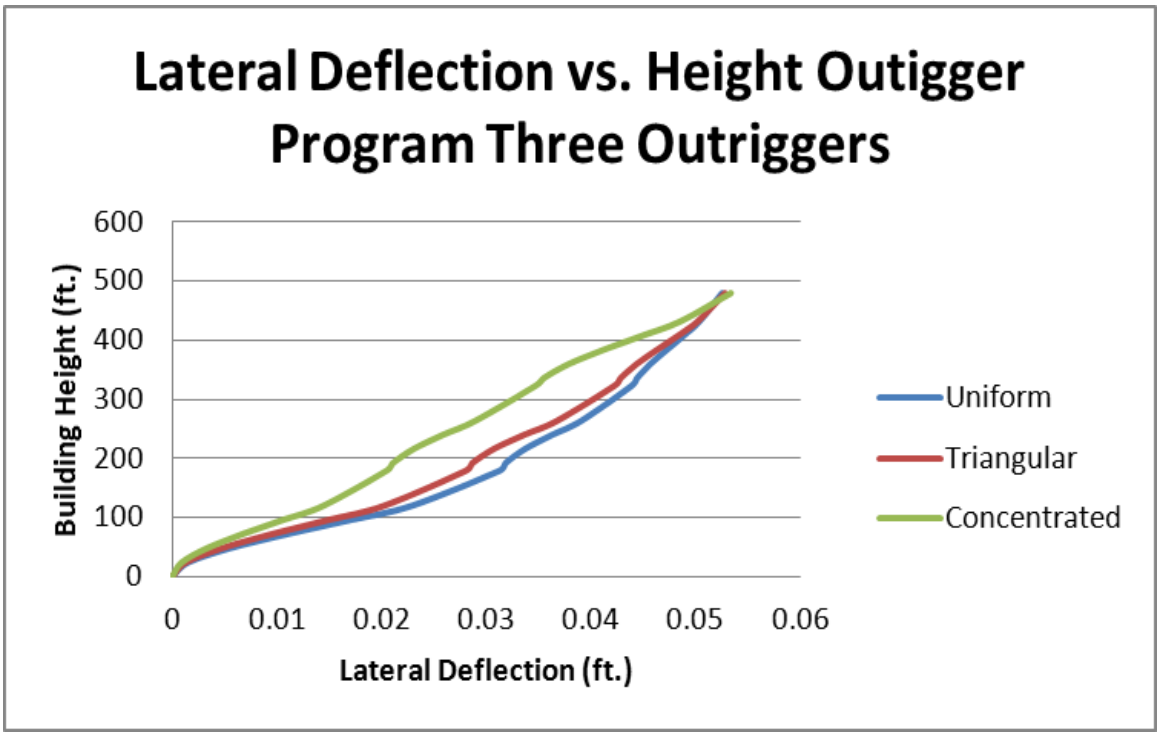

Figure 49: Example 9-1: 40 Story Composite Building, Lateral Deflection Outrigger Program, Three Outriggers

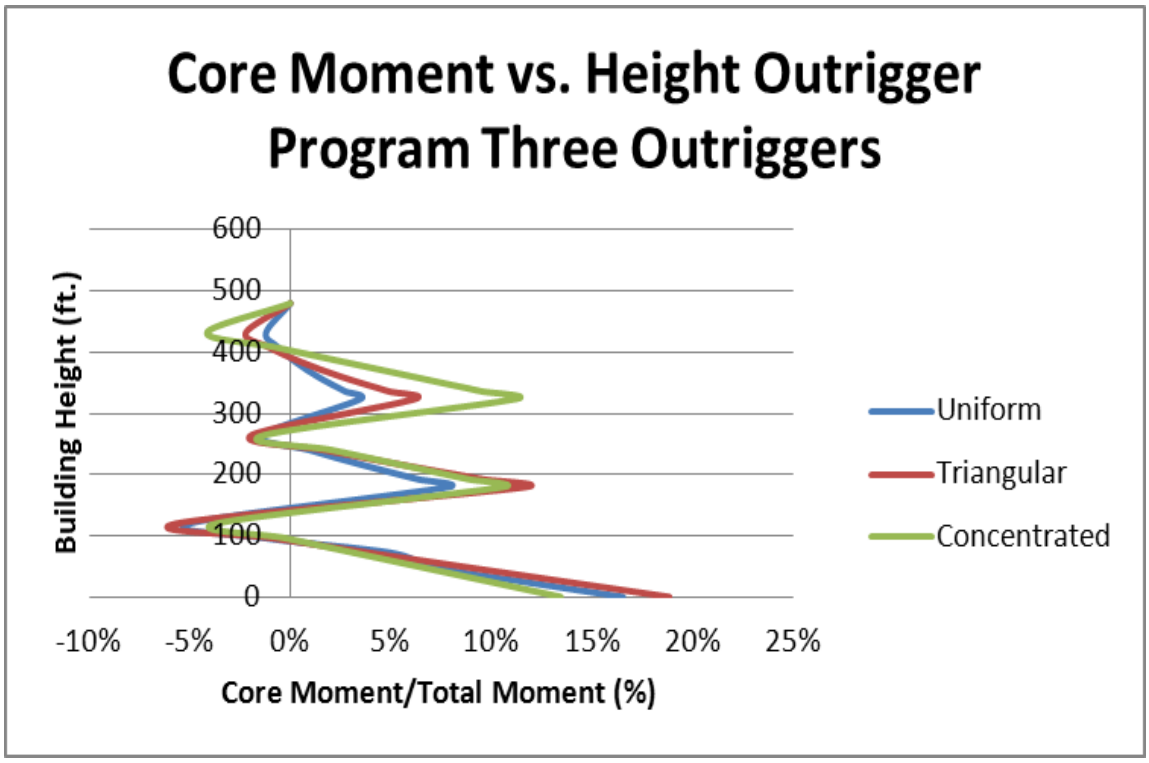

Figure 50: Example 9-1: 40 Story Composite Building, Core Moment Outrigger Program, Three Outriggers

3.4.2 Example 3-2: 60 Story Steel Building

3.4.2.1 Statement of the Problem

In this example the 60 story steel structure previously analyzed considering shear wall-frame interaction in Section 2.4.2 will be reanalyzed as an outrigger braced system using Outrigger Program and SAP2000. The frame will be analyzed for a uniformly distributed load with three different outrigger arrangements. Figures 51, 52, and 53 shows the SAP2000 models used for the one, two, and three outrigger analyses respectively.

The member properties are the same as those shown in Table 6 except that the new X brace are W36x330 sections. The outriggers have been located per Table 11 (using the uniform load values) to provide maximum drift reductions.

3.4.2.2 Methods of Analysis

The 60 story bent will be analyzed approximately via the rigid outrigger approach and the results compared to those of an "exact" matrix analysis. Arrangements of one, two, and three outriggers will be used for comparison for a uniformly distributed load case.

For the SAP2000 analyses the columns will be considered continuous through the joints. All girders except those within and surrounding the outriggers are assumed pin-connected at both ends. The bracing members in the vertical and horizontal trusses are modeled as plane frame members. The column connections to the foundation are considered fixed except where the truss bracing members meet the base. Load is input as a positive X uniform load along the left exterior column line of Figures 51, 52, and 53. To allow a "pure" comparison of the lateral load analyses no member self-weight is considered. Results are compared in Section 3.4.2.3.

Table 19: Input Data for Outrigger Program-60 Story Steel Building

E=518400 k/ft^2	1: D1=420 ft.
XI=1302.0 ft^4	2: D1=252 ft., D2= 516 ft.
EC=4176000 k/ft^2	3: D1=180 ft., D2=348 ft., D3=564 ft.
AC=5.22 ft^2	Load 1,
DC=75 ft.	1: W_o=0.600 k/ft.
H=750 ft.	
N= Any value greater than cero	

Note:

Story height= 12 ft.

AC= 6*125.25 in2

Concrete core wall: width= 25 ft., thickness= 1 ft.

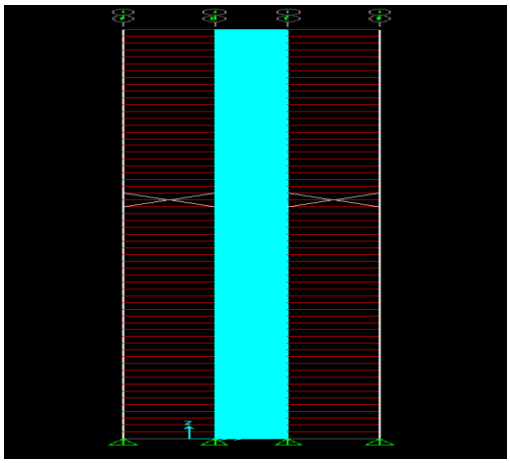

Figure 51: SAP2000 Model Example 3-2 with One Outrigger

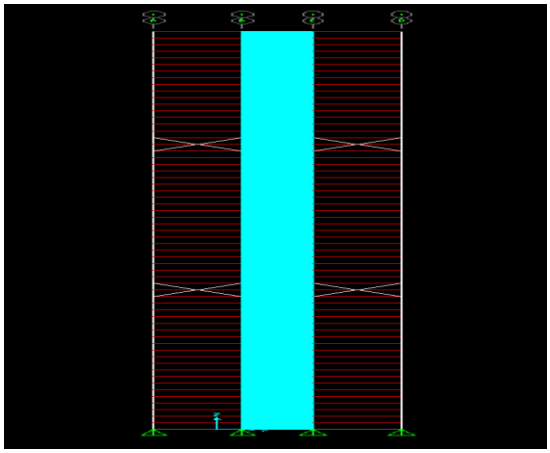

Figure 52: SAP2000 Model Example 3-2 with Two Outriggers

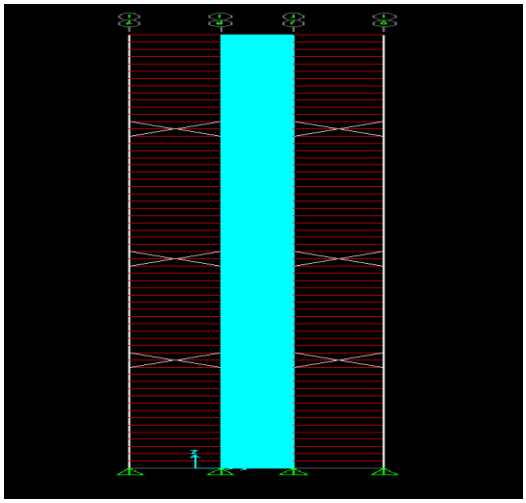

Figure 53: SAP2000 Model Example 3-2 with Three Outriggers

3.4.2.3 Results

Table 20 show the comparison of the Outrigger Program output files for the one, two, and three outrigger cases respectively, and SAP2000 outputs, outputs for SAP2000 is not included here.

As show in Table 20 the differences are in the range of 2 in maximum.

Table 20: Outrigger Program vs. SAP2000

	Lateral Displacement (in)	
Number of Outriggers	SAP2000	Outrigger Program
1	9.2393	11.6874
2	7.386	9.8341
3	6.5485	8.9966

3.5 Discussion of Results

The examples presented show the rigid outrigger approach yields results adequate for preliminary analysis and member sizing. The accuracy as compared to an exact analysis will depend on core properties and actual outrigger stiffness. The preliminary analysis allows rapid re-analysis which allows parametric studies to be accomplished in the design office for a variety of configurations.

The results for example 3-1 shows that the varied load types had minimal effect on the overall moment distribution in the core. The uniform and triangular distributed load cases are almost identical for core moment results. The single concentrated load case cannot be considered a good approximation to the actual total wind or seismic loading and since load type has negligible effect on the Outrigger Program analysis time or input preparation it should not have to be used as such. The concentrated load case produces greater outrigger resisting moments and for that reason the maximum drifts for all three loadings are approximately equal. The greater deflections usually expected for the P case are reduced due to its large M_i values. This is most evident in the middle stories of the two and three outrigger cases.

The accuracy of the rigid outrigger approach as compared to a matrix analysis is shown in the data for example 3-2. The Outrigger program neglects axial deformation, cannot account for the outrigger flexural deformation, and is unable to account for the rotation due axial deformation of the bracing members. The latter effect is partially accounted for through the use of the truss efficiency factors. Another reason for the greater SAP2000 drift is the fact that the actual outrigger resisting moments are less than those for the rigid outrigger cases. Based on the actual amount of moment reduction in the core from directly above to directly below each outrigger the SAP2000 outrigger resisting moments are much less than those from the rigid cases.

Note found that the greater outrigger resisting moments of the rigid outrigger case will cause an underestimation of the moment in the core of the real structure in sections away from the outriggers. It

is also interesting that the lower outriggers in the real structure have less of an effect on the moment reduction than the upper outriggers. The rigid outrigger approach is based on uniform column stiffness when in reality each of the average column stiffness below any outrigger will normally increase for a lower outrigger. Using the actual column stiffnesses around the outrigger would decrease the resisting moments of the outriggers near the top of the structure and provide more accurate results. Also better results would be expected for a monolithic core whose flexural stiffness can be more accurately represented.

The drift reduction in addition of one rigid outrigger yields a substantial reduction in the maximum drift from that of the pure cantilever. Subsequent reductions show the "diminishing returns" of adding additional outriggers. Overall the rigid outrigger approach can be considered accurate for preliminary design use. The ratio of analysis time between the Outrigger Program and SAP2000 programs is infinitesimal especially when preparation of input time is factored in.

IV. FRAMED AND BUNDLED TUBE STRUCTURES

4 Introduction

For structures of extreme height it is economical to utilize the exterior shell of the structure to resist lateral loads. Rather than individual elements providing lateral stiffness in a flexural or shear mode as in the shear wall frame structures, the framed tube incorporates the entire building plan in resisting lateral load in the ideal case a neutral axis can be considered to run perpendicular to the loaded direction and through the building's centroid. Upon lateral loading; one half the perimeter columns will be in tension and the other half in compression. In frame tubes the shear lag effect will cause warping of the floor slabs and secondary deformations in the interior partitions. Therefore, it is essential to accurately predict this behavior.

Section 4.l will discuss some of the methods previously presented for analyzing frame tube structures. Not all of the methods discussed can be considered approximate in nature. A method for analyzing framed tubes with equivalent plane frames was introduced by Coull and Subedi ref (103) and also by Rutenberg ref (127). Here the symmetry of the tube structure is capitalized on. Khan and Amin ref (128) also used equivalent plane frames to present design curves based on equivalent 10 story models. Equivalent plane frame analyses performed on framed tubes of uniform properties led to the development of design tables for framed tubes bySchwaighofer and Ast ref (129). The uniformity and regular column and girder spacing also make the tube system ideal for finite element type analyses ref (139), (131), and (2).

The orthotropic plate appr6ach introduced by Coull and Bose ref (52) for analysis of framed tubes and subsequently expended by Coull and Ahmed ref (10) for deflections of framed tubes and by Coull, Bose and Ahmed [54] for analysis of frame tubes is presented in Sections 4.2, 4.3, and 4.4. A computer program called Frame Tube Program was developed by the author to provide preliminary assessment of lateral and vertical deflections of framed and single tube structures. Previously, LeFrancois introduced program FRMTUB at W.P.I. ref (63) which provides the user with preliminary stresses and member forces of a single tube model. Stress resultants can be obtained using the equivalent tube parameters output by Frame Tube Program .One examples utilizing Frame Tube Program are presented in Section 4.5.

4.1 5.1 Literature Review

By recognizing the dominant behavioral modes of the tube structure the 3-dimensional model can be reduced to that of an equivalent plane frame [103]. We can idealize the framed tube behavior as consisting of axial deformation of the panels' normal to the applied load (flanges) and the frame action of the panels parallel to the applied load (webs). Neglecting out-of-plane effects due to rigid floor slabs allows rational application of a planar analysis.

Figure 54a shows a plan view of a doubly symmetric framed tube structure. By observing the conditions of symmetry only one quarter of the structure need be modeled (ECG). The equivalent plane frame for the structure of Figure 54a is shown in Figure 54b. Appropriate boundary conditions are shown. The panels are linked with members who are modeled to sustain compatibility and transfer vertical shear only. Hence only vertical

interaction forces are transferred to panel CG. This is easily accomplished by using relatively large stiffness properties for the link members.

Rutenberg utilized a method of successive approximations to provide for torsional analysis of framed tubes using equivalent plane frames ref (127). The method is also applicable to tube-in-tube structures. Rutenberg uncoupled the interaction of orthogonal frames by vertically constraining the corners at each floor level to allow a torsional analysis with plane frames. Here again a symmetric structure and assumption of rigid floors is required.

Khan and Amin ref (128) developed influence curves for the assessment column axial forces and girder shears of framed tubes of any proportion and height (within practical range). This was accomplished by repeated computer analyses of an equivalent 10 story tubes using various non-dimensional parameters to describe the tubes relative column and girder stiffnesses. Also suggested is a manner for preliminary framed tube analysis which utilizes equivalent end channels to represent the actual effective tube that results due to the shear lag effect.

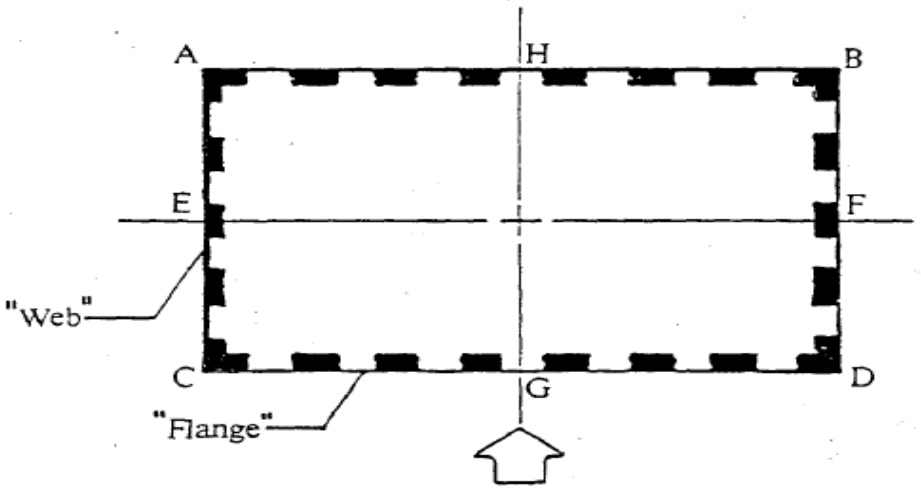

(a) Plan of Framed Tube

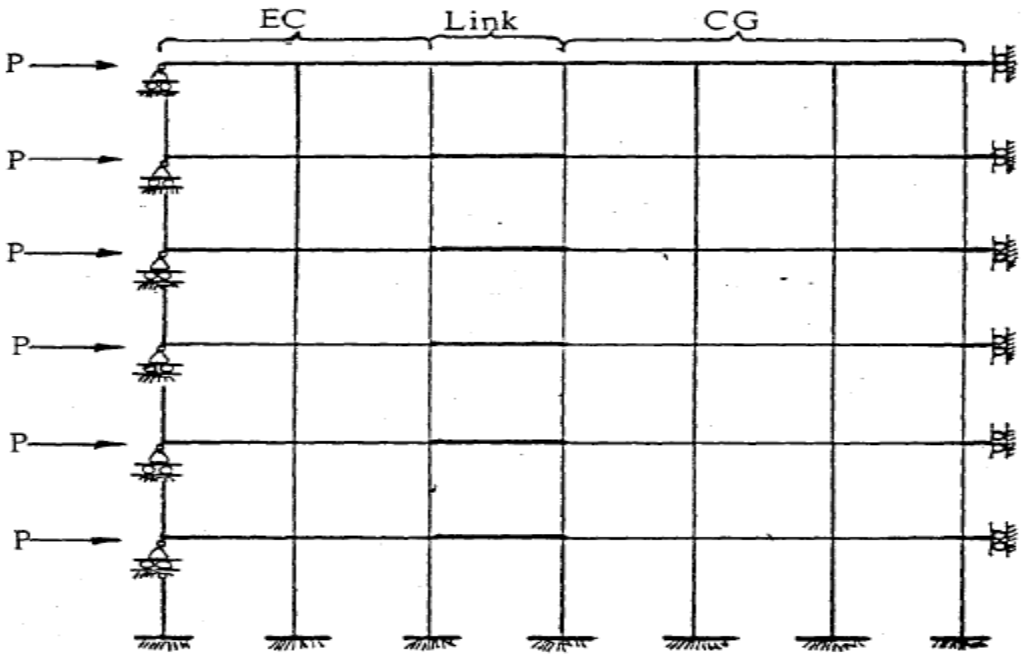

(b) Quarter Structure Plane Frame Model

Figure 54: Plane Frame Analysis of 3-D Tube

Owing to the regular frame pattern of the tube faces finite element approaches have been presented to analyze the framed tube. "Elements" which represent a column-girder intersection are introduced by Khan and Stafford Smith ref (130). The element is in the shape of a "+" with the overall width of one bay and height of one story. An element to represent edge columns is also given. The stiffness parameters can be derived using strength of material theory or the finite element method. This approach, although accurate, would be time consuming for preliminary analysis.

DeClercq and Powell introduced a "macroelement" ref (131). Here a section of the regularly spaced columns and girders which may consist of several stories and bays are idealized as a single macroelement Therefore, large numbers of discrete members can be lumped together simplifying the model. Each node of the macroelement has vertical and rotation (in-plane) degrees of freedom. In addition, the horizontal displacement at the top, middle and bottom of each element is considered. Supermacroelements called "corner space elements" are derived to represent a single multistory column. Deformations are considered to only occur at the nodes and only planar action of the macroelement is considered. A typical section of a tube planar frame section and its equivalent macroelement is shown in Figures 55a, and b.

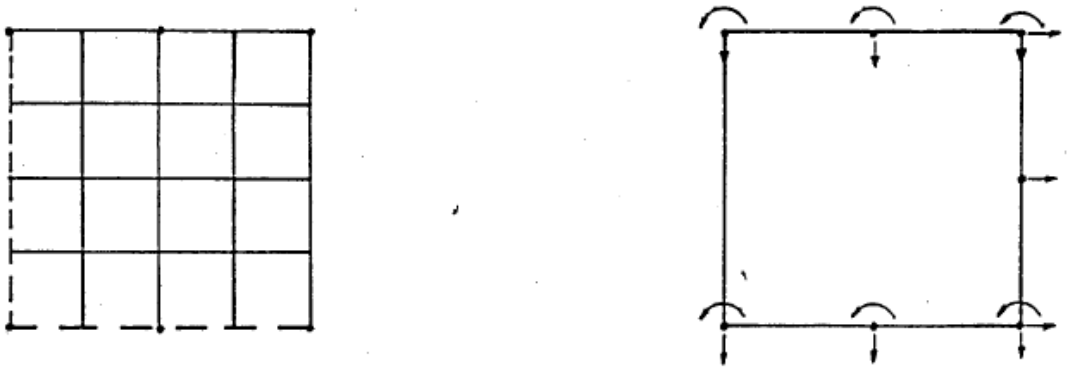

Figure 55: Macroelement Model of tube frame section

Of interest is also the orthotropic membrane approach of Ha, Fazio, and Moselhi ref (2). This approach can be labeled a discrete-continuum method because although the tube panels are modeled as an equivalent continuum, the panels are then analyzed per a finite element representation of many membrane elements. Unlike the approach of Khan and Stafford Smith ref (130), the idealized structure requires no cutouts for the window openings. Points of inflection are assumed at the mid-span of all members. The equivalent elastic properties of a section of the frame bounded by four points of inflection are derived by imposing the deformations of the frame unit on the membrane element when both are subject to statically equivalent shear or normal forces ref (2).

The method discussed hereafter is similar to that of Ha, et al., but instead of subdividing the equivalent plate panel into finite elements, the equivalent elastic properties of a plate segment representing an entire tube face are derived and the governing equations solved in closed form.

4.2 The Equivalent Orthotropic Plate Method for Analysis of Framed Tube Buildings

4.2.1 Introduction

Unlike previous methods discussed in Section 4.1, the approach used to develop the program Frame Tube presented in Section 4.5 is a continuum approach and therefore provides closed form solutions for stresses, member forces and deflections. However, by integrating over the applicable tributary area forces in any discrete element of the structure can be ascertained. The equivalent orth6tropic plate method, originally developed by Coull and Bose ref (52), also allows for parametric study and rapid re-analysis since the building behavior can be identified through simple numerical constants which are a function of geometry and material properties. A summary of the complete approach is given in Section 4.2.1.1.

Like any approximate method, the dominant action of the structure must be identified. From here on "side panels" will refer to those exterior frames that are parallel to the applied load (web panels) and "normal panels" will refer to those that are perpendicular (flange panels) to the applied lateral load. As explained in Section 1.2.4, the framed tube deformations are primarily those due to axial strain in the normal and corner columns and shearing strain (rigid jointed frame action) in the side panels. Compatibility of the panels is assured through vertical shear forces at the corners. An appropriate elastic modulus is used to model axial and shearing stiffnesses in the orthotropic plates. Floor slabs are assumed rigid in plane and therefore out-of-plane actions are neglected in all panels. Only linearly elastic behavior is considered and connections at the foundation are assumed rigid.

Geometrically, the spacing of the beams and the columns are assumed uniform throughout the height. Side panels are assumed identical and normal panels are also assumed identical. The building properties are assumed uniform throughout the height, but uniform estimates of segmented structures can be used. The normal and side panels can be of different width, but all sides must be of equal height and orthogonally connected. Bay sizes may differ horizontally but this is unlikely in this type of structure and aside from larger story heights in the first or second levels, story heights are usually also constant. A model of the equivalent orthotropic plate structure and a typical floor plan are given in Figures 57 and 56 respectively. This method has been extended for torsional analysis of framed tubes ref (122). For convenience a summary of the algorithm is given in Section 4.2.1.1. The details of the method for single and quad-tubular structures follow. Details of the torsional approach are not given here but, the algorithm is identical to that presented within for flexural analysis only.

4.2.1.1 Synopsis of Approach

An outline of the method for analyzing framed tube structures using equivalent orthotropic plate panels is presented below. The outline can apply to the analysis of bundled tube structures with the addition of some simplifying assumptions (Section 4.3.1).

1. Replace each tube grid with an orthotropic plate with properties that represent the appropriate stiffnesses of the beams and columns.

2. From the defined stress state of an orthotropic plate element and using the theory of elasticity obtain element equilibrium equations.

3. Define orthotropic stress-strain relations for normal and side panels.

4. Model the anticipated distribution of vertical stress in the normal panel as a parabolic function.

5. Repeat for side panels using cubic function.

6. Using comer compatibility and that of overall moment capability at any height reduce the unknowns to a single function *(S).*

7. Rewrite the vertical stress equations in terms of this single function.

8. Substitute these equations into the equilibrium equation and determine additional stress functions.

9. Write equation for strain energy (U) stored in the entire structure in terms of the stress functions.

10. Using the calculus of variations minimize the strain energy ref (135).

11. From step 10 the governing second order differential equation is obtained along with the boundary conditions.

12. Solve the differential equation based on the lateral load type and obtain the solution for the function S.

13. Substitute S into stress equations to obtain stresses at any height.

14. Forces are obtained by integrating the appropriate stress function over the appropriate tributary area of plate.

15. Deflections are obtained by integrating the strain equations obtained from the stress-strain-displacement relationship with the appropriate boundary condition.

4.2.2 Stresses and Member Forces

The orthotropic plate model of a framed tube structure is shown in Figure 57. The normal panels are of length 2b and the side panels are 2c wide. The positive x, y, and z directions and the notation for stresses in the normal and side panels are also shown. σ_z and σ'_z represent the vertical stress in the flange and web panels respectively, and $\sigma_y$and $\sigma_x$represent the axial stress in the girders. Shear stresses of the panels are defined by τ_{yz} and τ_{xz}.The building height is given by H.

The stress state of a differential element in the normal panel shown in Figure 57 is shown in Figure 58. From the force equilibrium of this element and a corresponding element in the side panel the following equations can be written:

$$\frac{\partial \sigma_y}{\partial x} + \frac{\partial \tau_{yz}}{\partial z} = 0 \quad ; \quad \frac{\partial \sigma_z}{\partial z} + \frac{\partial \tau_{yz}}{\partial y} = 0 \qquad \text{Equation 127}$$

$$\frac{\partial \sigma_x}{\partial x} + \frac{\partial \tau_{xz}}{\partial z} = 0 \quad ; \quad \frac{\partial \sigma'_z}{\partial z} + \frac{\partial \tau_{xz}}{\partial x} = 0 \qquad \text{Equation 128}$$

Equations (127) and (128) represent the normal and side panels respectively. The orthotropic stress-strain relations for the panels are given by ref (52):

$$\sigma_y = E_y \varepsilon_y + E_{yz} \varepsilon_z \; ; \quad \sigma_z = E_z \varepsilon_z + E_{yz} \varepsilon_y \; ; \quad \tau_{yz} = G_{yz} \gamma_{yz} \qquad \text{Equation 129}$$

for the normal panel and :

$$\sigma_x = E_x x + E_{xz}\varepsilon'_z \; ; \; \sigma'_z = E'_z\varepsilon'_z + E_{xz}\varepsilon_x \; ; \tau_{xz} = G_{xz}\gamma_{xz} \qquad \text{Equation 130}$$

for the side panel.

Here E and E represent modulus of elasticity and direct strain, and G and y represent, shear modulus and shearing strain respectively. Cross elasticity terms can be neglected and since spacing and properties of the columns and girders are assumed constant we can write:

$E_z=E'_z=E$; $G_{xz}=G_{yz}=G$ Equation 131

In determining the elastic properties of the equivalent tube the elastic modulus E can be represented by the elastic modulus of the columns for a uniform structure because in this case the area of any single column will be equal to the plate thickness times the bay width

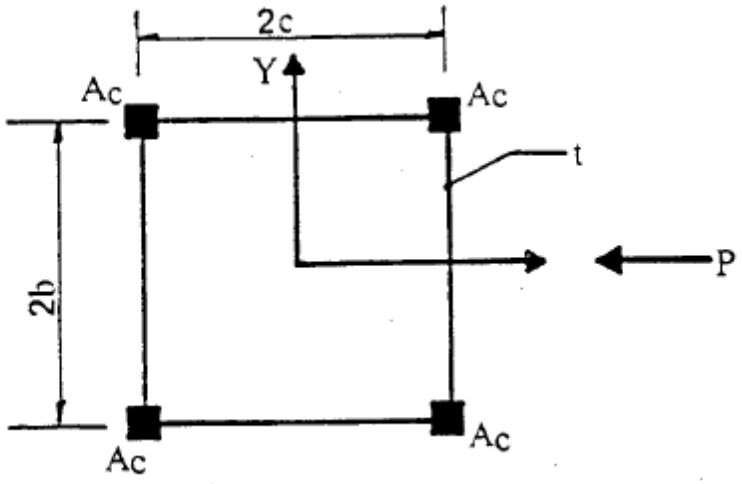

Figure 56: Plan of Substitute Structure-Single Tube

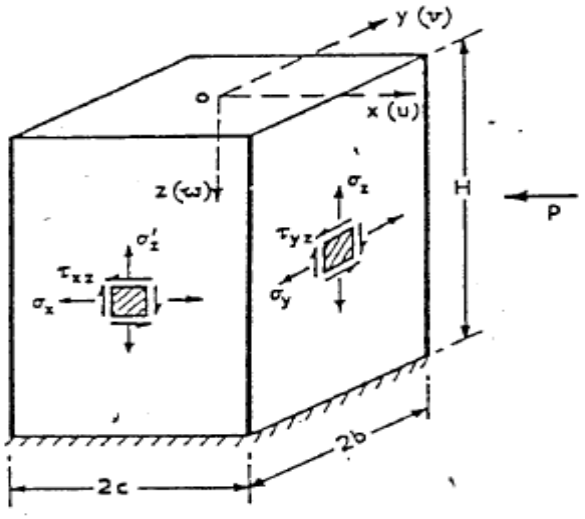

Figure 57: Notation for Stress-single tube ref (52)

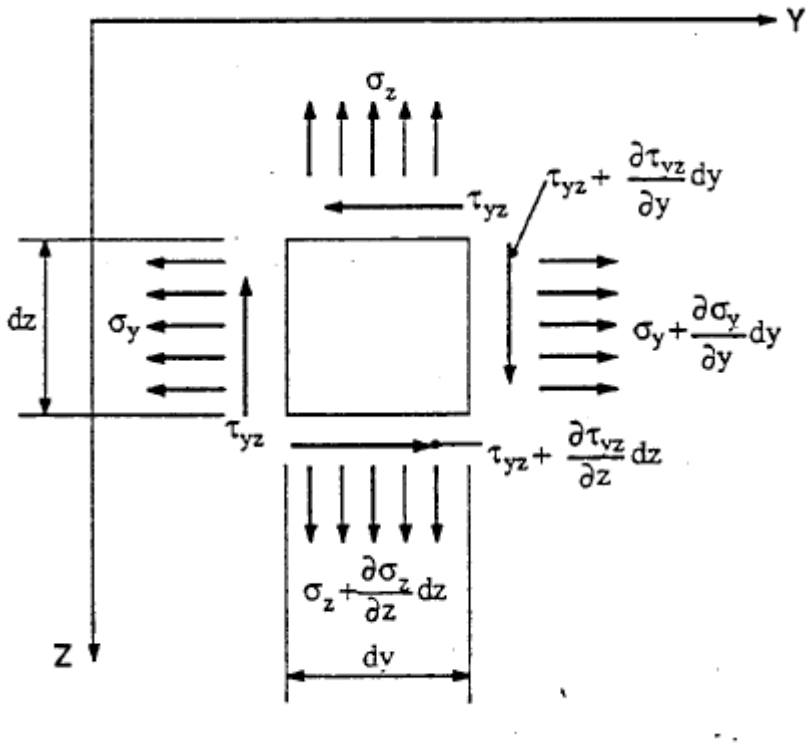

Figure 58: Stress State of differential element in normal panel of orthotropic plate

modulus is used to represent the plate shearing behavior in order to model the anticipated shear lag in the panels.

To determine G we proceed as we did for the frame elements of shear wall-frame interactive structures in Chapter II. Here however finite joint size must be accounted for due to the relative size and spacing of the girders and columns. Figures 59a and 59b show the tube grid and equivalent plate subjected to a shearing force Q. A single column line of the tube grid is shown subjected to a unit shearing force Q in Figure 59c. The columns are constrained to deflect equally at each floor level and points of contraflexure are assumed at the mid-span of all girders. t_1 and t_2 represent the infinitely rigid dimensions of the typical girder-column connection. t_1 equals column width along any face and t2 equals girder depth. d_1 and d_2 are the total lengths of the adjacent beams of moment of inertia Id_1 and Id_2. h is the story height and Ic is the column moment of inertia.

By equating the load-displacement relationships of the plate in Figure 59b and the column line in Figure 59c, the shearing rigidity, GA, of the equivalent plate, (for a uniform structure with $d_1 = d_2 = d$ and $Id_1 = Id_2 = Id$), reduces to ref (52):

$$\boldsymbol{GA} = \frac{\mathbf{12}\boldsymbol{EIc}}{\boldsymbol{e}^{\mathbf{2}}}\left(\mathbf{1}+\frac{\boldsymbol{t_2}}{\boldsymbol{e}}\right)\frac{\mathbf{1}}{\left(\mathbf{1}+\left(\frac{\mathbf{1}}{\boldsymbol{e}}\right)\frac{\boldsymbol{Ic}\left(\mathbf{1}+\frac{\boldsymbol{t_2}}{\boldsymbol{e}}\right)}{\boldsymbol{Id}\left(\mathbf{1}+\frac{\boldsymbol{t_1}}{\boldsymbol{l}}\right)^{\mathbf{2}}}\right)^{\mathbf{2}}} \quad \text{Equation 132}$$

where: $e = h - t_2$, $l = d - t_1$

This equation can be applied to exterior columns by setting Id of one adjacent beam equal to zero. This is equivalent to multiplying (l/e) by 2 in eq. (132).The total shearing stiffness of the equivalent plate is equal to the sum of the GA terms for a single story level. Non-uniform

structures would require calculation of an average GA value. The artificial shear modulus for a uniform structure is found by dividing a panel GA by that panels cross sectional area. G for buildings of unequal spacing in normal and side panels would be determined by averaging the G from each panel. Shearing deformations of the beams, columns, and the joints can be incorporated ref (123), but inclusion of shearing deformations is only necessary for unusual structures of very high member size to spacing ratios ref (124).

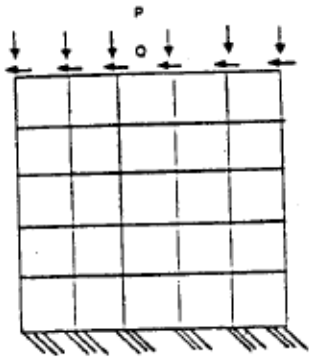

(a) Framed Tube Grid

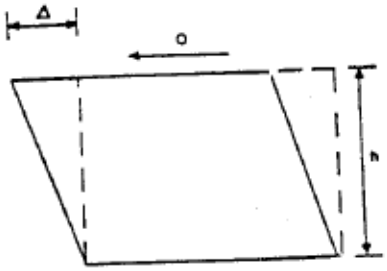

(b) Shear Def. of Plate Element

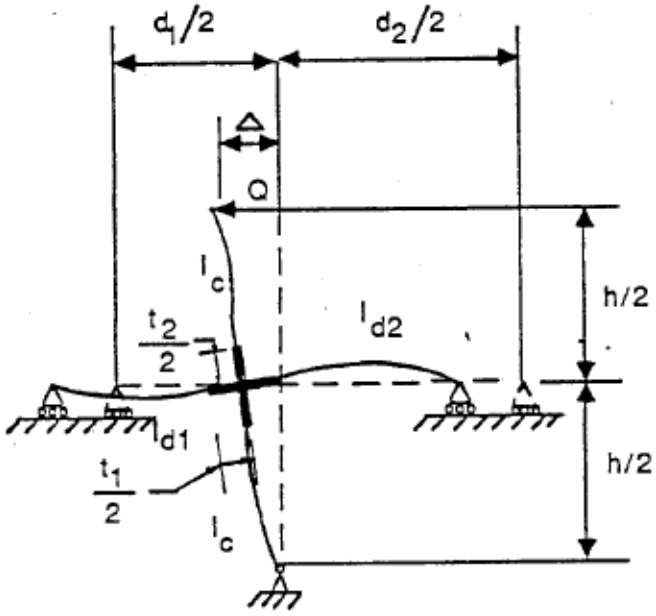

(c) Horizontal Deformation of One Column Line in Framed Tube

Figure 59: Shear behavior in frame with rigid connections ref (52)

We can now proceed in determining the stresses in the equivalent tube. The distribution of vertical stresses in the normal panel due to the shear lag effect is assumed to be given by ref (52):

$$\sigma_z = \frac{M_c}{I} + S_o + \left(\frac{y}{b}\right)^2 S \qquad \text{Equation 133}$$

Where S_o and S are functions of the height coordinate z.

The first term in eq. (133) is the normal stress per basic beam theory. The moment of inertia of the equivalent tube cross section shown in Figure 56 is found to be:

$$I = \frac{4}{3}tc^2(3b + c) + 4c^2A_c \quad \text{Equation 134}$$

Here t is the equivalent tube thickness and Ac represents the cross sectional areas of the corner columns in excess of the ordinary column cross sectional area. If all the columns are of equal area, then Ac equals zero. The tube thickness is equal to the sum of the cross sectional areas of the columns, (at some level z), divided by the width of the applicable side.

Therefore the normal panel cross sectional area would be given by 2tb.

Similarly the distribution of vertical stresses in the side panels is assumed to be ref (52):

$$\rho'_z = \frac{Mx}{I} + \left(\frac{x}{c}\right)^3 S1 \quad \text{Equation 135}$$

where S1 is also a function of z.

In eq. (133) only even powers are used due to symmetry. In eq. (135) only odd powers are used due to skew-symmetry of the stress distribution. By incorporating the corner

compatibility and moment equilibrium equations the vertical stresses can subsequently rewritten in terms of the single function S(z) as ref (52):

$$\sigma_z = \frac{Mc}{I} - \left(\frac{1}{3}m - \left(\frac{y}{b}\right)^2\right) S \quad \text{Equation 136}$$

$$\sigma'_z = \frac{Mx}{I} + \left(1 - \frac{1}{3}m\right)\left(\frac{x}{c}\right)^3 S \quad \text{Equation 137}$$

$$\sigma_c = (\sigma_z)_{y=b} = \frac{Mc}{I} + \left(1 - \frac{1}{3}m\right) S \quad \text{Equation 138}$$

where m=(5b+3c+ *15Ac/t) I* (5b+c+5Ac/t) and σ_c represents the corner column axial stress.

By substituting eqs.(136) and (137) into eqs. (127) and (128) and integrating, the other stress components become ref (52):

$$\sigma_y = \frac{b^2 c}{2I}\left(\left(\frac{y}{b}\right)^2 - 1\right)\left(\frac{d^2M}{dz^2}\right) - \frac{b^2}{12}(2m\left(\frac{y}{b}\right)^2 - \left(\frac{y}{b}\right)^4 - (2m-1))\frac{d^2s}{dz^2} \quad \text{Equation 139}$$

$$\tau_{yz} = -y(\left(\frac{c}{I}\right)\left(\frac{dM}{dz}\right) - \frac{1}{3}(m - \left(\frac{y}{b}\right)^2)\frac{dS}{dz} \quad \text{Equation 140}$$

$$\sigma_x = \left(\frac{c^3}{2I}\right)\left[2\left(\frac{1}{3} - \frac{b}{c} + \frac{Ac}{ct}\right) + \left(1 + \frac{2b}{c} + \frac{2Ac}{ct}\right)\left(\frac{x}{c}\right) - \frac{1}{3}\left(\frac{x}{3}\right)^3\right]\frac{d^2M}{dz^2} - (1 - \frac{1}{3}m)(\frac{c^2}{20})((\frac{x}{c}) - (\frac{x}{c})^5)\frac{d^2S}{dz\text{^}2} \quad \text{Equation 141}$$

$$\tau_{xz} = (\frac{c^2}{2I})(1 + \frac{2b}{c} + \frac{2Ac}{ct} - \left(\frac{x}{c}\right)^2)\frac{dM}{dz} \quad \text{Equation 142}$$

The integration constants were evaluated from the following boundary conditions ref (52):

(a) At x=+c; $\sigma_x = \frac{P}{2t} = -\frac{1}{2t}\frac{d^2M}{dz^2}$ Equation 143

Where P equals the magnitude of the uniformly distributed load.

(b) At x=-c; $\sigma_x = 0$ and at y=±b; $\sigma_y = 0$ Equation 144

(c) At the corner $(\tau_{xz})_{x=c} + (\tau_{yz})_{y=b} = \frac{Ac}{t}\frac{\partial\sigma_c}{\partial_z}$ Equation 145

in which τ_{yz} is skew-symmetric with respect to the y axis.

(d) Each side frame is assumed to sustain one half of the total shear (F) or:

$$\frac{F}{2} = t\int_{-c}^{c} \tau_{xz}\, dx = \frac{1}{2}\int_{0}^{z} P\, dz = \frac{1}{2}\frac{dM}{dz}$$ Equation 146

The total strain energy in the substitute structure is now given by:

$$U = t\int_{0}^{H}\{\int_{-b}^{b}(\frac{{\sigma^2}_z}{E} + \frac{{\tau^2}_{yz}}{G})dy + \int_{-c}^{c}(\frac{{\sigma^2}_c}{E} + \frac{{\tau^2}_{xz}}{G})dx\}dz + \frac{2Ac}{E}\int_{0}^{H} {\sigma^2}_c\, dz$$ Equation 147

Horizontal strains are considered negligible in the strain energy equation. By substituting the stress functions of eqs. 136, 137, 138, 140 and 142 into the strain energy equation, integrating with respect to x and y, and minimizing the resulting integral per the calculus of variations, (the integral must be a minimum per the principle of least work), yields the following governing differential equation ref (52):

$$\frac{d^2S}{dz^2} - \left(\frac{k}{H}\right)^2 S = \lambda^2 \frac{d^2\sigma_b}{dz^2}$$ Equation 148

With: $$k^2 = \frac{15GH^2}{Eb^2}\left(\frac{\frac{1}{5}(5m^2-10m+9)+(3-m)^2(\frac{c}{b})(\frac{1}{7}+\frac{Ac}{ct})}{\frac{1}{7}(35m^2-42m+15)+\frac{1}{15}\left(\frac{c}{b}\right)^3(3-m)^2}\right)$$ Equation 149

$$\lambda^2 = \frac{3\left((5m-3)-\left(\frac{1}{7}\right)\left(\frac{c}{b}\right)^3(3-m)\right)}{\left(\frac{1}{7}\right)(35m^2-42m+15)+\left(\frac{1}{15}\right)\left(\frac{c}{b}\right)^3(3-m)^2}$$ Equation 150

And $$\sigma_b = \frac{Mc}{I}$$ Equation 151

The resulting boundary conditions for the structure assumed encastre at the base and free at the top are ref (52):

At z=0; S=0 Equation 152

At z=H; $$\frac{dS}{dz} - \lambda^2\frac{d\sigma_b}{dz} = 0$$ Equation 153

The complete solution to eq.(148) depends on the load type. Since k^2 is always positive for practical values of (b/c) and *(Ac/ct)* ref (52) the homogeneous solution can be expressed by eq. [5.2.2-26] since there will be nu imaginary roots of the characteristic equation:

$$\boldsymbol{S = Acosh\left(\frac{k}{H}\right)z + Bsinh\left(\frac{k}{H}\right)z}$$ Equation 154

The dominant stress functions can now be expressed by the following equations:

$$\boldsymbol{\sigma_z = \sigma_b - \left(\frac{1}{3}m - \left(\frac{y}{b}\right)^2\right)\sigma_b(H)F1F2}$$ Equation 155

$$\boldsymbol{\sigma'_z = \sigma_b\left(\frac{x}{c}\right) + \left(1 - \frac{1}{3}m\right)\left(\frac{x}{c}\right)^3\sigma_b(H)F1F2}$$ Equation 156

$$\boldsymbol{\tau_{yz} = \frac{y}{H}\frac{d\,\sigma_b}{d\xi} + \frac{y}{3H}\left(m - \left(\frac{y}{b}\right)^2\right)\sigma_b(H)F1F3}$$ Equation 157

$$\boldsymbol{\tau_{xz} = \frac{c}{2H}\left(\left(1 + \frac{2b}{c} + \frac{2Ac}{ct} - \left(\frac{x}{c}\right)^2\right)\frac{d\,\sigma_b}{d\xi} + \left(1 - \frac{1}{3}m\right)\left(\frac{c}{4H}\right)\left(\frac{1}{5} - \left(\frac{x}{c}\right)^4\right)\right)\sigma_b(H)F1F3}$$ Equation 158

Here ξ represents a dimensionless height coordinate given by z/H. The values for,σ_b, $\frac{d\,\sigma_b}{d\xi}$, F1, F2, and F3 are shown in Table 21 for the three standard loading cases. P is equal to the value of the concentrated load at the top of the structure, the value of a uniformly distributed load, or the maximum value of a linearly distributed load at the top of the structure when P=0 at z=0. In BUNTUBE they are designated P, P0, and P1 respectively. The girder axial stresses are of little consequence in the preliminary analysis and determination of member sizes.

Member forces are found by integrating the appropriate stress function over the appropriate tributary area For column axial stress that area would be one half a bay width on either side of the applicable column line, (defined by an x or y location), at some level z.

For girder forces the tributary area would be one half of a story height above and below the girder at some level z. For example, the axial force in a side column "i" is given by:

$$N_{si} = t \int_{Xi+\frac{d}{2}}^{Xi+\frac{d}{2}} \sigma'_z \, dz \qquad [5.2.2\text{-}31]$$

which when substituting eq. [5.2.2-11] for σ'_z and integrating becomes:

$$N_{si} = \frac{tdXi}{c}\left(\sigma_b + \left(1 - \frac{1}{3}m\right)\left(\frac{1}{c^2}\right)\left(Xi^2 + \frac{d^2}{4}\right)\sigma_b(H)F1F2\right) \quad [5.2.2\text{-}32]$$

Similar expressions for the axial forces in the normal panel and the shears in the columns and the girders can be obtained ref (52). Since Framed tube program was not developed to calculate member forces the remaining equations will not be given.

Table 21: Design function for framed Tube analysis ref (52)

TABLE 5.2.2.1

Design Functions For Framed Tube Analysis [52]

Fct.	Conc. Load	Uniformly Distributed Load	Triangularly Distributed Load
σb	$\frac{PcH}{I}\xi$	$\frac{PcH^2}{2I}\xi^2$	$\frac{PcH^2}{2I}(\xi^2 - \frac{1}{3}\xi^3)$
$\frac{d\sigma b}{d\xi}$	$\frac{PcH}{I}$	$\frac{PcH^2}{I}\xi$	$\frac{PcH^2}{2I}(2\xi - \xi^2)$
F1	λ^2	λ^2	λ^2
F2	$\frac{\sinh k\xi}{k\cosh k}$	$\frac{2}{k^2}\left[\frac{\cosh k(1-\xi) + k\sinh k\xi}{\cosh k} - 1\right]$	$\frac{3}{k^2}\left[\frac{2k\cosh k(1-\xi) + (k^2-2)\sinh k\xi}{2k\cosh k} - (1-\xi)\right]$
F3	$\frac{\cosh k\xi}{\cosh k}$	$\frac{2}{k}\left[\frac{k\cosh k\xi - \sinh k(1-\xi)}{\cosh k}\right]$	$\frac{3}{k^2}\left[\frac{(k^2-2)\cosh k\xi - 2k\sinh k(1-\xi)}{2\cosh k} + 1\right]$

4.2.3 Deflections

In order to determine the displacements of the orthotropic tube model we require the stress-strain-displacement relationships for a differential element of the orthotropic plate. Since out of plane actions are neglected due to the assumption of rigid floor slabs these relationships can be derived for a planar element Also, because we are only considering elastic response, higher powers of strain or displacement derivatives can be neglected. The following derivation is derived from reference ref (125).

Consider the differential element of the orthotropic tube side panel shown in Figure 60, which deforms from the original position ABCD to position A'B'C'D'. The deformed length of the left edge A'D' is:

$$(\boldsymbol{A'D'})^2 = \left(\boldsymbol{dz} + \frac{\partial \omega'}{\partial z}\boldsymbol{dz}\right)^2 + \left(\frac{\partial u}{\partial z}\boldsymbol{dz}\right)^2 \quad \text{Equation 159}$$

and the z direction strain is given by:

$$\boldsymbol{\varepsilon_z'} = \frac{\boldsymbol{A'D' - AD}}{\boldsymbol{AD}} \quad \text{Equation 160}$$

Since AD=dz we get $\boldsymbol{A'D'} = (\mathbf{1} + \boldsymbol{\varepsilon_z'})\boldsymbol{dz}$ Equation 161

Squaring eq. (161), equating it with eq. (159) and dividing through by $(dz)^2$ yields:

$$(1 + 2\varepsilon_z' + (\varepsilon_z')^2) = \left(1 + 2\frac{\partial \omega'}{\partial z} + \left(\frac{\partial \omega'}{\partial z}\right)^2 + \left(\frac{\partial u}{\partial z}\right)^2\right) \quad \text{[5.2.3-4)}$$

By neglecting higher order terms we get (in conjunction with Hooke's Law):

$$\boldsymbol{\varepsilon_z'} = \frac{\partial \boldsymbol{\omega'}}{\partial \boldsymbol{z}} = \frac{\boldsymbol{\sigma_z'}}{\boldsymbol{E}} \quad \text{Equation 162}$$

The shear strain γ_{xz} is defined as the change in angle of the initially rectangular differential element. From Figure 60 the change in angle from DAB to D'A'B' is given by:

$$\gamma_{xz} = \frac{\partial \omega'}{\partial y} dx \left(\frac{1}{dx}\right) + \frac{\partial u}{\partial z} dz \left(\frac{1}{dz}\right)$$

Or

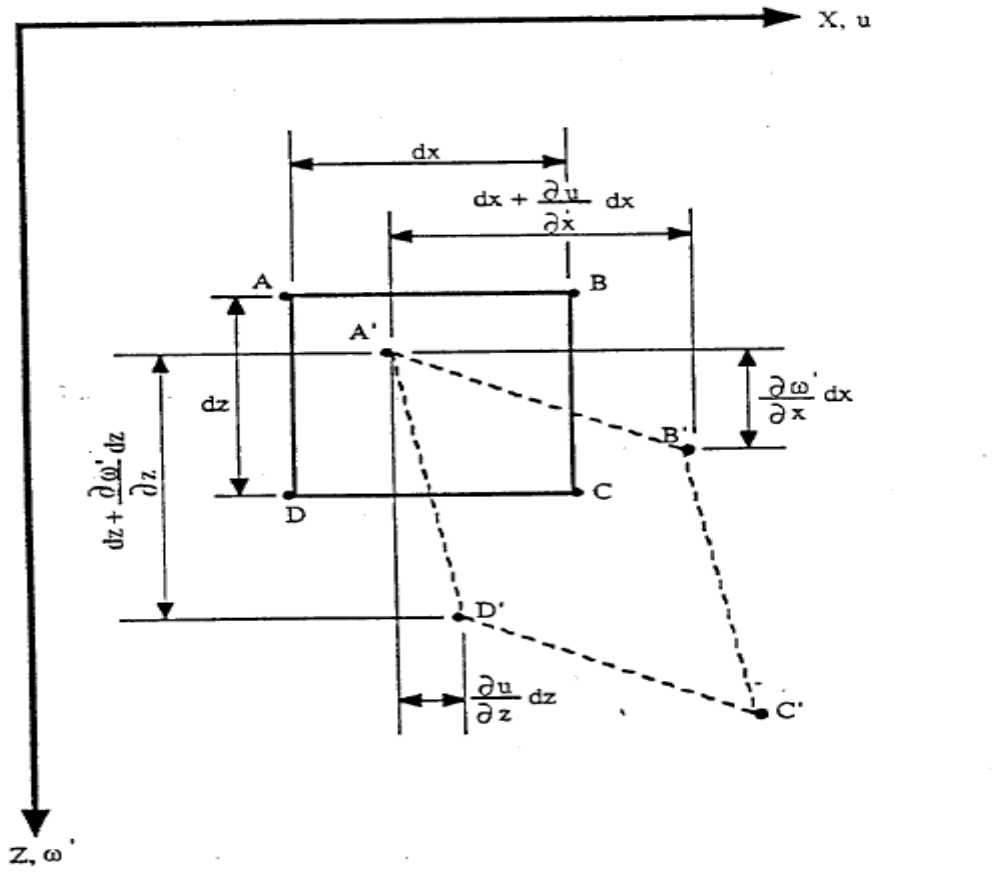

Figure 60: Displaced state of differential element in side panel of orthotropic plate ref (125)

$$\boldsymbol{\gamma_{xz}} = \frac{\partial \omega'}{\partial x} + \frac{\partial u}{\partial z} = \frac{\tau_{xz}}{G}$$ Equation 163

. Thus the stress-strain-displacement relationships for the side panels are given by eqs.

(162) and (163) and similarly for the normal panel by:

$$\boldsymbol{\varepsilon_z = \frac{\partial \omega}{\partial x} = \frac{\sigma_z}{E}}$$ Equation 164

where u and ω are defined in Figure 57.

No relationship for γ_{xz} is necessary since a normal panel is assumed not to deflect laterally for a structure symmetric in the plane of loading.

The normal and side panel shear stress equations are now rewritten as follows ref (10):

$$\boldsymbol{\sigma_z = \frac{Mc}{I} - \phi S}$$ Equation 165

$$\boldsymbol{\sigma'_z = \frac{Mc}{I} + \gamma \left(\frac{x}{c}\right)^3 S}$$ Equation 166

$$\boldsymbol{\tau_{xz} = \frac{c^2}{2I}\left(g1 - \left(\frac{x}{c}\right)^2\right)\frac{dM}{dz} + \gamma\left(\frac{c}{4}\right)\left(\frac{1}{5} - \left(\frac{x}{c}\right)^4\right)\frac{dS}{dz}}$$ Equation 167

where: $\alpha = \frac{b}{c}, \beta = \frac{Ac}{ct},\ g1 = 1 + 2\alpha + 2\beta\ , \gamma = 1 - \frac{m}{3}, \phi = \phi(y) = \frac{m}{3} - \left(\frac{y}{b}\right)^2$

and for a uniformly distributed load of magnitude P:

$$M = \frac{Pz^2}{2}\ , \qquad S = \frac{Pc\lambda^2 H^2}{k^2 I}(\cosh(k\xi) + K1\sinh(k\xi) - 1)$$

with $K1 = \frac{k - \sinh(k)}{\cosh(k)}$

By substituting eq. (166) into eq. (162), integrating, and incorporating the boundary condition that $\omega' = 0$ at z=H, the vertical displacements in the side panel become ref (10):

$$\boldsymbol{\omega' = \frac{PH^3 x}{6EI}(\xi^3 - 1) + \frac{Pc\lambda^2 H^2}{k^3 EI}\gamma\left(\frac{x}{c}\right)^3 (\sinh(k\xi) + K1\cosh(k\xi) - k\xi)}$$ Equation 168

Then by substituting eqs. (168) and (169) into eq. (164), integrating, and incorporating the boundary condition that u=O at z=H, the lateral deflection at the neutral axis (x=O) becomes ref (10):

$$\boldsymbol{u = -\frac{PH^4}{24EI}(3 + \xi^4 - 4\xi) + (\frac{Pc^2H^2}{4GI})(g1(\xi^2 - 1) + \left(\frac{\lambda^2\gamma}{5k^2}\right)(F1 + K1F2))} \quad \text{Equation 169}$$

where: $F1 = F1(\xi) = \cosh(k\xi) - \cosh(k)$, $\quad F2 = F2(\xi) = \sinh(k\xi) - \sinh(k)$

Note that at the top of the building (z=0), the first term in eq. (169) reduces to the deflection of a pure cantilever subjected to a uniformly distributed load. Therefore the second term represents the lateral deflection due to the "shear racking" of the side panels. The vertical displacements in the normal panel are found by substituting eq. (165) into eq. (164), integrating, and incorporating the boundary condition that $\omega = 0$at z=H. It follows that:

$$\boldsymbol{\omega = -\frac{PcH^3}{6EI}(1 - \xi^3) - (\frac{Pc\lambda^2H^3}{k^3EI})\phi(\sinh(k\xi) + K1\cosh(k\xi) - k\xi)} \quad \text{Equation 170}$$

In order to avoid round off error in the computer due to the extreme difference in magnitude between $k\xi$and its hyperbolic sine or cosine the expression in the parenthesis attached to the second term above and in eq. (168) is rewritten as:

$$\boldsymbol{SKC = \frac{\sinh(k\xi)\cosh(k) + k\cosh(k\xi) - \sinh(k)\cosh(k\xi) - k\xi\cosh(k)}{\cosh(k)}} \quad \text{Equation 171}$$

so that when z=H ie., $\xi = 1$, SKC=O. Examining the magnitudes of ω' andω across the applicable tube face at various levels will indicate the degree of shear lag. As with the lateral displacements the second term of eqs. (168) and (170) gives the vertical displacement due to

the shear lag effect. For the case of a triangularly distributed load the tube deflections are given by ref (10):

$$\omega' = \frac{PH^3x}{24EI}(4\xi^3 - \xi^4 - 3) + \left(\frac{Pc\lambda^2H^3}{k^2EI}\right)\gamma\left(\frac{x}{c}\right)^3\left(\frac{1}{k^2} + \frac{1}{k}\sinh(k\xi) + K2\cosh(k\xi) - \xi + \frac{1}{2}\xi^2\right)$$ Equation 172

$$u = -\frac{PH^4}{120EI}\left(5\xi^4 - \xi^5 - 15\xi + 11\right) + \frac{Pc^2H^2}{4GI}\left(\frac{1}{3}g1(3\xi^2 - \xi^3 - 2) + \left(\frac{\lambda^2\gamma}{5k^2}\right)(F1 + kK2F2 + (\xi - 1))\right)$$ Equation 173

$$\omega = \frac{PcH^3}{24EI}(4\xi^3 - \xi^4 - 3) - \frac{Pc\lambda^2H^3}{k^2EI}\phi\left(\frac{1}{k}\sinh(k\xi) - \xi + \frac{1}{2}\xi^2 + \frac{1}{k^2} + K2\cosh(k\xi)\right)$$ Equation 174

where $K2 = \frac{k^2 - 2 - 2k\sinh(k)}{2k^2\cosh(k)}$

Proceeding similarly for the case of a concentrated load of magnitude P applied at the top of the structure, the tube displacements reduce to:

$$\omega' = \frac{PH^2x}{2EI}(\xi^2 - 1) + \left(\frac{Pc\lambda^2H^3}{k^2EI}\right)\gamma\left(\frac{x}{c}\right)^3\left(\frac{F1}{\cosh(k)}\right)$$ Equation 175

$$u = -\frac{PH^3}{6EI}(2 - 3\xi + \xi^3) + \left(\frac{Pc^2H}{4GI}\right)\left(g1(\xi - 1) + \left(\frac{\lambda^2\gamma}{10k}\right)\left(\frac{F2}{\cosh(k)}\right)\right.$$ Equation 176

$$\omega = -\frac{PcH^2}{2EI}(1 - \xi^2) - \left(\frac{Pc\lambda^2H^2}{k^2EI}\right)\phi\left(\frac{F1}{\cosh(k)}\right)$$ Equation 177

In order to avoid the round off errors previously discussed for the uniformly distributed load case, the terms involving K2 were expanded to a form similar to eq. (171). Equations for the rotations (θ) of the tube structure when subjected to the three standard torque loadings corresponding to the three lateral load cases discussed above have also been developed by Coull and Ahmed ref (10). They will not be presented here.

4.3 Computer Program BUNTUBE

4.3.1 Program Description and Use

The equations for lateral and vertical deflections given in Sections 5.2.3 and 5.3.3 have been incorporated into a computer program called Framed Tube Program. Framed Tube Program will allow the user to analyze single tube structures. The program was in Matlab® graphical user interface and compiled withversion2009a.. The structure may consist of a single tube, but must be symmetrical about two axes. Additional assumptions and/or restrictions are given below:

1. All columns and girders must have equal properties on all sides and at all heights.

2. Corner columns may be larger than "face" columns but their properties must be uniform with height.

3. Story heights must be uniform.

4. All columns and girders must be of the same material.

5. Bay widths must be uniform horizontally and vertically.

6. All material behaves linear elastically.

7. For the quad-bundled tube the exterior panels must contain an odd number of column lines so that the interior panels will intersect the exterior panels at a column line. (An appropriate warning is written on the screen at execution time)

8. All panels must be orthogonally connected.

9. All tubes of a quad-bundled tube must have equal overall height

Average uniform properties can be used for buildings of segmented vertical stiffness properties. Similar approximating adjustments can be made to analyze buildings with uneven story heights and bay widths, but normally for this type of structure these assumptions are reasonable. The last assumption could be eliminated by applying the transfer matrix method to allow stopping individual tubes at various heights.

The output file consists of a full input echo, the lateral deflections at regularly spaced locations along the height and the normal and side panel vertical deflections for each column line at equally spaced points along H. Also output are the equivalent tube parameters which can be used along with Table 21 to calculate stresses as required. After each analysis the user has the choice of restarting the program without exiting the program environment.

4.3.2 Example 4-1: 16 Story Framed Tube

4.3.2.1 Statement of the Problem

In order to allow for comparison between the orthotropic plate approximate analysis technique and a more exact matrix analysis, which may occur during the final design phase, a 16 story concrete uniform framed tubes will be analyzed using Framed Tube Program and SAP2000. This concrete structure was originally analyzed by Chan ref (133) and subsequently by Moselhi ref (132).

The building plan is shown in Figure 61. The global coordinate system shown is consistent for both the Framed Tube Program and SAP2000 analyses except that the SAP2000 z axis is in the opposite direction of that for Framed Tube Program. Each frame of the tube consists of 13 regularly spaced columns giving a bay width of 8'-6"on all sides and at all elevations. All columns are 1'-6" x

1'-6" in plan and all girders are 0'-8" wide and 2'-0" deep. The elastic and shearing modules are 432000 k/ft^2 and 172800 k/ft^2 respectively for all members.

Table 22 is the input data for the Framed Tube Program analysis. A uniformly distributed load of 4.08 k/ft., corresponding to a wind pressure of 40 psf. on the normal face, represents the design load. Also shown are the calculated equivalent tube parameters as output by Framed Tube Program.

Due to symmetry one quarter of the plan shown in Figure 61 is modeled for the SAP2000 analysis. The SAP2000 model is shown in Figure 62.The story heights at which the output will be compared are indicated.

Table 22: Example 4-1 16 story, Framed Tube Program Input parameters

Modulus of elasticity	4.32E+05
Number of segment for output	16
Building Height	192
Story height	12
BLDG. width in X direction	102
BLDG. width in Y direction	102
Number of columns lines in Y direction	13
Number of columns lines in X direction	13
Area of corner columns	2.25E+00
Magnitude of distributed load	4.08
Equivalent tube thickness	0.286765
Equivalent shear modulus of plates	6.78E+03
Moment of inertia of tube about Y axis	2.03E+05
Geometric parameter	1.33E+00
Differential equation constant 2	1.16E+00
Differential equation constant 1	1.79E+00
Column area	2.25E+00
Column inertia	4.22E-01
column with	1.50E+00
Girder area	1.34E+00
Girder inertia	4.47E-01
Girder depth	2.00E+00

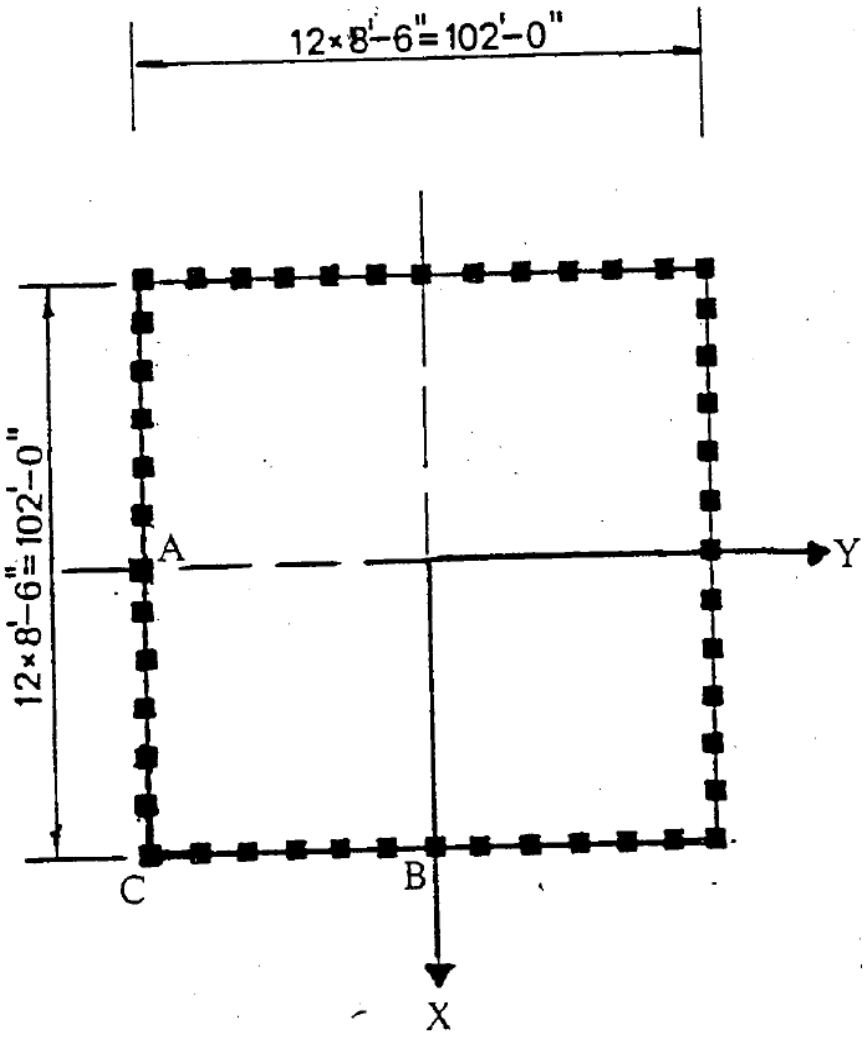

Figure 61: Plan view example 4-1 ref (32)

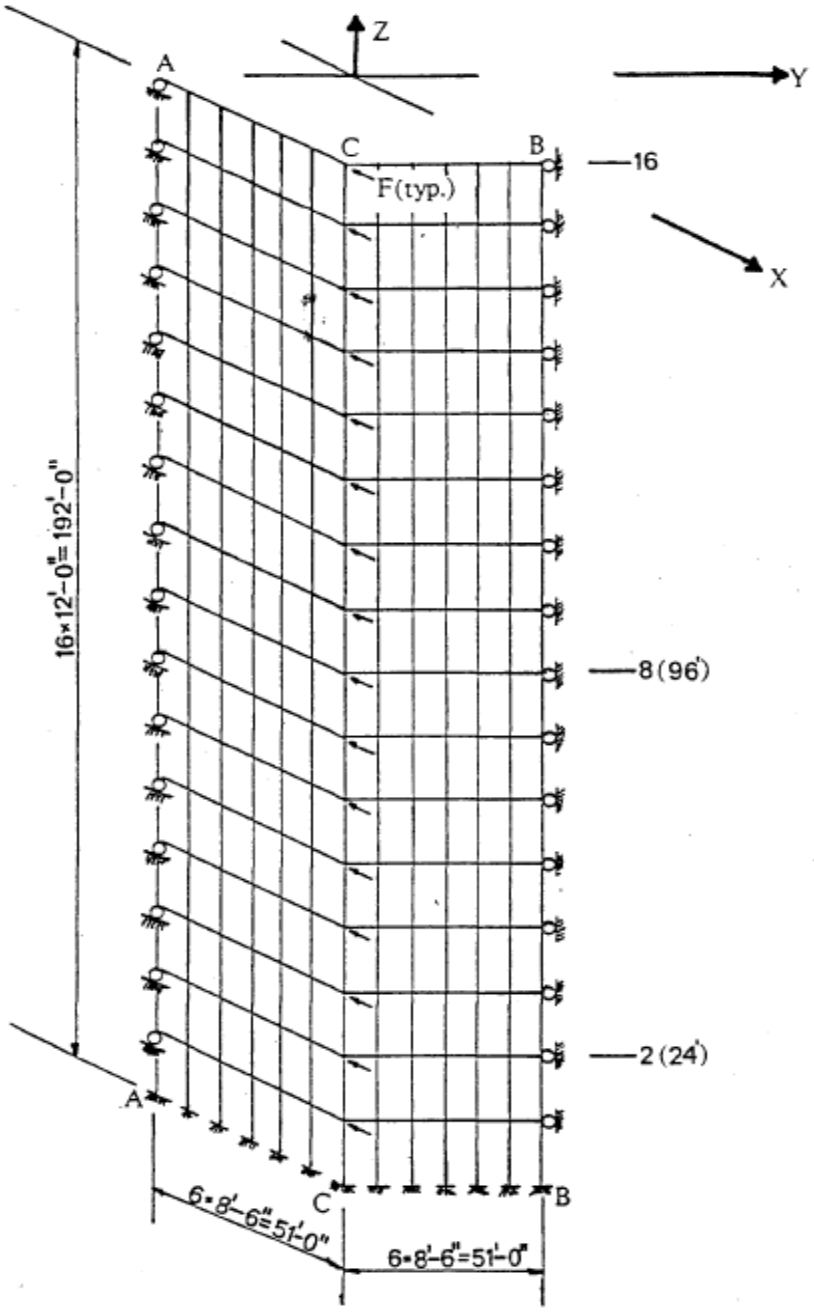

Notes: 1. F= 12.74 Kips

Figure 62: SAP2000 model example 4-1

4.3.2.2 Methods of Analyses

The 16 story framed tube will be analyzed using both Framed Tube Program and SAP2000. The Framed Tube Program analysis will be carried out on a full three dimensional model of the structure. It can be represented in the output by a single normal and side panel due to symmetry. A uniformly distributed load of 4.08 k/ft., producing a base overturning moment of 75202.56 k/ft., is used for comparison. This load was used by Moselhi to analyze this structure and is used here to allow a comparison to the Moselhi approach.

For the SAP2000 analysis story shears will be used to mimic the uniformly distributed load. Figure 62 indicates the force F, applied at each story level. The overturning moment produced by the F forces totals one quarter of the total overturning moment. To allow a one quarter model to be used appropriate boundary conditions are utilized at the story levels. The base is considered rigidly fixed. To represent the rigid joint sizes the girders will be stopped at the column face(s) and infinitely rigid links will be used to model the width of each column and likewise the depth of each girder. At the top story the columns will be "stopped" one half of a girder depth from the actual SAP2000 joint and a rigid link inserted to represent the remaining distance.

4.3.2.3 Results

Figure 63 compares the lateral deflection of the 16 story framed tube using Framed Tube Program, and SAP2000.

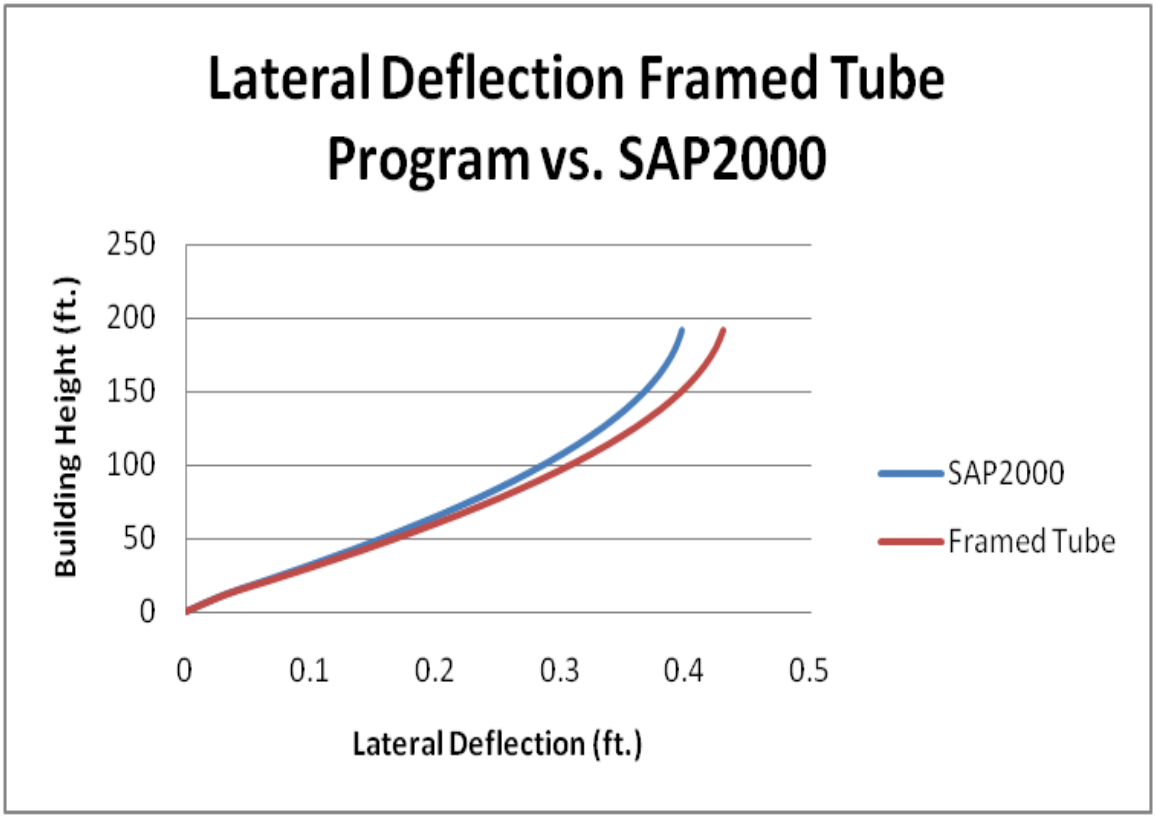

Figure 63: Lateral Deflection example 4-1 Framed Tube Program vs. SAP2000

4.4 Discussion of Results

Framed Tube Program provides a good preliminary estimation of the lateral deflections. In this example Framed Tube Program was within 32% of the SAP2000 results. The orthotropic plate approximations are a more constrained model of the structure than a discrete matrix analysis. Axial girder strains are neglected by the Framed Tube Program analysis and also, the frame racking effects near the lower stories of the real structure are greater relative to those at upper stories. In other words the interstory drift cannot be accurately modeled with a parabolic distribution. If the artificial shear modulus used in the orthotropic plate approach could be varied with height in relative proportion to the actual racking effects that are expected better comparative results could be obtained. Also the rigid floor slabs cannot be conveniently modeled in a quarter tube approach

using SAP2000. For this reason the SAP2000 model is more flexible as reflected in the high torsional moments that developed in the lower level columns of the side frames due to out of plane translation. As with any approximate analysis approach the inherent characteristics of the real structure will affect the comparative accuracy of the method. For the framed tube better results will occur for tubes with relatively stiff girders and small window openings.

v. CONCLUSIONS AND RECOMMENDATIONS

5 Conclusions

The computer programs presented within; Wall Frame Program for analysis of shear wall or truss-frame interactive structures in two dimensions, Outrigger Program for the analysis of multi-outrigger braced tall buildings, and Framed Tube Program for the preliminary assessment of deflections in a single tube structure, have proven to satisfy the requirement set forth for approximate analysis tools. Each Resource Level Knowledge Module is fast, easy to use and reasonably accurate for preliminary design. The incorporation of graphics has made some programs more useful for structural assessment.

It was found that the accuracy of an approximate method as compared to a matrix analysis is affected by the inherent properties of the structure. Shear wall-frame structures with an inherent flexural behavior will be more closely approximated by the shear-flexural cantilever theory, (which is the basis for Wall Frame 2D program). Stiffer frames in these types of structures were found to have a great influence on the shear and moment distribution between the frame and the flexural components. Although the stiffer frame will reduce drift near the top of the structure it is usually more economical to proportion the vertical resisting elements to sustain a greater percentage of the lateral load effects.

The accuracy of using an equivalent uniform stiffness for structures of non-uniform vertical stiffness was found to be a reasonable approximation. Drifts can be expected to be slightly overestimated and core moments and shears slightly underestimated near the base. The speed of this analysis and also the capability within Wall Frame 2D Program to calculate the shearing stiffness of the frames for horizontal as well as vertical non-uniformity versus the relatively extensive input preparation required for a transfer matrix approach make this program attractive for preliminary design ref (76). In cases of radical changes in stiffness the designer should exercise good judgment in applying a uniform stiffness approximation.

The accuracy of analyzing outrigger braced structures can be improved by including the effects of outrigger flexibility in the analysis. The user can expect an underestimation of up to 40% of the actual lateral drift for structures analyzed per the rigid outrigger approach.

The rigid outrigger approach was found to give most inaccurate results for a single outrigger structure. Also, outrigger resisting moments calculated based on the axial forces in the exterior columns only, will be overestimated and since these moments will be less in the real structure the Outrigger program within will yield base core moments less than those in the real structure. Outrigger moments will increase as the outrigger is moved lower in the structure (subsequently reducing core moments) but this will sacrifice the drift reduction due to the outrigger. Adding additional outriggers will further reduce drift, but each additional outrigger has a lesser and lesser effect on the structure. More than four outriggers in one structure can be considered in justifiable from a lateral deflection standpoint. Lateral load type effects the optimum location of the outrigger for drift reduction. It was found that a uniformly distributed load provides the most accurate results for load types that produce equal base overturning moments.

Using an assumed parabolic variation for the shear lag in a framed tube was found to underestimate the deflections near the comer columns and slightly overestimate the deflections at the middle of the normal face of the tube. The accuracy of the method decreases near the base of the structure. A comparison to a SAP2000 analysis for a 16 story concrete framed tube structure has shown that displacements can be estimated to within 33%.

The knowledge modules presented can be rationally applied in a knowledge based approach to tall building design. Additional research is required to establish an environment integrating conceptualization, preliminary member sizing and analysis, global evaluation, and optimization of a tall buildings structural system. With the advent of faster and more powerful computers, demand for

research into approximate analysis of tall buildings has declined in recent years. The time required to perform extensive matrix analyses has been reduced with the advent of automatic mesh generators and computer aided design and drafting (CADD) systems. These developments however, are not always readily available, (or affordable) to the average engineer. The approximate analysis techniques are invaluable in this respect and also they "force" the user to have or quickly obtain an understanding of tall building behavior.

5.1 Recommendations for Future Research

In order to establish an integrated and complete design environment for tall buildings the following research should be conducted:

1. Approximate dynamic analysis

2. Development of modules to calculate vertical and lateral loads

3. Development of modules to perform vertical load analysis

4. Software should be developed to manipulate the data from several analyses and allow global evaluation of structural systems

5. Development of modules for partial tube, tube-in-tube, braced tubes and composite structural systems

6. As an aside, perform a detailed investigation of floor slab rigidity ref (71).

The following direct improvements to the software presented within are suggested:

1. Improve SWLFRM-3D to allow a distribution of moment in the frame elements to be directly output.

2. Add outrigger flexibility capabilities to outrigger Program.

3. Add additional subroutines to Framed Tube program that will provide for stresses, member forces and torsional analysis.

4. Apply the transfer matrix method to allow direct analysis of non-uniform framed tubes or allow for stopping individual tubes in a bundled tube system at different story levels.

5. Add graphical capabilities to Framed Tube program to observe shear lag in the normal and side panels of single and quad-bundled tubes.

6. Add subroutines to accommodate perforated walls (Wall Frame Program) and cores directly.

7. Incorporate an interactive system whereby the user can input story shears (as calculated from an applicable code), and the program will calculate the equivalent lateral load using a uniform, triangular and/or concentrated load.

8. Allow for superposition of the results from more than one analysis.

REFERENCES

1. Iyengar, S.H., et. al., "Elastic Analysis and Design", Chapter SB-2, Structural Design of Tall Buildings, Tall Building Monographs, ASCE, Vol. SB, 1979, pp. 617-804.

2. Ha, Kinh, H., Fazio, Paul, Moselhi, Osama, "Orthotropic Membrane For Tall Building Analysis", Jml. of the Struc. Div., ASCE, Vol. 104, No. ST9, Sept., 1978,pp 1495-1505.

3. J.Connor, P.Jayachandran, D.Sriram, "Knowledge Based Approach For Preliminary Design of Tall Buildings", Proposal to NSF, March 1987.

4. Stafford Smith, B., and Coull, A., "Elastic Analysis of Tall Concrete Buildings", SOA Report 21-1, Technical Committee No. 21, ASCE-IABSE Joint Committee on Planning and Design of Tall Buildings, 1972, pp. 157-170.

5. Khan, F.R., "On Some Special Problems of Analysis and Design of Shear Wall Structures", Tall Buildings, Pergamon Press Ltd., London, 1967, pp. 321-347.

6. Stamato, M.C., "Three Dimensional Analysis of Tall Buildings", Report No. 24-4, Proceedings of ASCE-IABSE International Conference on Planning and Design of Tall Buildings, Vo1.3, Lehigh University, Bethelem, PA., 1972, pp. 683-899.

7. Coull, A. and Smith, B.S., "Analysis of Shear Wall Structures", Tall Buildings, Proceedings of a Symposium at the University of Southampton, Pergamon Press Ltd., London, 1967.

8. Coull, A., Stafford Smith, B., "Recent Developments in Elastic Analysis of Tall Concrete Buildings", Developments in Tall Buildings 1983, Hutchinson Ross Publishing Co., Stroudsburg, Penn., 1983, pp.569-580.

9. Stafford Smith, B., "Recent Developments in the Methods of Analysis for Tall Building Structures", Civil Engineering arid Works Review, Vol. 65, 1970.

10. Coull, A. and Ahmed, A., "Deflections of Framed-Tube Structures", Journal .of the Struc Div., ASCE, Vol. 104, No. ST5, May 1978, pp. 857-862.

11. Heidebrecht and Smith., "Approximate Analysis of Tall Wall-Frame Buildings", Jrnl . of the Struc. Div., ASCE, Vo1.99, No.STI, Feb., 1973, pp.199-221.

12. Maher, M.L., and Fenves, S.J., Hi-Rise: A Knowledge-Based Expen System for the Preliminary Structural Design of High Rise Buildings, Department of Civil Engineering, Report No. R85-146, Carnegie-Mellon University, Pittsburgh,PA. Jan., 1985.

13. Taranath,B.S., "Optimum Belt Truss Locations for High-Rise Structures", AISC Engineering Journal, Vol. 11, First Quarter, 1974, pp. 18-21.

14. Fitzsimmons, N., "History and Philosophy of Tall Buildings", Proceedings, International Conference on Planning and Design of Tall Buildings, Vol.1, Lehigh Univ., 1972, pp.41-52.

15. Beck, H., "Contribution to the Analysis of Coupled Shear Walls", Journal. ACI, Vol. 59, No.8, August 1962, pp. 1055-1070.

16. Salmon, Charles, G., and Johnson, John, E., Steel Structures .Design and Behavior, 2nd Ed., Harper and Row, New York, 1980, pg.4.

17. Khan, Fazlur, "The Bearing Wall Comes of Age", Architectural and Engineering News, Vol.10, No.10, Oct., 1968, pp.78-85.

18. Sitzenstock, R.P., "Evolution of the High-Rise Office Building", Progressive Architecture, Vol. 44, Sept. 1963. pp. 146-157.

19. Khan, P.R., "Evolution of Structural Systems for High Rise Buildings in Steel and Concrete", Seminar on the Design of Tall Buildings, New York, 1973.

20. Iyengar, S.H., "Structural Systems - An Update", Advances in Tall Buildings, Van Nostrand Reinhold Co., New York, 1986, pp. 149-162.

21. "Optimizing the Structure of the Skyscaper", Architectural Record, Oct, 1972.

22. Liauw, T.C., "Evolution of New Structural Systems for Tall Buildings", Proceedings of the Regional Conference of Tall Buildings, Asian Institute of Technology, Bangkok, Thailand, Jan. 23-25,1974, pp.115-125 .

23. Kozak, J., "Structural Systems of Tall Buildings in Steel or Combined Steel and Concrete ",Proceedings, 10th Regional Conference on Planning and Design of Tall Buildings, Bratislava, Czechoslovakia, April 1973 , pp. 118-134.

24. Committee 3 of the Council on Tall Buldings and Urban Habitat, "Structural Systems", Chapter SC-l, Tall Building Systems and Concepts, Tall Building Monographs, ASCE, Vol. 5C, 1980, pp. 3-61.

25. Gero, J.S., "The Behavior of Building Structures Under Lateral Loads", Australia and New Zealand Conference on the Planning and Design of Tall Buildings, Sydney, Australia, 1973.

26. Iyengar, S.H., "Recent Developments in Composite High-Rise Systems", Advances in Tall Buildings, Van Nostrand Reinhold Co., New York, 1986, pp. 379-388.

27. Ruderman, J., "High Rise Steel Office Buildings in the United States", The Structural Engineer, Vol. 44, No.1, Jan. 1965. pp. 23-30.

28. Fintel, M., "Deflections of High-Rise Concrete Buildings", Journal. ACI, July 1975, pp. 324-328.

29. Iyengar, S.H., "Preliminary Design and Optimization of Steel Building Systems", Proceedings, ASCE-IABSE International Conference on Tall Buildings, Vol. 2, Lehigh Univ., 1972, pp. 185-201.

30. Asfour, Grant "Methods of Structural Analysis and Design of Tall Buildings", Independent Study Submittedfor MSCE Degree, Department of Civil Engineering, Worcester Polytechnic Institute, MA, June 1981.

31. Picardi, E.A." Structural System- Standard Oil of Indiana Building", Journal. of the Struc. Div. ASCE, Vol. 99, ST4, April 1973, pp. 605-620.

32. Paxton, W.E., Colaco, J.P., et.al., "Concrete Framing Systems For Tall Buildings", Chapter CB-3, Structural Design of Tall Concrete and Masonry Buildings, Tall Building Monographs, ASCE, Vol. CB, 1978, pp. 49-107.

33. Coull, A., and Irwin, A.W., "Model Investigations of Shear Wall Structures", 1rnl. of the Struct. Div., ASCE, Vol. 98, No. ST6, June 1972, pp. 1223-1237.

34. Fintel, M., "Staggered Wall Beams for the Multistory Buildings", Civil Engineering, ASCE, Vol. 38, No.8, August 1968, pp. 56-59.

35. Balcke, H.P., Kloiber, L.A. and Nohn, A.C., Staggered Truss Building Systems", Civil Engineering, ASCE, Vol. 39, No. 11, Nov. 1969, pp. 56-59.

36. Heidebrecht, A.C., amd Swift, R.D., "Analysis of Asymmetrical Coupled Shear Walls", 1rnl.of the Struc. Div., ASCE, Vol. 97, No. ST5, 1971, pp. 1407-1422.

37. Gluck, J., "Lateral Load Analysis of Irregular Shear Wall Multi-Story Structures", ACI Journal., Vol. 67, No.7, 1970, pp.548-553.

38. Rosman, R., "Analysis of Spatial Concrete Shear Wall Systems", Proceedings, Institute of Civil Engineers, London, England, Supplement Paper 1'2665, 1970, pp. 131-152. .

39. Biswas, J.K. and Tso, W.K., "Three Dimensional Analysis of Shear Wall Buildings Subject to Lateral Load", 1rnl of the Struc.Div., ASCE, Vol. 100, No.ST5, Proc. Paper 10537, 1974, pp. 1019-1036.

40. Coull, A. and hwin, A.W., "Load Distribution in Multi Story Shear Wall Structures", Proceedings, 8th Congress of IABSE, New York, 1968.

41. Kahn, F.R., "Optimization Approach for Concrete High Rise Structures", Response of Multistory Concrete Structures to Lateral Forces. ACI Spec. Pub., SP-36, 1973, pp.13-37.

42. Colaco, J.P., Coull, A. and Stafford-Smith; B., "Elastic Analysis", Chapter CB-5, Structural Design of Tall Concrete and Masonry Buildings, Tall Building Monographs, ASCE, Vol. CB, 1978, pp. 147-168.

43. Derecho, A.T., "Frames and Frame-Shear Wall Systems", Response of Multi-Story Concrete Structures to Lateral Forces, ACI Spec. Pub., SP-36, 1973, pp. 13-37.

44. Macleod, Ian, A .. "Shear Wall-Frame Interaction, A Design aid With Commentary",PCA Special Publication, 1971.

45. Salim, Irawin, "The Behavior of Flexible Outrigger Braced Tall Buildings", Thesis Submittedfor Master of Engineering Degree, Department of Civil Engineering and Applied Mechanics, McGill University, Montreal, Quebec, May 1980.

46. Taranath, B.S., Optimum Belt Truss Locations for High-Rise Structures", The Structural Engineer, Vol. 53, No.8, 1975, pp. 345-347.

47. Stafford Smith, B., and Nwaka, 1.0., "The Behavior of Multi-Outrigger Braced Tall Buildings", American Concrete Institute Special Publication of Papers for Symposium on Reinforced Concrete Structures, Sponsored by Committee 442,1980.

48. Iyengar, S.H., "Structural Systems for two Ultra High-rise Structures",Australia and New Zealand Conference on the Planning and Design of Tall Buildings, Sydney, Australia, 1973.

49. Schueller Wolfgang, High Rise Building Structures, John Wiley & Sons, N.Y., 1977.

50. Khan, F.R., "Multi-Story Buildings: Recent Structural Systems in Steel for High-Rise Buildings", DeIngenieur, Vol.82, No.28, July 1970, pp. 1381-1392.

51. Feld, L.S., "Superstructure for 1350-ft World Trade Center", Civil Engineering-ASCE, June 1971, pp. 66-70.

52. Coull, A., Bose, B., "Simplified Analysis of Frame-Tube Structures", Journal. of the Struc. Div., ASCE, Vol. 101, No. ST11, Nov. 1975, pp. 2223-2240.

53. Iyengar, Hal S., "Bundled-Tube Structure for Sears Tower", Civil Engineering Journal, ASCE, Nov. 1972.

54. Coull, A., Bose, B., and Ahmed, A.K., "Simplified Analysis of Bundled-Tube Structures", Journal. of the Struc. Div., ASCE, Vol. 108, No.ST5, May 1982, pp. 1140-1153.

55. Khan, P.R., "Current Trends in Concrete High Rise Buildings", Tall Buildings, Pergamon Press Ltd., London, 1966.

56. Colaco, J P.," Partial Tube Concept for Mid-Rise Structures", Engineering Journal ,AISC, 4th Quarter, 1986, Vol. 11, No.4, pp. 81-85.

57. Khan, F.R., "The John Hancock Center", Civil Engineering-ASCE, Oct. 1967 .

58. Jayachandran, P., "Optimized Analysis and Design of Tall Buildings for Seismic and Wind Drift-Acceleration Criteria", Proposal to NSF, Sept 1977.

59. Clarke, D.Computer Aided Structural Design~ John Wiley and Sons Ltd., Chichester, England,1978.

60. An Editorial., "Expert Systems", Fire Technology, Vol. 23, No.1, Feb. 1987, pg. 1.

61. Yehia, Nabil, A.B., and Bechara, Rabih, M., "A Simple Knowledge-Based Design Approach", Concrete International, Vol. 10, No.1, Jan. 1988.

62. Spillers, W.R., "Artificial Intelligence and Structural Design", Journal of the Srruc. Div., ASCE, Vol. 92, ST6, Dec. 1966, pp. 491-496.

63. LeFrancois, D.R., "Approximate Methods of Analysis and Preliminary Design of Tall Buildings", Thesis Submittedfor MSCE Degree, Department of Civil Eng., Worcester Polytechnic Institute, Worcester, MA., July 1981.

64. Bandel, R., "Frames Combined with Shear Trusses under Lateral Loads", Proc. ASCE, Vol. 88, No. ST6, Dec. 1962, pp. 227-243.

65. Stafford Smith, B., et al, " A Generalized Approach to the Deflection Analysis of Braced Frame, Rigid Frame, and Coupled Wall Structure", Canadian Journal of Civil Engineering, Vol. .8. , 1981, pg. 230.----

66. Khan, F.R., and Sbarounis, J.A., "Interaction of Shear Walls and Frames", Proceedings, ASCE, Vol. 90, No. ST3, June 1964, pp. 285-335.

67. Clough, RW., King, I.P., and Wilson, E.L., "Structural Analysis of Multistory Buildings", Journal. of the Struc. Div., ASCE, Vol. 90, June 1964, pp. 19-34.

68. Panne, A.L., "Design of Combined Frames and Shear Walls", Tall Buildings, Pergamon Press Ltd., London, 1967, pp. 291-320.

69. Jenkins, W.M. and Harrison, T., "Analysis of Tall Buildings with Shear Walls under Bending and Torsion", Tall Buildings, Pergamon Press Ltd., London, 1967, pp. 413-444.

70. Winokur, A. and Gluck, J., "Lateral Loads in Asymmetric Multistory Structures", Jrnl. of the Struc.Div., ASCE, Vol. 94, No. ST3, Proc. Paper 5842, March, 1968.

71. Quadeer, A. and Stafford Smith, B., "The Bending Stiffness of Slabs Connecting Shear Walls", ACI Proc., Vol. 66, No.6, 1969, pp. 464-477.

72. Sieczkowski, J., et al., "Simplified Method of Analysis of Frame-Wall Systems", Advances in Tall Buildings, Van Nostrand Reinhold Co., New York, 1986, pp. 433-450.

73. Coull, A., and Adams, N.W., "A Simple Method of Analysis of the Load Distribution in Multistory Shear Wall Structures", ACI Spec. PUb., SP-36, 1973, pp. 187-205.

74. Gluck, J., "Lateral Load Analysis of Asymmetric Multistory Structures", Journal of the Struc. Div., ASCE, Vol. 96, No. ST2, Feb., 1970, pp. 317-332.

75. Mortelmans, F.K.E.C. et.al., "Approximate Method for Lateral Load Analysis of High Rise Buildings", Journal of the Struc.Div., ASCE, Vol. 107, No. ST2, August 1981, pp. 1589-1609.

76. [Seetharamulu, K., and Kumar A., "The Analysis of Tall Building Structures by the Transfer Matrix Mathed", Proceedings of the Regional Conference on Tall Buildings,

National/Regional Conference(Bangkok, Thailand, January 23-25,1974), Asian Institute of Technology, Bangkok, Thailand, pp. 367-379.

77. Balendra, T., "A Simplified Model for the Lateral Load Analysis of Asymmetrical Buildings", Engineering Structures, Vol. 5, July 1983, pp. 154-162.

78. Coull, A., and Smith, B.S., "Analysis of Shear Wall Structures", Tall Buildings, Proceedings of a Symposium at the University of Southampton, Pergamon Press Ltd., London, 1966.

79. ACI Committeee442., "Response of Buildings to Lateral Forces", Proceedings, Journal. ACI, Vol. 68, No.2, Feb. 1971, pp. 81-106.

80. Rosman, R, "Laterally Loaded Systems Consisting of Wails and Frames", Tall Buildings, Pergamon Press Ltd., London, 1967, pp. 273-289.

81. Smith, B.S., "The Composite Behavior of Infilled Frames", Tall Buildings, Pergamon Press Ltd., London, 1967, pp. 481-495.

82. Cardan, B., "The Composite Behavior of Infilled Frames", Tall Buildings, Pergamon Press Ltd., London, 1967, pp. 481-495.

83. Gould, P.L., "Interaction of Shear Wall Frame Systems in Multistory Buildings', Jrnl. ACI, Proceeding No.1, Vol. 62, Jan. 1965, ppA5-70.

84. Coull, A., and Choudhury, J.R, "Stresses and Deflections in Coupled Shear Walls", ACI Proc., Vol. 64, No.2, 1967, pp.65-72.

85.]Marshall, M.G.,''The Analysis of Shear Wall Structures", MSc Thesis, University of Waterloo, Ontario, Sept., 1968.

86. Coull, A., and Choudhoury, J.R, "Analysis of Coupled Shear Walls", Journal. ACI, Sept. 1967, pp. 587-593.

87. Coull, A. and Purl, RD., "Analysis of Coupled Shear Walls of Variable Thickness ", Building Science, Vol. 2, No.2, 1967, pp. 181-188.

88. Coull, A. and Purl, RD., "Analysis of Coupled Shear Walls of Variable Cross-Section", Building Science, VoL2, No.4, 1968, pp. 313-320.

89. Schwaghofer, J., and Microys, H.F., "Analysis of Shear Walls Using Standard Computer Programs", Jrnl. ACI, Dec. 1969, Vol. 66, pp. 1005-1007.

90. Cheung, Victor W.T., and Tso, W.K., "Lateral Load Analysis for Buildings with Setback ", Journal of Structural Engineering, Vol. 113, No.2, Feb. 1987, pp. 209-227.

91. Conte, Samuel, D., and Deboor,Carl., Elementary Numerical Analysis ,3rd ed., Mcgraw-Hill Book Co., New York, 1980.

92. Choi, C.K. and Bang, M.S., "Plate Element with Cutout for Perforated Shear Wall",Jrnl.oftheStruc. Div., ASCE, Vol. 113, No.2, Feb., 1987.

93. Tham, L.G., and Cheung, Y.K., "Approximate Analysis of Shear Wall Assemblies with Openings", The Structural Engineer, Vol.'61B, No.2, June 1983.

94. Manual of Steel Construction, AISC, 13th ed., 2007.

95. Fleming, J.F., "Lateral Truss Systems in High Rise Buildings", Proceedings of the National Conference on Tall Buildings, Asian Institute of Technology , Bangkok, Thailand, 1974.

96. "Minimum Design Loads for Buildings and Other Structures", American National Standards Institute, ANSI-A58.1, 1982.

97. McNabb, J.W., and Muvdi, RR, Drift Reduction Factors for Belted High-Rise Structures", AISC Engineering Journal, 3rd Quarter, 1975, pp. 88-91.

98. McNabb, J.W. , and Muvdi, RR, "Discussion of Drift Reduction Factors for Belted High-Rise Structures", Engineering Journal AISC, 1st Quarter, 1977.

99. Rutenberg, A., "Earthquake Analysis of Belted High-Rise Building Structures"; Engineering Structures, Vol. 1, NoA, July 1979, pp. 190-196.

100. Stafford Smith, B. and Salim, I., "Parameter Study of Outrigger-Braced Tall Buildings", Jml. of the Struc. Div., ASCE, Vol. 107, No. ST1O, 1981, pp. 2001-2014.

101. Pancewicz, Z., and Arciszewski, T., "Approximate Statical Analysis of Bracing System Composed of Trussed Frames", Proceedings of Regional Conference on Planning and Design of Tall Buildings, Warsaw, Poland, Nov. 1972, pp.195-204.

102. Schwaighofer, J., and Tai, C., "Tables for the Analysis of Shear Walls With Two Vertical Rows of Openings", Publication No. 71-27, University of Toronto, Department of Civil Engineering, Nov. 1971.

103. Coull, A., and Subedi, N.K., "Framed Tube Structures for High-Rise Buildings", Jml.oftheStruc. Div., ASCE, Vol. 97, No. ST8, August 1971, pp. 2097-2105.

104. Coull, A., and Stafford Smith, B., "Torsion Analysis of Symmetric Building Structures", Jml. of the Struc. Div., ASCE, Vol. 99, No. ST1, 1973, Proc. Paper 9464, pg. 229.

105. Rutenberg, A., and Heidebrecht, A.C., "Approximate Analysis of Asymmetric Wall-Frame Structures", Building Science, London, Vol. 10, 1975, pg. 27.

106. Swaddiwudhipong, S., and Seng-Lee, L., "Core-Frame Interaction in Tall Buildings", Engineering Structures, Vol. 7, No.1, Jan. 1985, pp. 51-55.

107. Clough, Ray, W., and King, Ian, P., "Analysis of Three Dimensional Building Frames", Memoires Abhandlungen Publications, IABSE, Published by General Secretariart in Zurich, 24th Vol., 1964.

108. Weaver, W., Brandon, G.E., and Manning, T.A., "Tier Buildings With Shear Cores, Bracing and Setbacks", Computers and Structures, Vol. 1, 1971, pp.57-83.

109. Stamato, M.C., and Stafford Smith, B., "An Approximate Method for the Three Dimensional Analysis of Tall Buildings", Proceedings, Institution of Civil Engineers, Vol. 43, July, 1969, pp. 361-379. '

110. Hongladaromp, T., Lee, S.L., and Pithyachariyakul, P., "Analysis of Asymmetric Shear Wall-Frame Buildings", Proceedings of the Regional Conference of Tall Buildings, Bangkok, Thailand, Jan. 1974, pp. 353-365.

111. Danay, A., Gellert, M. and Gluck, 1., "The Axial Strain Effects on Load Distribution inNonsymmetric Tier Buildings", Building Science, Vol. 9, No.1, 1974, pp.29-38.

112. Clough, R., King, I.P., and Wilson, E.L., "Structural Analysis of Multistory Buildings", JmlStruc. Div., ASCE, Vol. 90, No.ST3, June 1964, pp.19-34.

113. Stamato, M.C., and Mancini, E., "Three Dimensional Interaction of Walls and Frames", JmlStruc.Div., ASCE, Vol.99, No. ST12, 1973, p. 2375.

114. Heins, C.P.Jr., and Seaburg, P.A., "Torsion Analysis of Rolled Steel Structures", Bethlehem Steel AlA File No. 13-A-1 , 1963.

115. Chajes, A., Principles of Structural Stability Theory, Prentice-Hall, Inc., Englewood Cliffs, New Jersey, 1974, pp. 106-110.

116. Rutenberg, A., and Tso, W.K., "Torsional Analysis of Perforated Core Structures", Jml.oftheStruc. Div., ASCE, Vol. 101, No. ST3, 1975, pp. 539-550.

117. Liauw, T.C. and Leung, K.W., "Torsional Analysis of Core Wall Structures by the Transfer Matrix Method", The Structural Engineer, April 1975, Vol. 53, No.4, pp. 187-193.

118. Taranath, B.S., "Torsion Analysis of Braced Multistory Cores", The Structural Engineer, Vol. 53, No.7, 1975, pp. 285-289.

119. Stafford Smith, B., and Taranath, B.S., "Analysis of Tall Core-Supported Structures Subject to Torsion", Proceedings, Institution of Civil Engineers, London, Vol. 53, 1972, p. 173.

120. Heidebrecht, A.C., and Stafford Smith, B., "Approximate Analysis of Open-Section Shear Walls Subject to Torsional Loading", JmlStruc.Div., ASCE, Vol. 99, No. ST12, Dec. 1973, pp. 2355-2373.

121. Coull, A., and Tawflk, S.Y., "Elasto-Plastic Analysis of Core Structures Subjected to Torsion ", Proceedings of Institute for Civil Engineers, Vol. 71, Part 2, pp. 789-804.

122. Coull, A., and Bose, B., "Torsion of Framed-Tube Structures", JmlStruc.Div., ASCE, Vol. 102, No. ST12, Dec. 1976, pp. 2366-2370.

123. Moselhi, 0., Fazio, P., and Zielinski, Z., Discussion of "Torsion of Frame-Tube Structures", by Coull, A., and Bose B., JmlStruc.Dov., ASCE, ST12, Dec. 1977, pp. 2426-2428.

124. Coull, A., and Bose, B., Closure to Discussion of "Torsion of Framed-Tube Structures", JmlSrruc. Div., ASCE, STlO, Oct. 1978, pp. 1673-1674.

125. McGuire, W., and Gallagher, R.H., Matrix Structural Analysis, John Wiley and Sons, New York, 1979, Ch. 12.

126. Personal Correspondence with T.Balendra,'National University of Singapore, Facsimile Feb., 12, 1988.

127. Rutenberg, A., "Analysis of Tube Structures for High-Rise Buildings", Proceedings of the 22nd National/Regional Conference on Tall Buildings, Asian Institute of Technology, Bangkok, Thailand, Jan. 1974, pp. 397-413.

128. Khan, F.R., and Amin, N.R., "Analysis and Design of Framed Tube Structures for Tall Concrete Buildings", Response of Tall Multistory Cone. Buildings to Lateral Forces, ACI Special Publication, SP-36, 1973.

129. Schwaighofer, J. Ast. P., "Tables for the Analysi~ of Framed Tube Buildings", Publication No. 72-01, University of Toronto, Department of Civil Engineering, March 1972.

130. Khan, M.A.H., and Stafford Smith, B., "A Simple Method of Analysis for Deflections and Stresses in Wall-Frame Structures", Building and Environment, Vol. II, Pergamon Press Ltd., London, 1976, pp. 69-78.

131. DeClercq, H., and Powell, G.H., "Analysis and Design of Tube-Type Tall Building Structures", Report No. EERC 76-5, Earthquake Engineering Research Center, College of Engineering, University of California, Berkeley, CA, Feb. 1976.

132. EI-Moselhi, O.E., "Analysis ofPetforated Walls and Tube-Type Tall Building Structures", Report No. CBS-44, Center for Building Studies, Faculty of Engineering, Concordia Univesity, Montreal, Quebec, June 1978.

133. Chan, P.C.K., "Static and Dynamic Analysis of Framed-Tube Structures", PHD. Thesis, Mcmaster University, Hamilton, Ontario, Canada, 1973.

134. Tsapatsaris, N., "A Knowledge Based Expert System for the Selection of Structural Systems for Tall Buildings", Thesis Submitted/or MSCE Degree, Department of Civil Engineering, Worcester Polytechnic Institute, Worcester, MA, July 1987.

135. Grandin, H.Jr, Fundamentals o/the Finite Element Method, MacMillan Pub.Co., New York, 1986, pp. 73-84.

136. Stafford Smith, B., "Modified Beam Method for Analyzing Symmetrical Interconnected Shear Walls", Journal ACI, Vol. 67, No. 12, 1970, pp. 977-980.

Appendix

60 Story composite Building input values for program ALPHA								
Ic (in^4)	Ig (in^4)	h (ft)	n	EQ. STORIES	Ef (ksi)	t (in)	Iw (in^4)	Ew (ksi)
3840	16800	12	3	5	29000	8	73728000	3605
4330	17900	12	3	5	29000	10	92160000	3605
4900	19500	12	3	5	29000	12	110592000	3605
5440	21100	12	3	5	29000	14	129024000	3605
6000	23300	12	3	5	29000	16	147456000	3605
6600	25700	12	3	5	29000	18	165888000	3605
7190	28500	12	3	5	29000	20	184320000	3605
8210	32100	12	3	5	29000	22	202752000	3605
9430	36000	12	3	5	29000	24	221184000	3605
10800	39600	12	3	5	29000	26	239616000	3605
12400	50600	12	3	5	29000	28	258048000	3605
14300	64700	12	3	5	29000	30	276480000	3605

Table 23: 36 concrete story building parameters

Number of segments	Segment No.	I (ft^4)	GA (Kips)	ALPHA (1/ft) (*10e-4)	Segment Length (ft)
6	1	49872	9500	5.874	20
	2	46042	8731	5.861	30
	3	42125	8674	6.107	30
	4	36662	7530	6.099	100
	5	32121	6750	6.169	130
	6	30091	6400	6.207	50
4	1	47574	9039	5.866	50
	2	37923	7794	6.101	130
	3	32121	6750	6.169	130
	4	30091	6400	6.207	50
2	1	45531	8902	5.951	80
	2	33080	6966	6.148	280
1	1	36080	7396	6.093	360

PRELIMINARY ANALYSIS OF WALL OR TRUSS-FRAMED BLDGS.
METHOD DEV. BY HEIDEBRECHT & SMITH
THIS METHOD TO BE USED FOR 2-DIMENSIONAL ANALYSIS.
REF: J. OF STRL. DIV, ASCE, VOL 99, NO. ST2. FEB. 1973
MADISON R. PAULINO M.S.C.E. W.P.I. 2010

Input Data:
Wind Load (Wo) (K/ft): 4.75000
Building Height (ft): 360.00
Truss or Wall Mon. of elasticity (K/ft^2): 5.52100e+005
Total moment of Inertia Truss or Wall (ft^4): 3.60800e+004
Alpha: 6.09300e-004
Number of output (N): 10.0

Height(ft)	Lateral Deflection	Shear Wall		Frame	
H	y	Moment	Shear	Moment	Shear
0.00	0.00000	3.04166e+005	1.71000e+003	3.63438e+003	0.00000e+000
36.00	0.00924	2.45752e+005	1.53533e+003	3.56602e+003	3.66779e+000
72.00	0.03451	1.93613e+005	1.36140e+003	3.37917e+003	6.59684e+000
108.00	0.07241	1.47723e+005	1.18813e+003	3.09891e+003	8.87085e+000
144.00	0.11995	1.08061e+005	1.01543e+003	2.74733e+003	1.05732e+001
180.00	0.17456	7.46065e+004	8.43213e+002	2.34350e+003	1.17869e+001
216.00	0.23405	4.73445e+004	6.71405e+002	1.90353e+003	1.25950e+001
252.00	0.29666	2.62615e+004	4.99920e+002	1.44054e+003	1.30800e+001
288.00	0.36101	1.13473e+004	3.28676e+002	9.64663e+002	1.33244e+001
324.00	0.42613	2.59492e+003	1.57589e+002	4.83079e+002	1.34107e+001
360.00	0.49146	0.00000e+000	-1.34212e+001	0.00000e+000	1.34212e+001

PRELIMINARY ANALYSIS OF WALL OR TRUSS-FRAMED BLDGS.
METHOD DEV. BY HEIDEBRECHT & SMITH
THIS METHOD TO BE USED FOR 2-DIMENSIONAL ANALYSIS.
REF: J. OF STRL. DIV, ASCE, VOL 99, NO. ST2. FEB. 1973
MADISON R. PAULINO M.S.C.E. W.P.I. 2010

Input Data:
Wind Load (W1) (K/ft): 7.12500
Building Height (ft): 360.00
Truss or Wall Mon. of elasticity (K/ft^2): 5.52100e+005
Total moment of Inertia Truss or Wall (ft^4): 3.60800e+004
Alpha: 6.09300e-004
Number of output (N): 10.0

Height(ft)	Lateral Deflection	Shear Wall		Frame	
H	y	Moment	Shear	Moment	Shear
0.00	0.00000	3.03803e+005	1.28250e+003	3.99727e+003	-2.27374e-013
36.00	0.00938	2.57856e+005	1.26592e+003	3.92788e+003	3.75258e+000
72.00	0.03555	2.12957e+005	1.22430e+003	3.73438e+003	6.89709e+000
108.00	0.07558	1.70007e+005	1.15762e+003	3.43835e+003	9.45355e+000
144.00	0.12669	1.29909e+005	1.06585e+003	3.06040e+003	1.14540e+001
180.00	0.18627	9.35677e+004	9.48932e+002	2.61980e+003	1.29427e+001
216.00	0.25196	6.18884e+004	8.06824e+002	2.13400e+003	1.39759e+001
252.00	0.32171	3.57795e+004	6.39453e+002	1.61819e+003	1.46218e+001
288.00	0.39382	1.61519e+004	4.46739e+002	1.08491e+003	1.49611e+001
324.00	0.46702	3.91953e+003	2.28589e+002	5.43567e+002	1.50865e+001
360.00	0.54053	0.00000e+000	-1.51029e+001	0.00000e+000	1.51029e+001

PRELIMINARY ANALYSIS OF WALL OR TRUSS-FRAMED BLDGS.
METHOD DEV. BY HEIDEBRECHT & SMITH
THIS METHOD TO BE USED FOR 2-DIMENSIONAL ANALYSIS.
REF: J. OF STRL. DIV, ASCE, VOL 99, NO. ST2. FEB. 1973
MADISON R. PAULINO M.S.C.E. W.P.I. 2010

Input Data:
Wind Load (P) (K/ft): 855.00000
Building Height (ft): 360.00
Truss or Wall Mon. of elasticity (K/ft^2): 5.52100e+005
Total moment of Inertia Truss or Wall (ft^4): 3.60800e+004
Alpha: 6.09300e-004
Number of output (N): 10.0

Height(ft)	Lateral Deflection	Shear Wall		Frame	
H	y	Moment	Shear	Moment	Shear
0.00	0.00000	3.02957e+005	8.55000e+002	4.84326e+003	0.00000e+000
36.00	0.00952	2.72247e+005	8.51156e+002	4.77284e+003	3.84361e+000
72.00	0.03676	2.41669e+005	8.47722e+002	4.57143e+003	7.27768e+000
108.00	0.07972	2.11206e+005	8.44696e+002	4.25375e+003	1.03039e+001
144.00	0.13642	1.80846e+005	8.42076e+002	3.83443e+003	1.29236e+001
180.00	0.20488	1.50572e+005	8.39862e+002	3.32811e+003	1.51382e+001
216.00	0.28315	1.20371e+005	8.38051e+002	2.74933e+003	1.69487e+001
252.00	0.36925	9.02274e+004	8.36644e+002	2.11264e+003	1.83559e+001
288.00	0.46121	6.01275e+004	8.35639e+002	1.43253e+003	1.93606e+001
324.00	0.55709	3.00565e+004	8.35037e+002	7.23498e+002	1.99633e+001
360.00	0.65492	-3.89480e-011	8.34836e+002	3.89480e-011	2.01641e+001